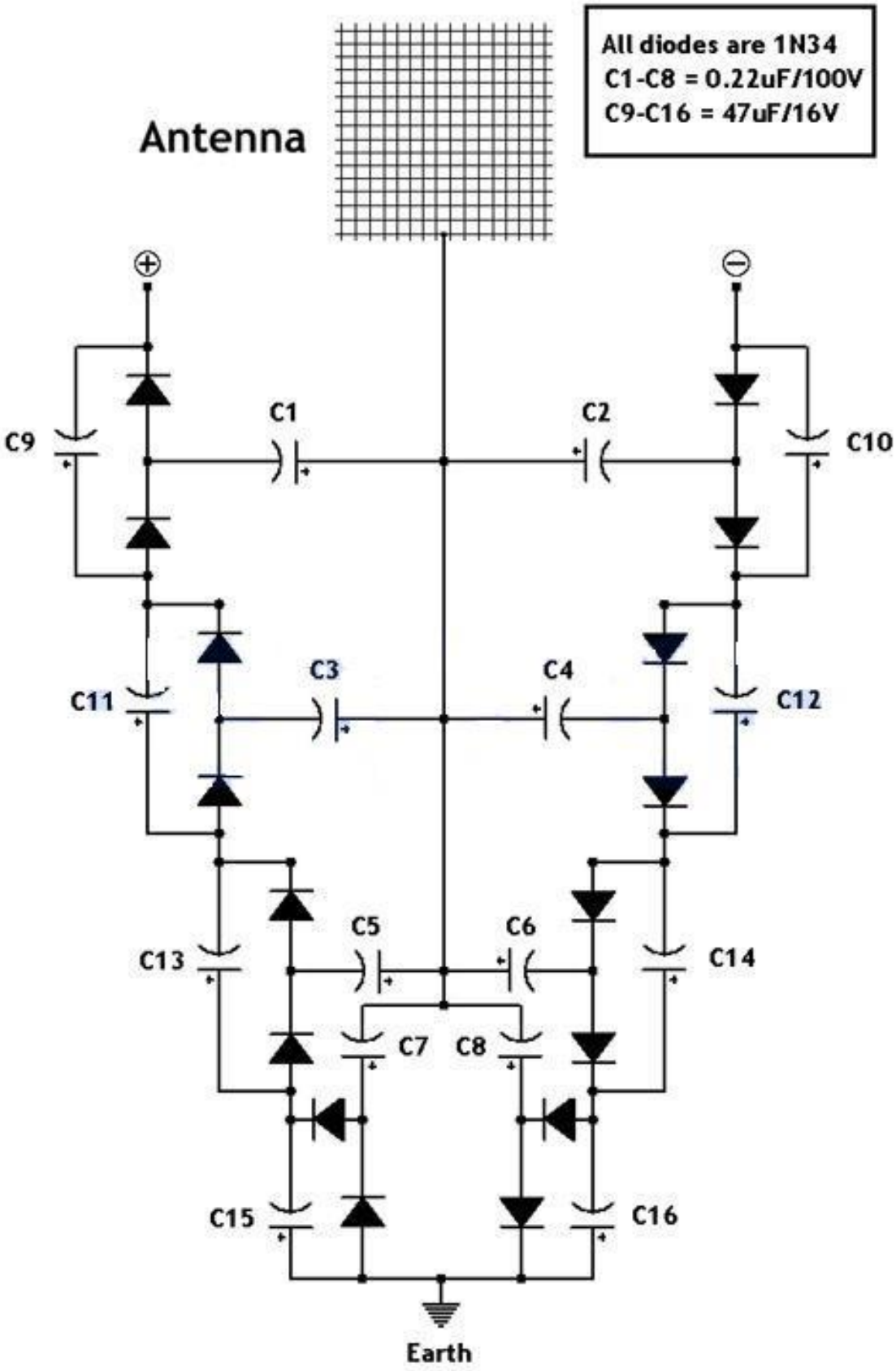
All diodes are 1N34
C1-C8 = 0.22uF/100V
C9-C16 = 47uF/16V
Antenna
C1
C2
C3
C4
C5
C6
C7
C8
C9
C10
C11
C12
C13
C14
C15
C16
Earth

FIG. 1

APM-2 SCHEMATIC DIAGRAM

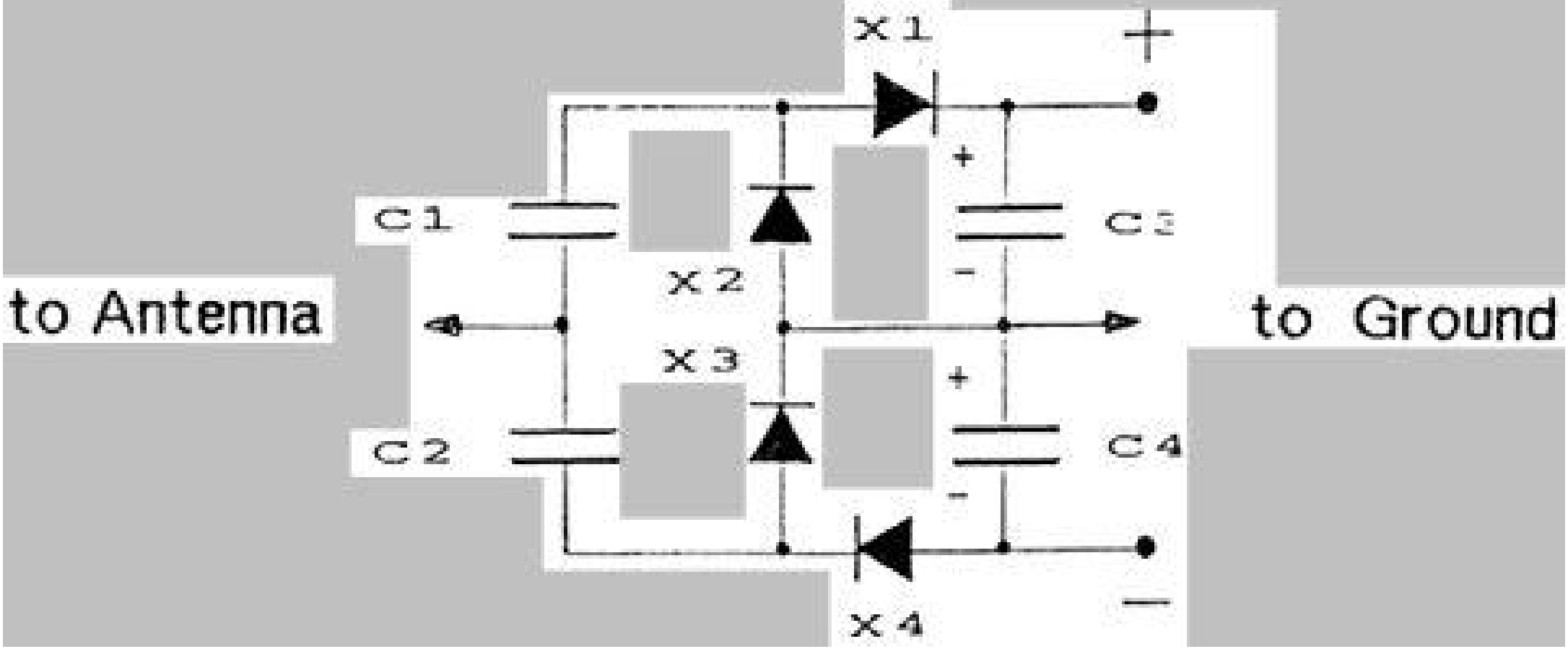

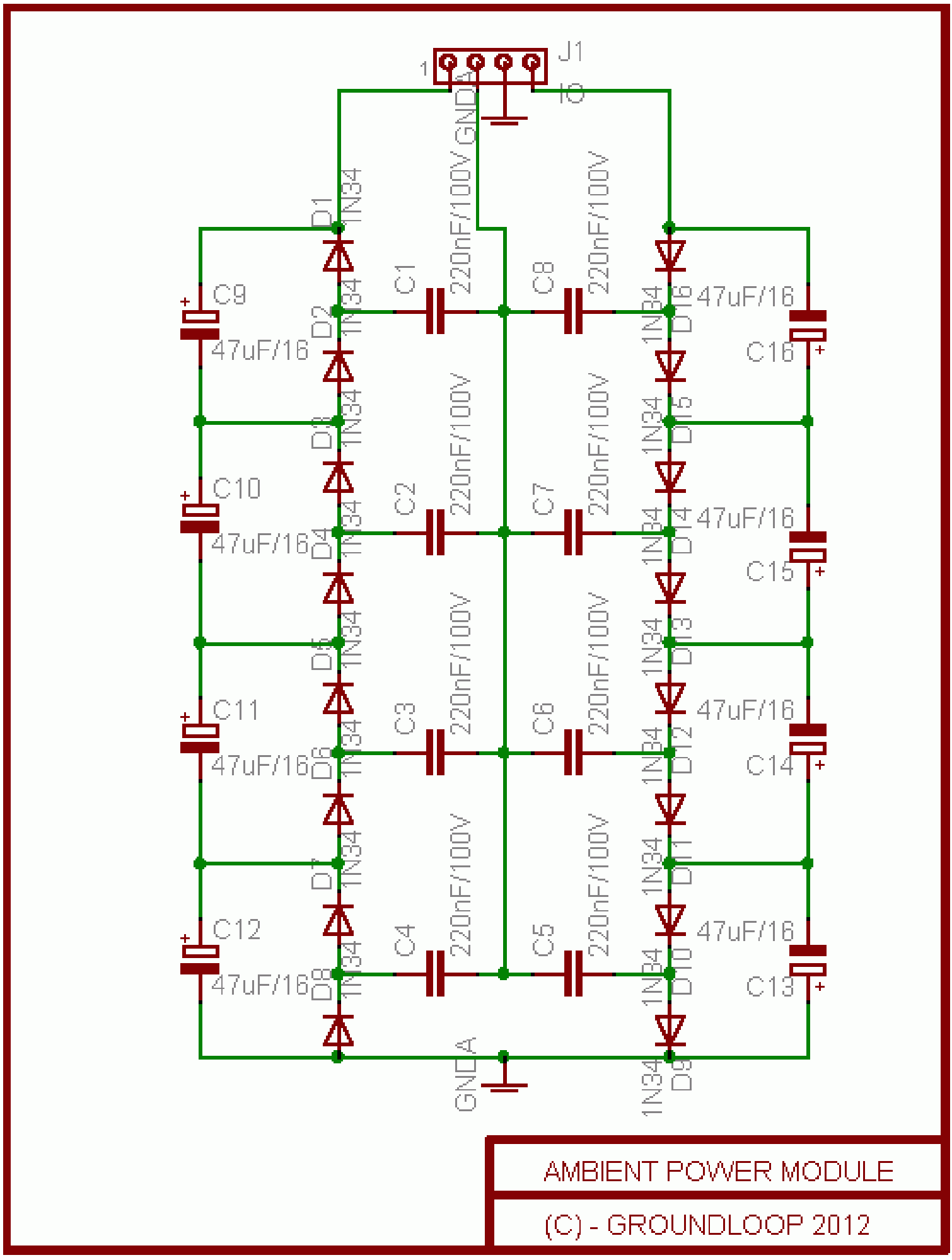
J1
1
4
IO
GND
D1
1N34
C1
220nF/100V
C8
220nF/100V
C9
47uF/16
D2
1N34
D16
1N34
47uF/16
C16
D3
1N34
D15
1N34
C2
220nF/100V
C7
220nF/100V
C10
47uF/16
D4
1N34
D14
1N34
47uF/16
C15
D5
1N34
D13
1N34
C3
220nF/100V
C6
220nF/100V
C11
47uF/16
D6
1N34
D12
1N34
47uF/16
C14
D7
1N34
D11
1N34
C4
220nF/100V
C5
220nF/100V
C12
47uF/16
D8
1N34
D10
1N34
47uF/16
C13
GND
A
D9
1N34
AMBIENT POWER MODULE
(C) - GROUNDLOOP 2012

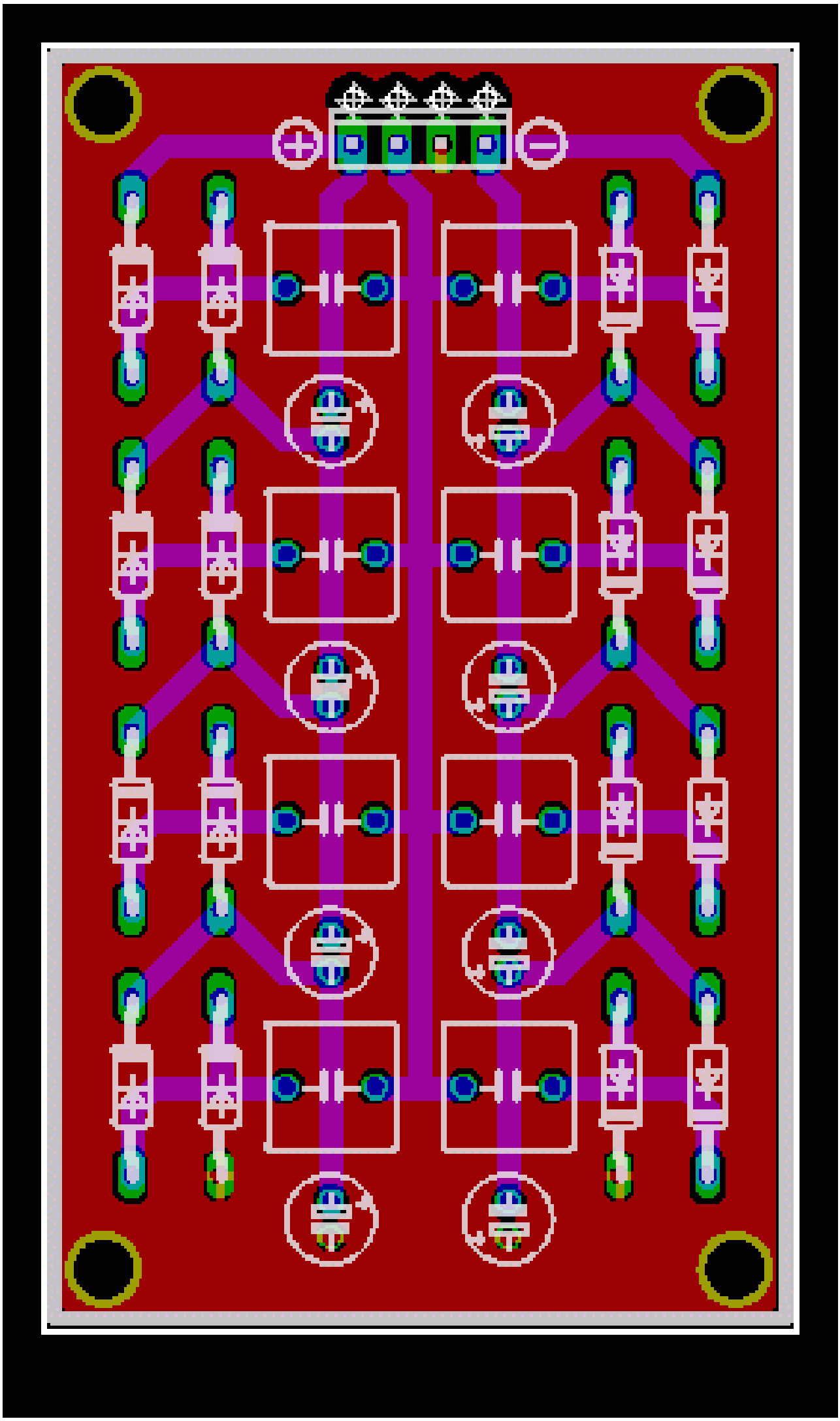

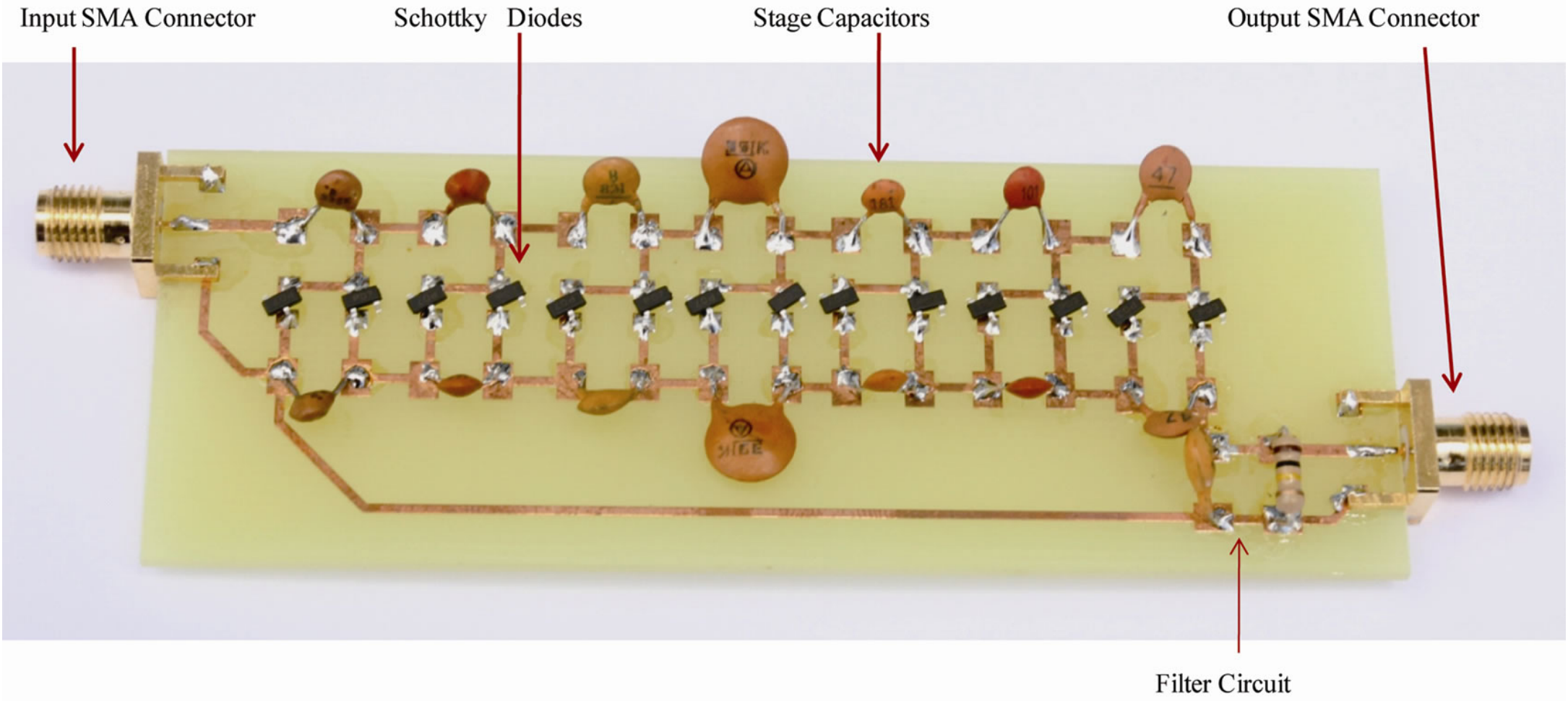
Input SMA Connector
Schottky Diodes
Stage Capacitors
Output SMA Connector
Filter Circuit

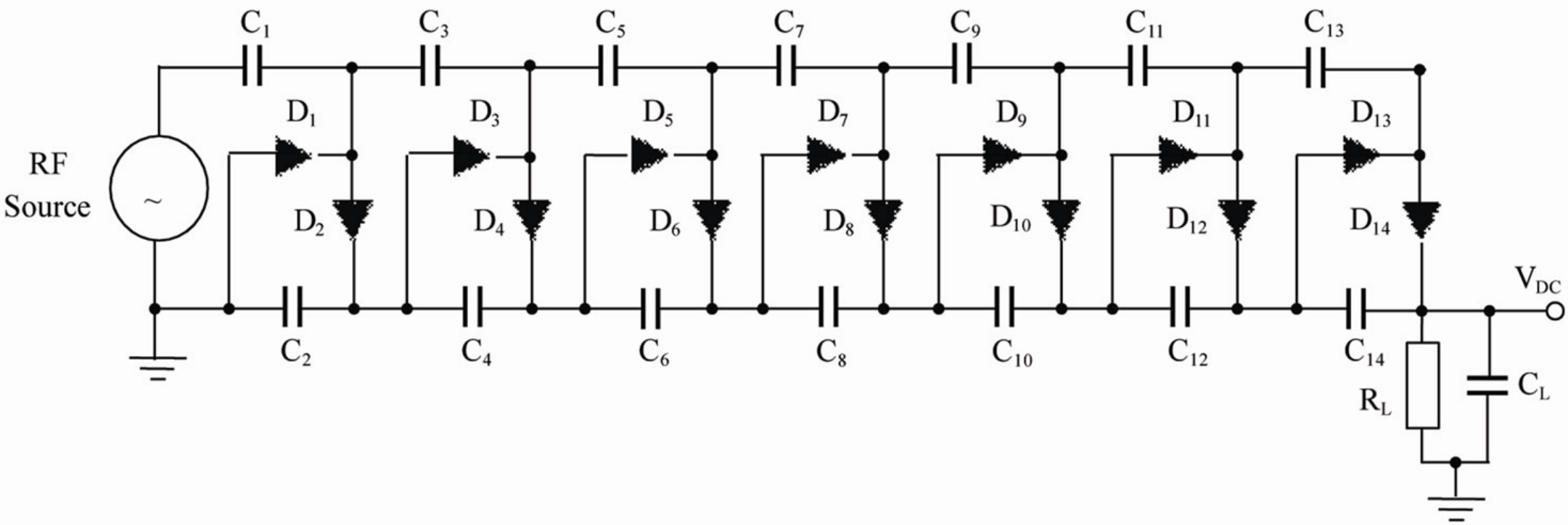
C1
C3
C5
C7
C9
C11
C13
D1
D3
D5
D7
D9
D11
D13
RF
Source
~
D2
D4
D6
D8
D10
D12
D14
VDC
C2
C4
C6
C8
C10
C12
C14
RL
CL

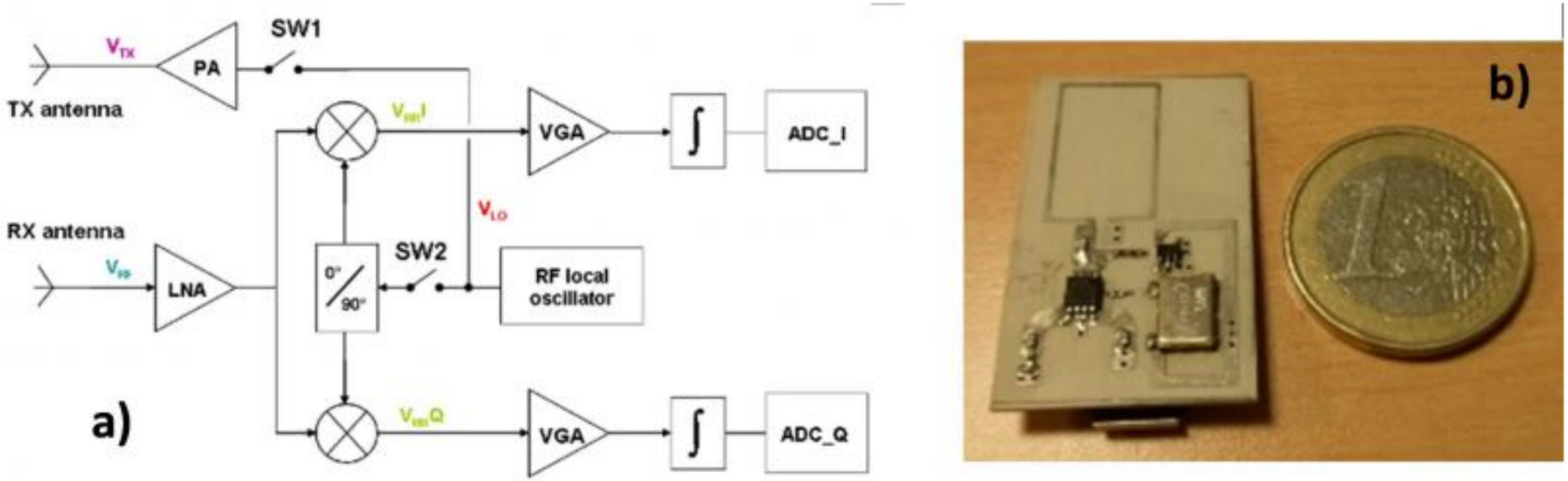

Fig 5.2. a) RF-reader architecture and b) Miniaturized RFID tag

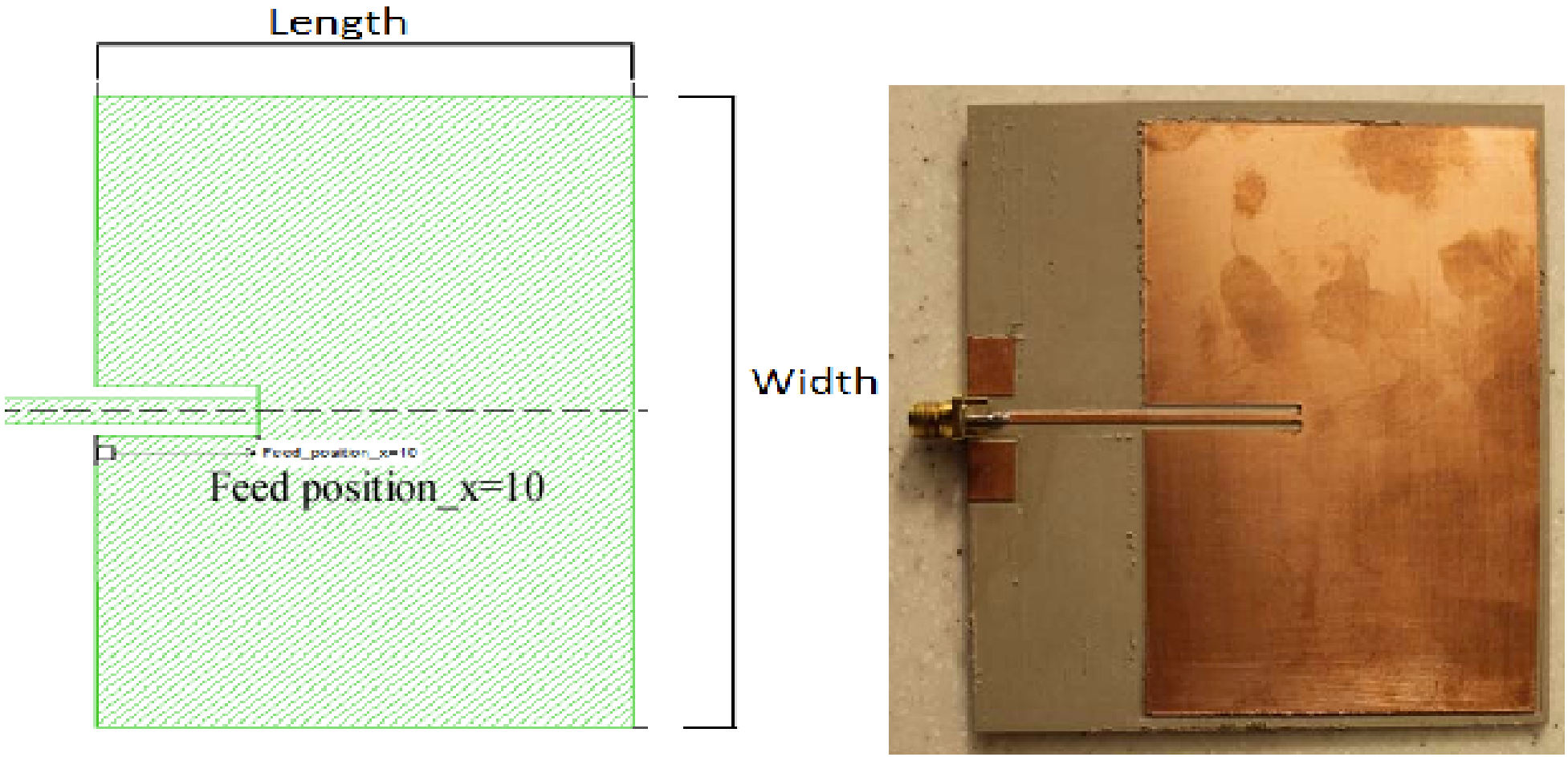

Fig. 3. RF Energy receiving antenna layout and manufactured prototype

Fig. 3. RF Energy receiving antenna layout and manufactured prototype

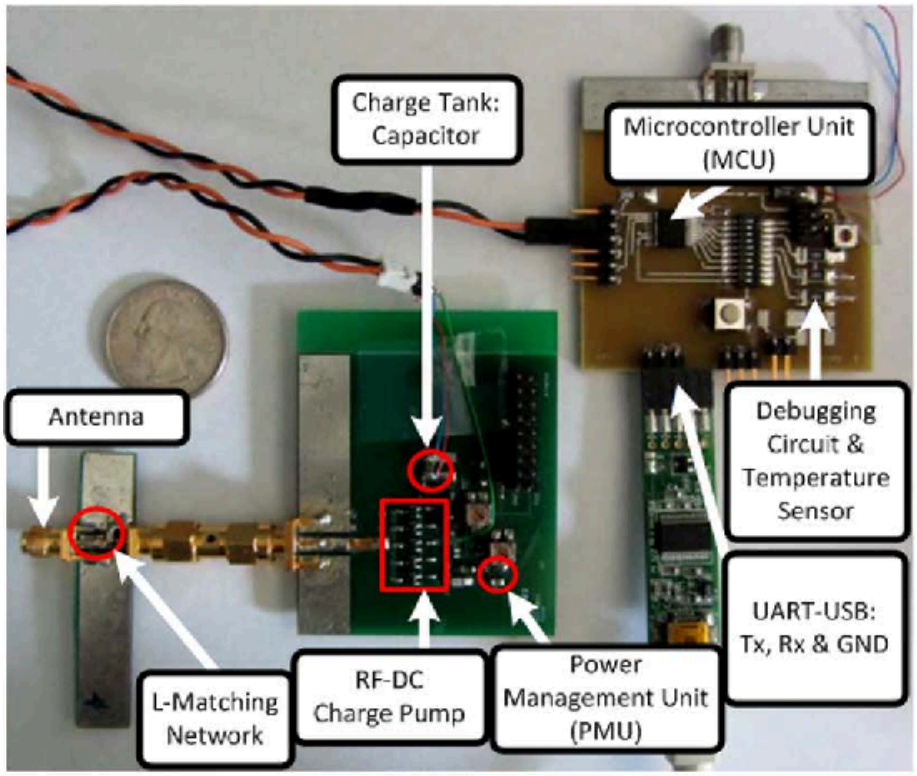
Charge Tank: Capacitor
Microcontroller Unit (MCU)
Antenna
Debugging Circuit & Temperature Sensor
UART-USB: Tx, Rx & GND
L-Matching Network
RF-DC Charge Pump
Power Management Unit (PMU)

(a)

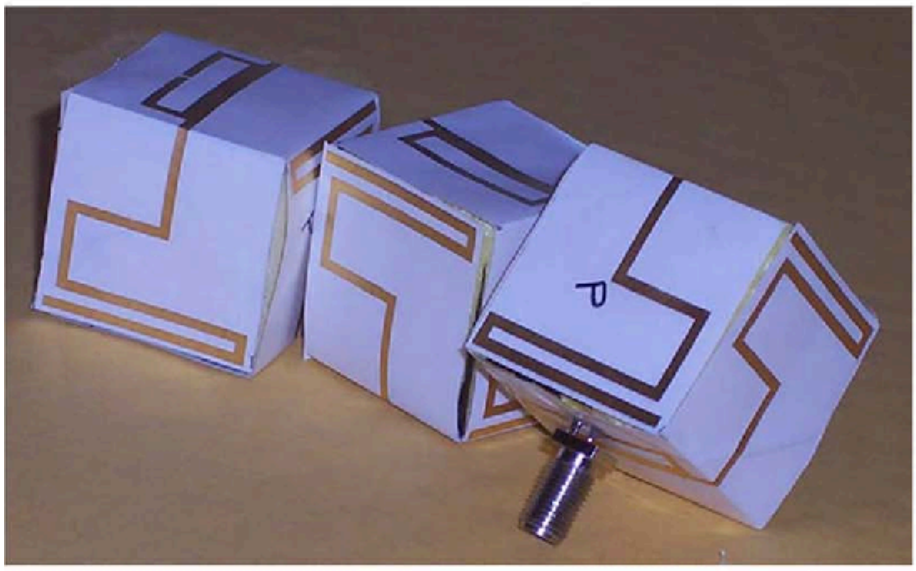

(b)

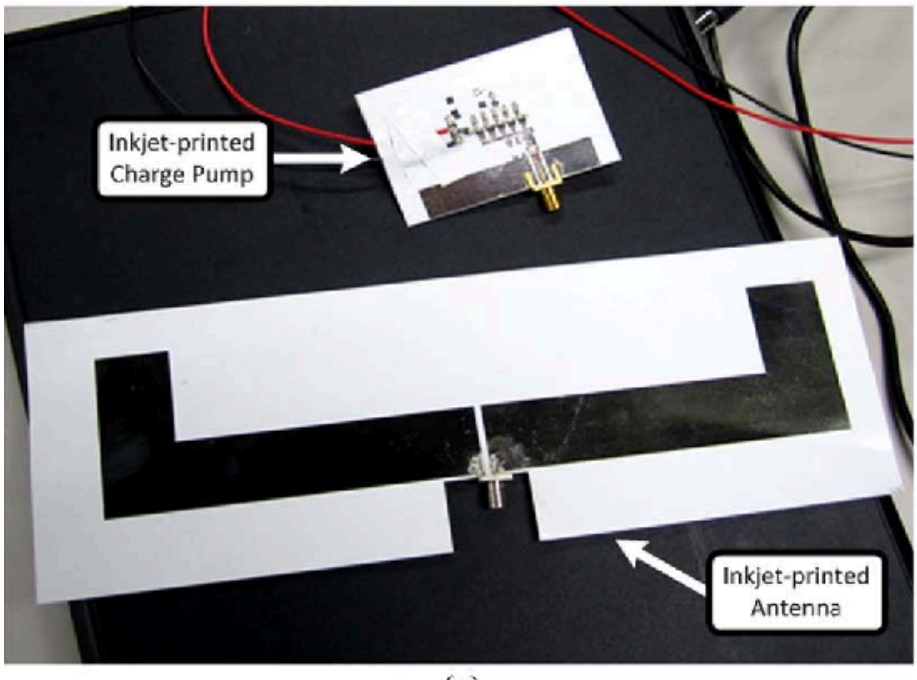
Inkjet-printed Charge Pump
Inkjet-printed Antenna

(c)

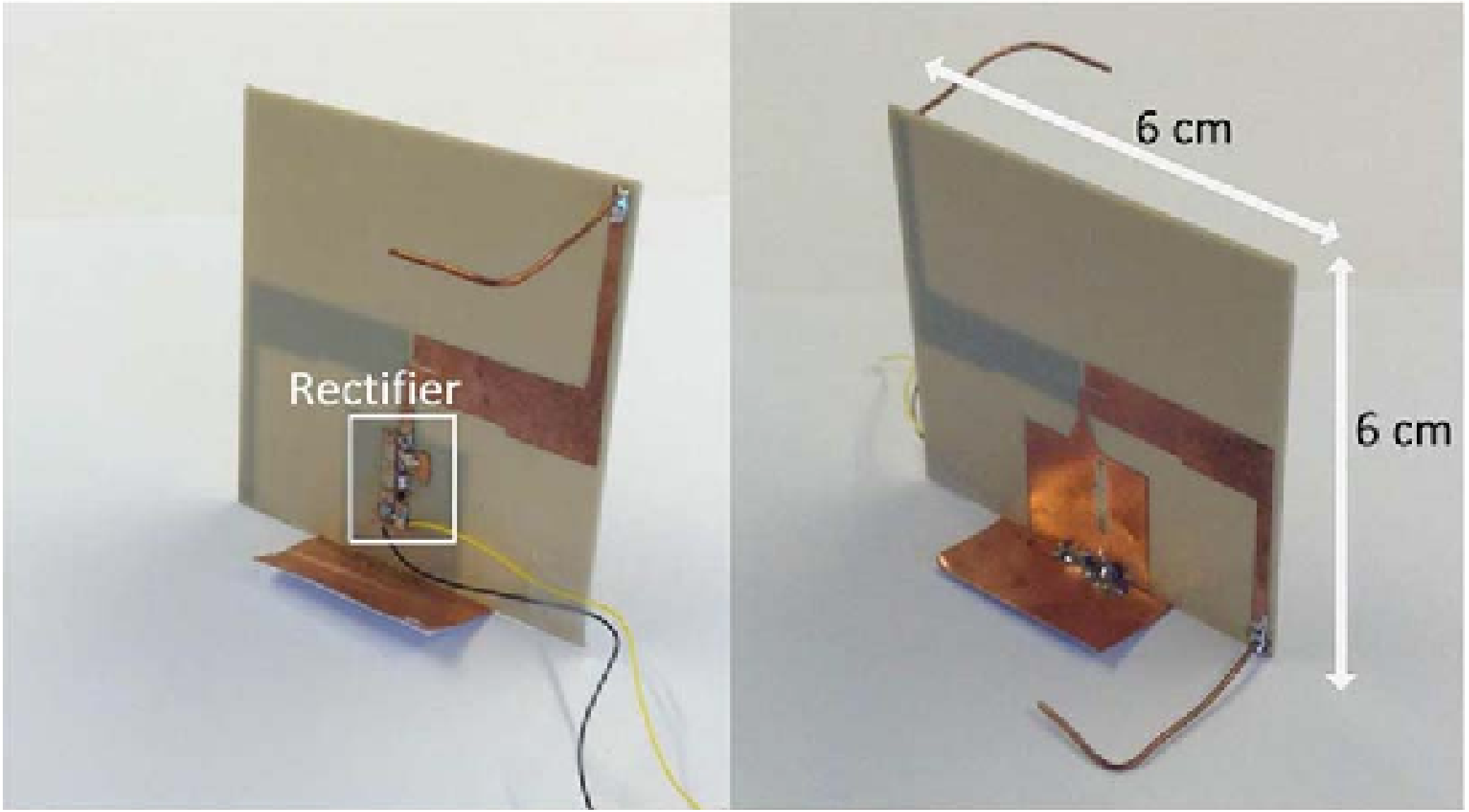

Fig. 16. Fabricated dual-band rectenna prototype [17].

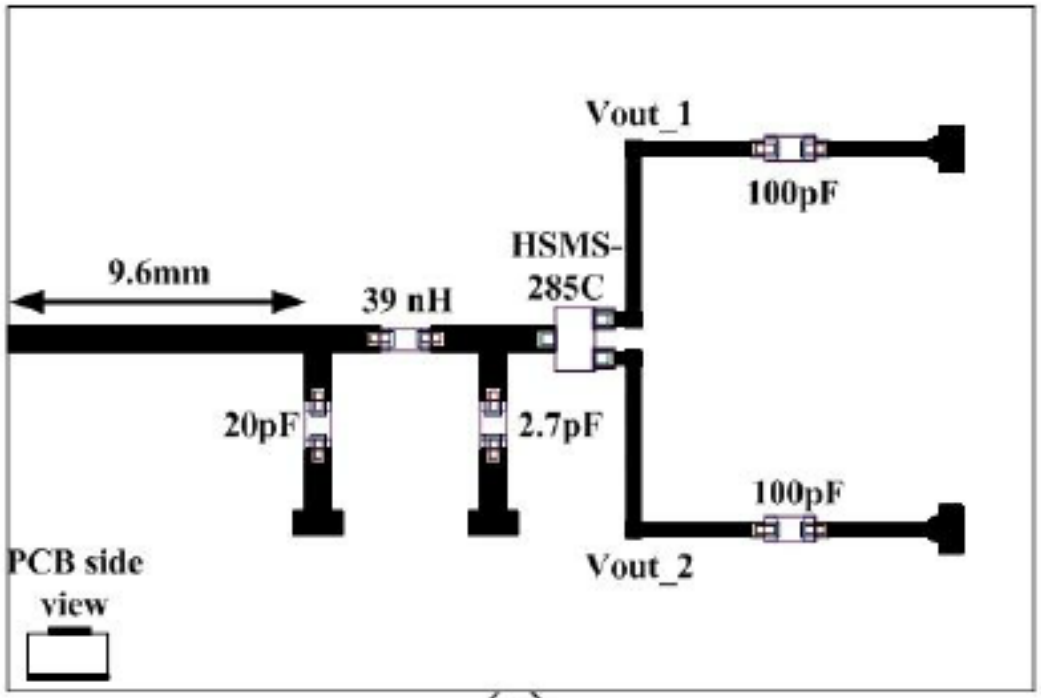
Vout_1
100pF
HSMS-
285C
9.6mm
39 nH
20pF
2.7pF
100pF
PCB side
view
Vout_2

(a)

(b)

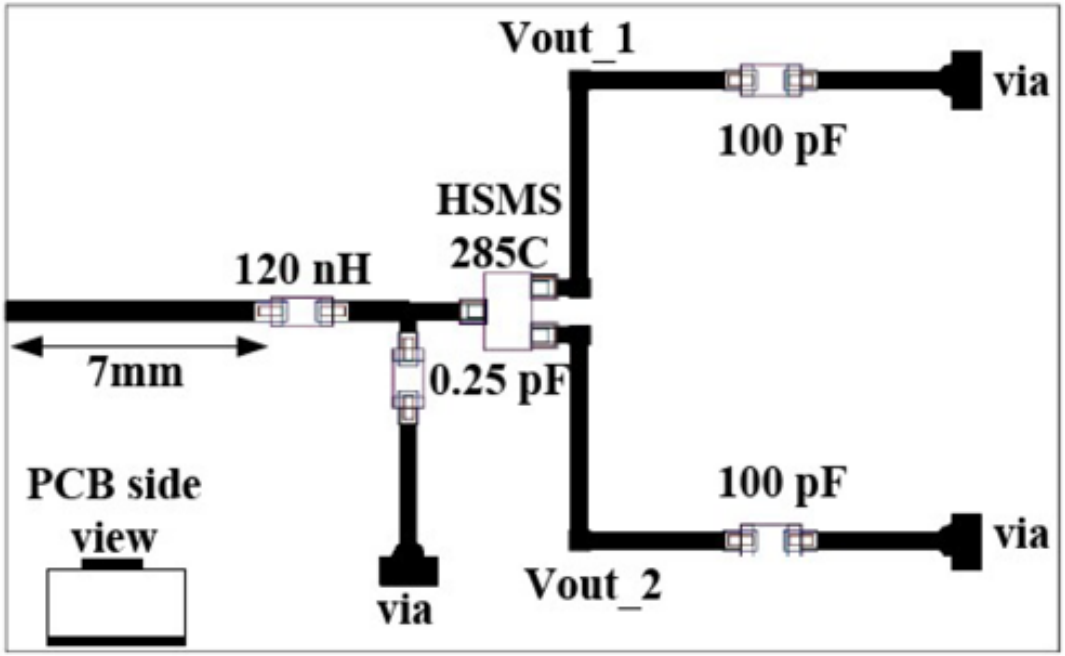
Vout_1
via
100 pF
HSMS
285C
120 nH
7mm
0.25 pF
PCB side
view
100 pF
via
via
Vout_2

(c)

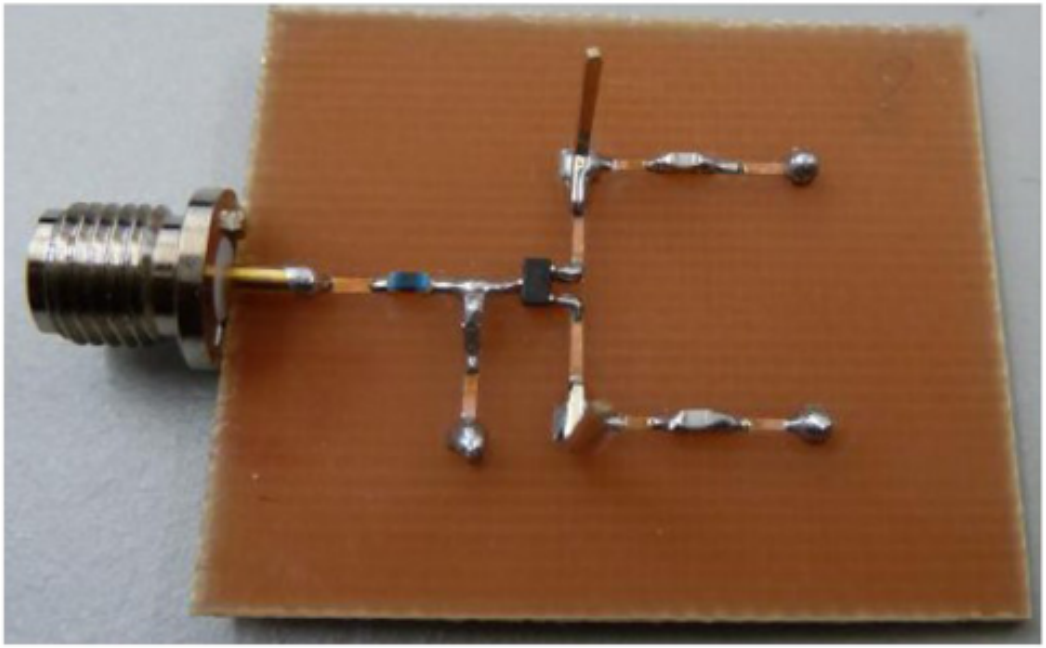

(d)

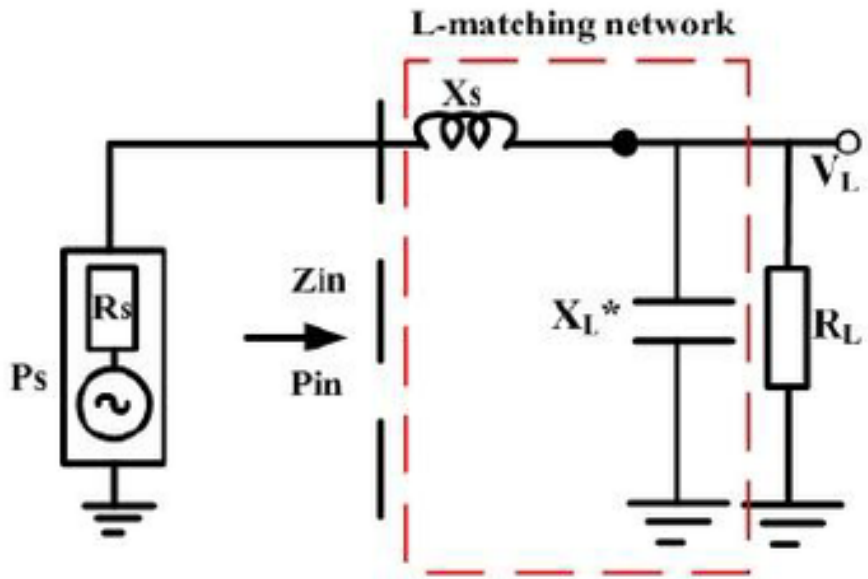
L-matching network
Xs
V_L
Rs
Ps
Zin
Pin
X_L*
R_L

(a)

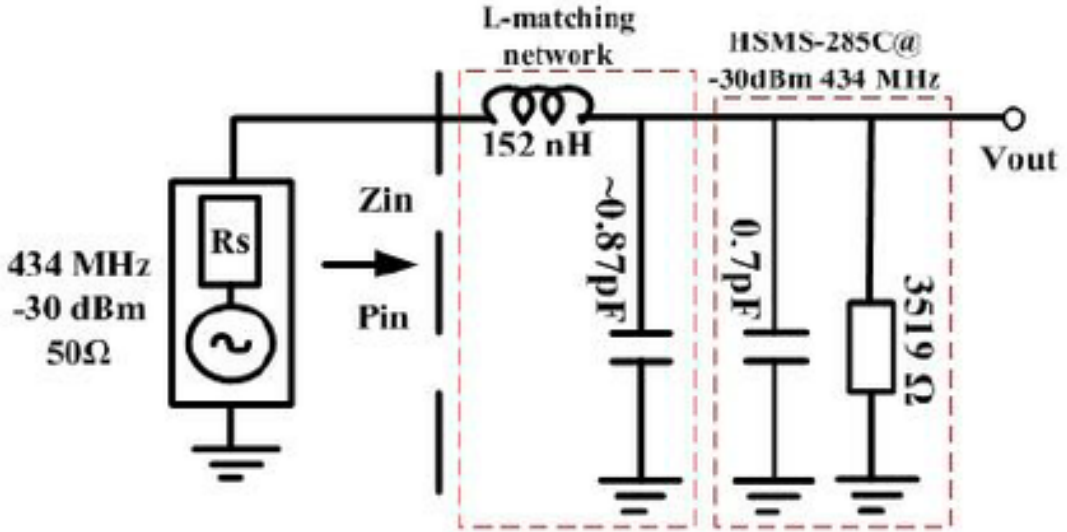
L-matching network
HSMS-285C@ -30dBm 434 MHz
152 nH
Vout
Rs
434 MHz
-30 dBm
50Ω
Zin
Pin
~0.87pF
0.7pF
3519 Ω

(b)

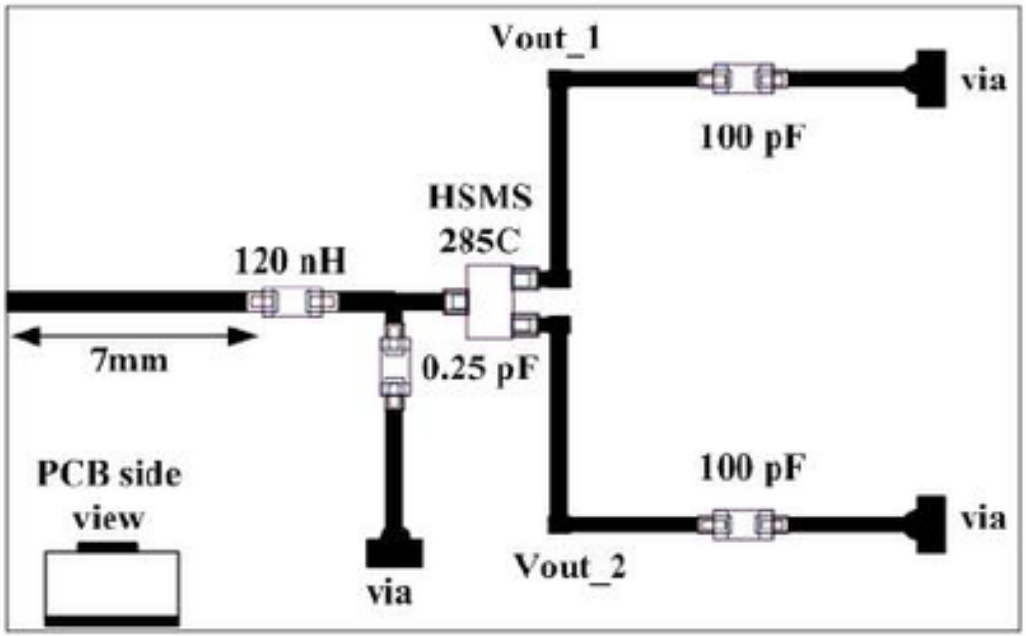
Vout_1
via
100 pF
HSMS
285C
120 nH
7mm
0.25 pF
PCB side
view
100 pF
via
via
Vout_2

(c)

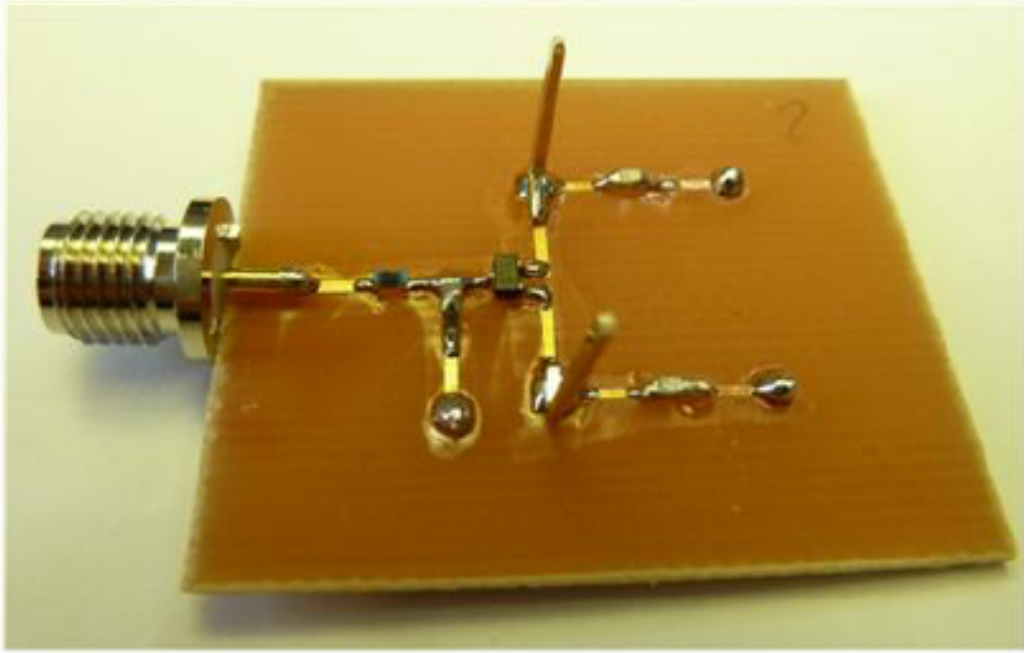

(d)

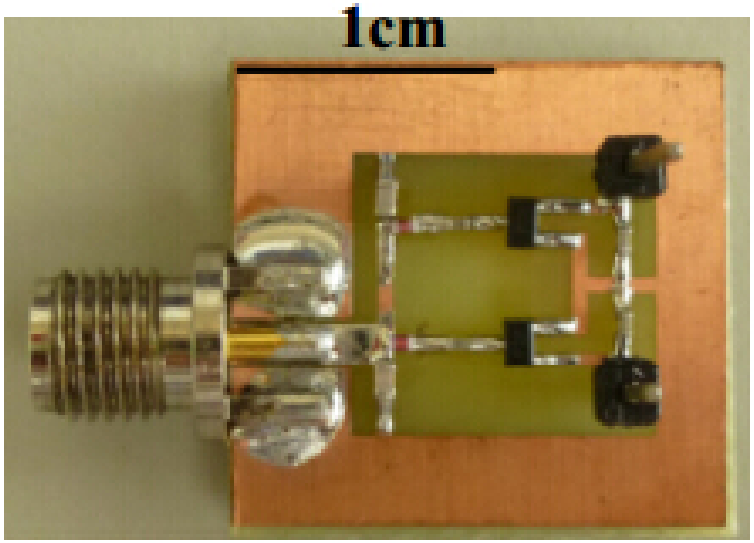
1cm

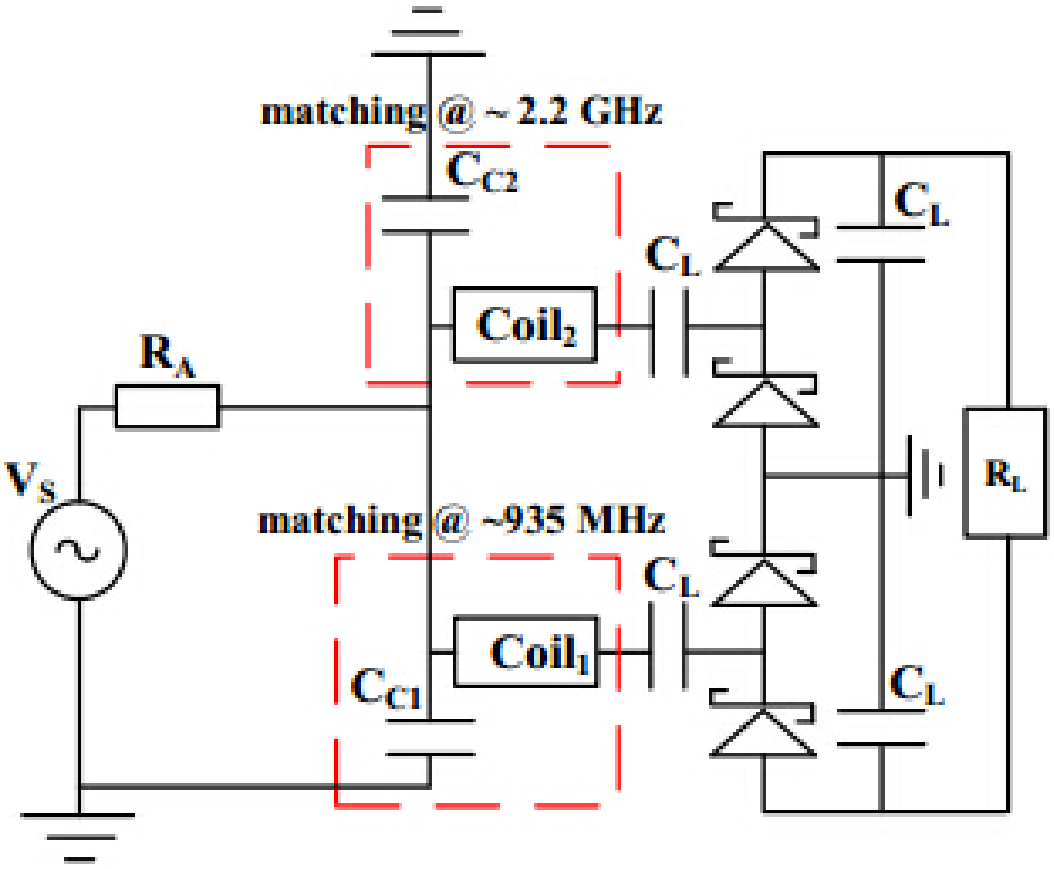
matching @ ~ 2.2 GHz
C_{C2}
C_L
C_L
$Coil_2$
R_A
V_S
matching @ ~935 MHz
C_L
$Coil_1$
C_{C1}
C_L
R_L

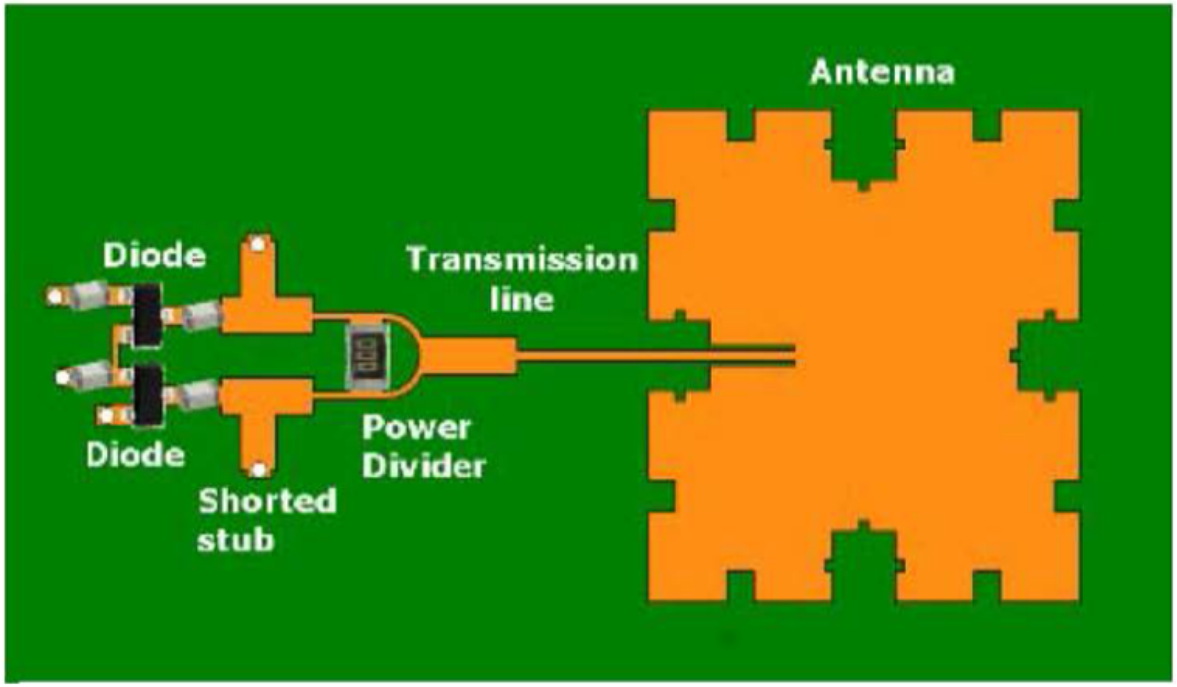
Antenna
Diode
Transmission line
Diode
Power Divider
Shorted stub

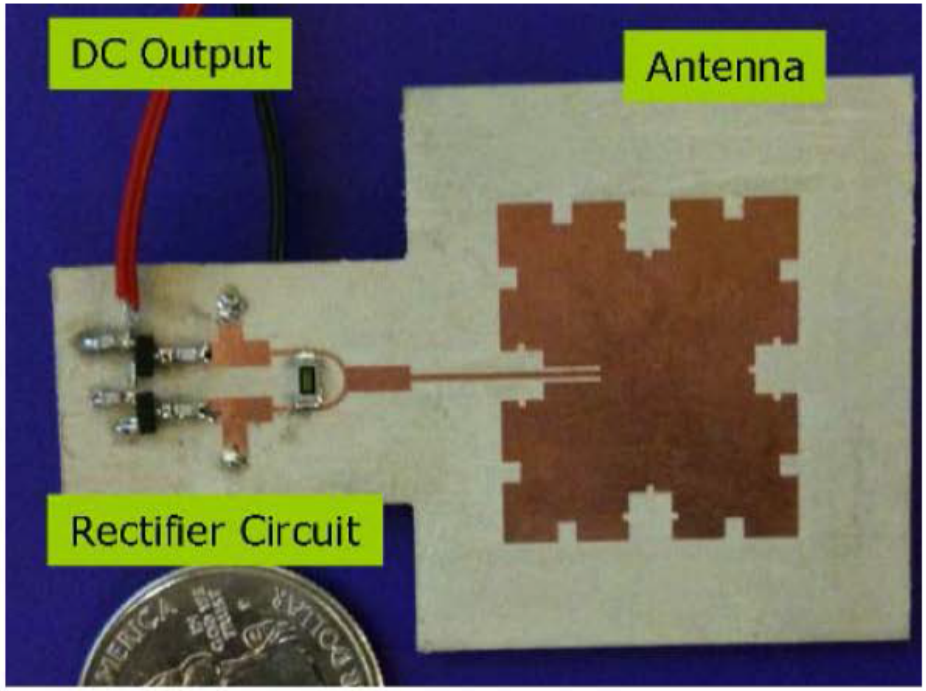
DC Output
Antenna
Rectifier Circuit

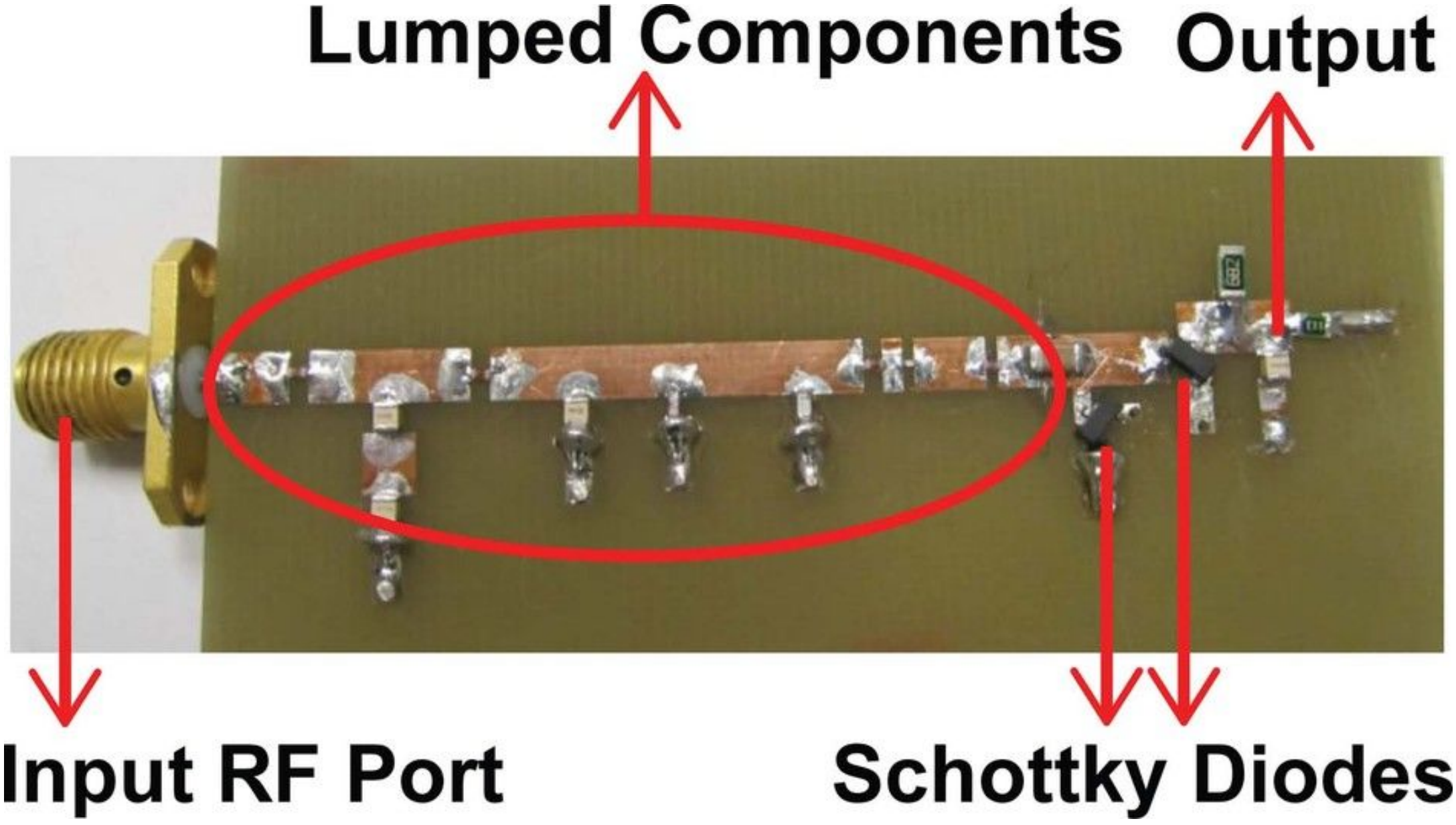
Lumped Components
Output
Input RF Port
Schottky Diodes

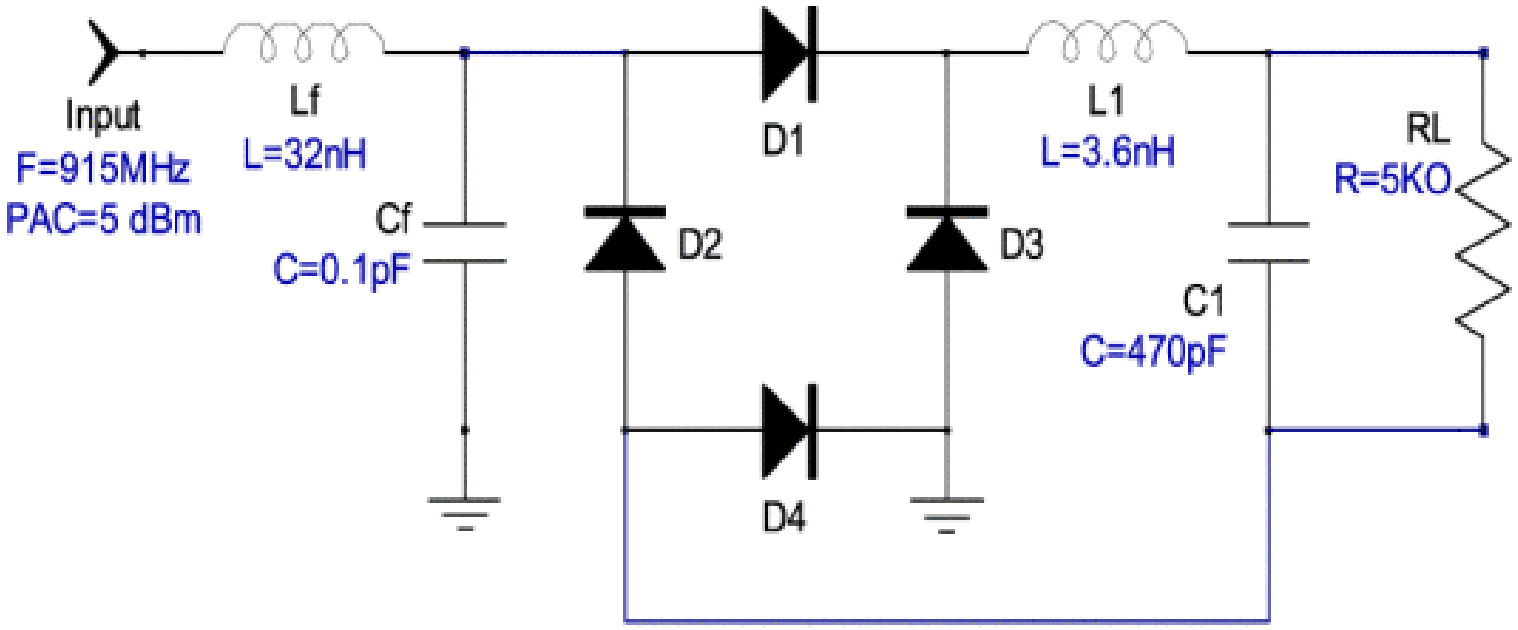
Input
F=915MHz
PAC=5 dBm
Lf
L=32nH
Cf
C=0.1pF
D1
D2
D3
D4
L1
L=3.6nH
C1
C=470pF
RL
R=5KO

(a)

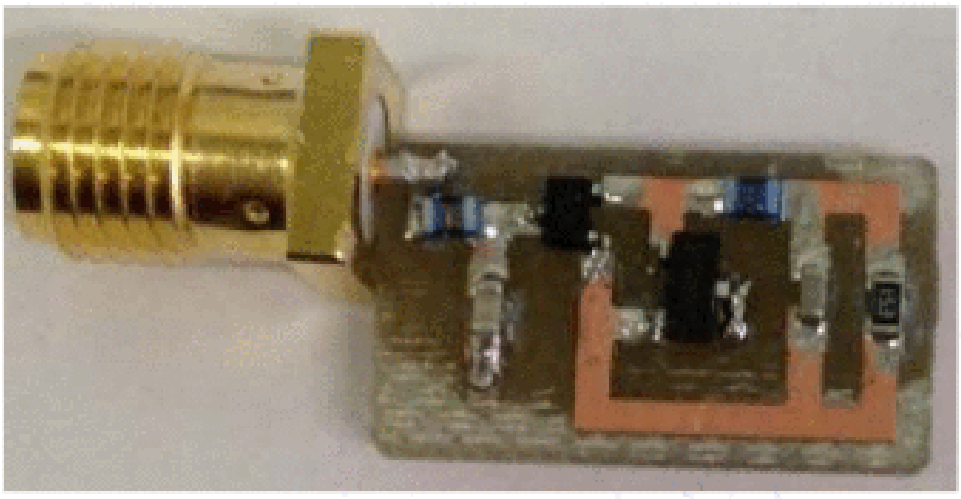

(b)

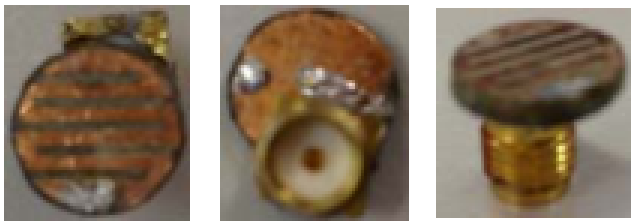

FIGURE 5. **(a) Top view of the PIFA. (b) Bottom view of the PIFA. (c) Complete three-layer PIFA.**

C. ANTENNA PERFORMANCE

The designed antenna is simulated using the EM simulation software XFdtd to devise its parameters. The return loss response and the input impedance of the antenna is also

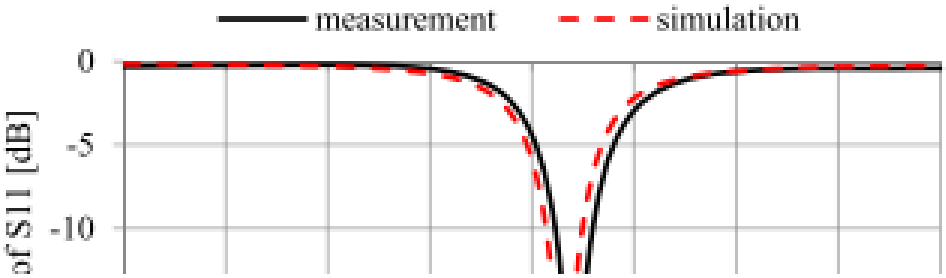

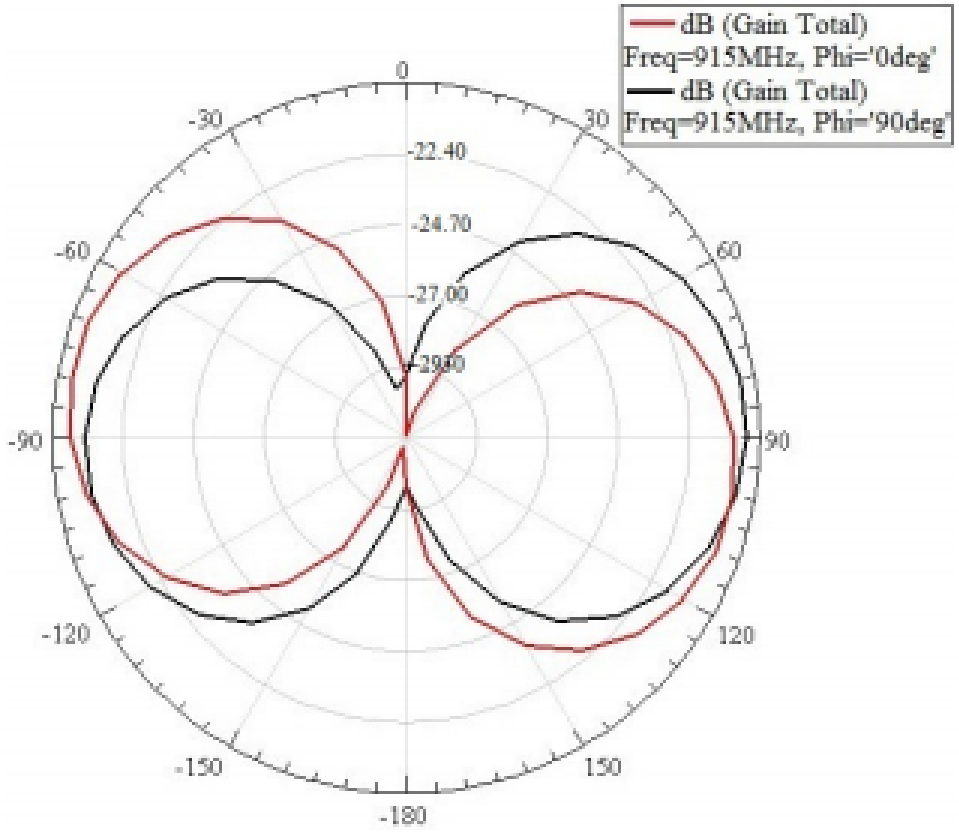

FIGURE 7. **2D far field gain pattern of the proposed three-layer PIFA in free space.**

VI. RECTIFIER DESIGN, FABRICATION AND ANALYSIS

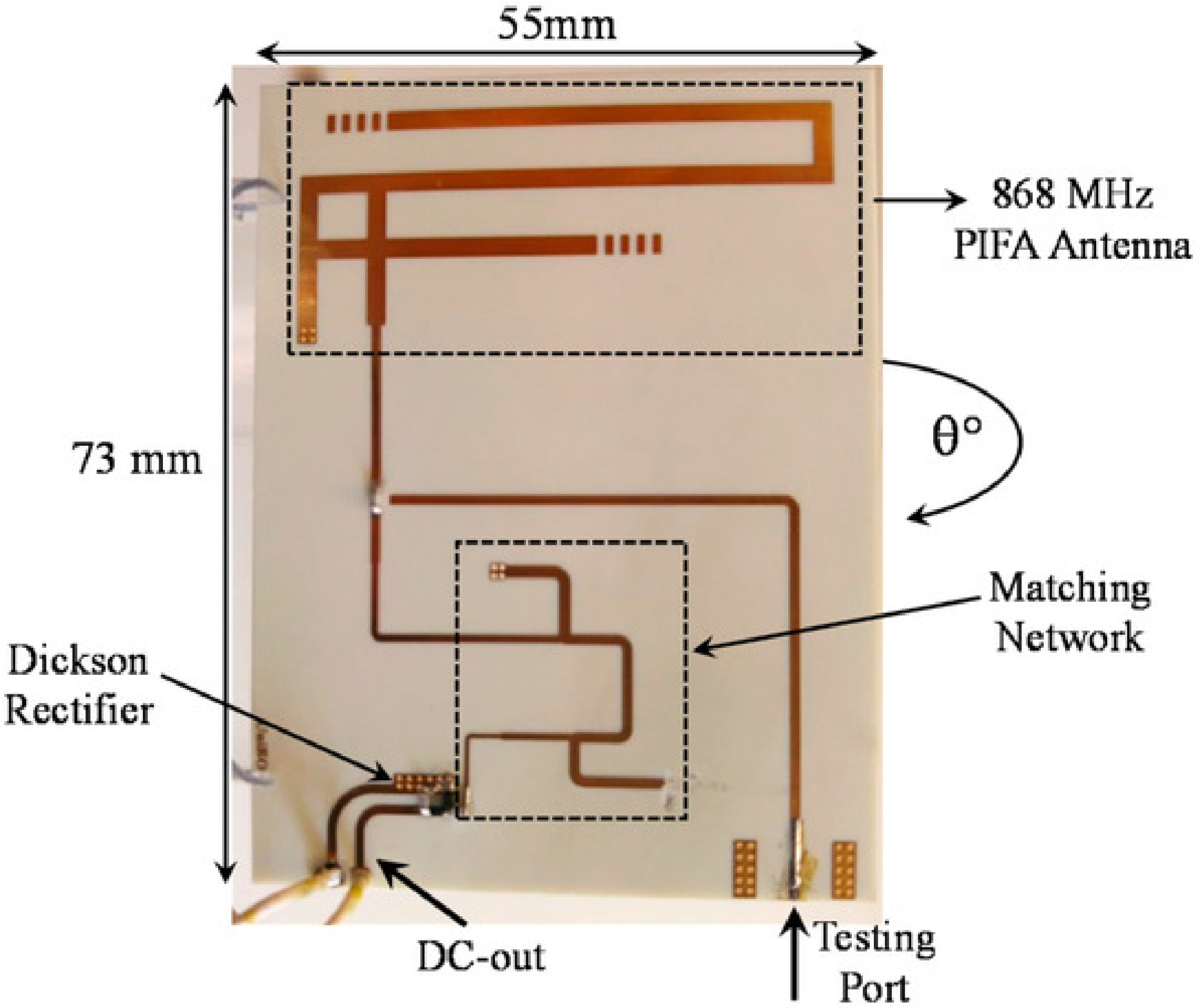
55mm
868 MHz
PIFA Antenna
73 mm
θ°
Matching
Network
Dickson
Rectifier
DC-out
Testing
Port

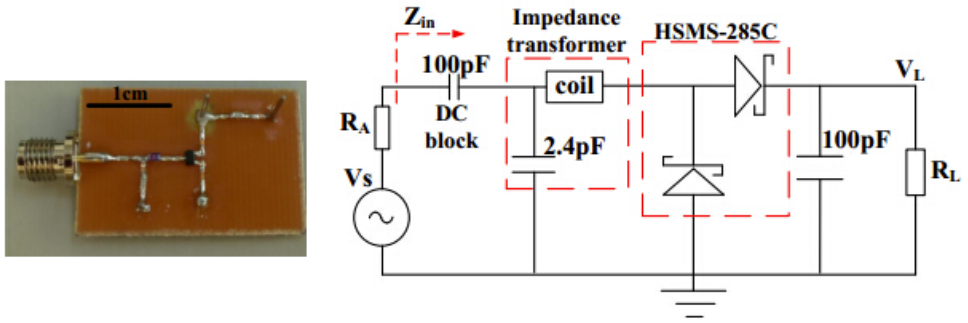

Figure 4. PCB of the realized RF harvester at 930MHz using a HSMS-285C diode voltage doubler. The HSMS-285C has the following spice parameters I_S = 3μA, C_j = 0.18pF and R_S= 25. *Coil* = 38.5nH at 900MHz with a Q_u of 69. The chip capacitors have Q_u of about 1000 at 900MHz.

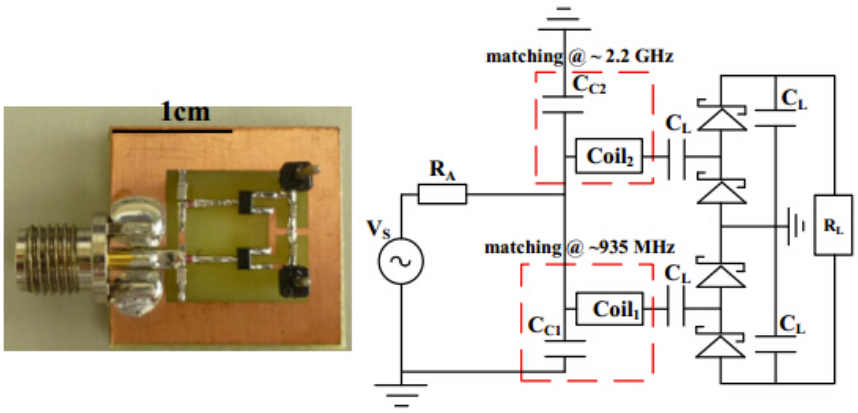

Figure 6. Picture and circuit layout of the dual-band RF harvester. The harvester is matched at 935MHz and 2.2GHz. Schottky diodes are HSMS-285x series. C_{C1}=2.7pF, $Coil_1$ =39nH; $Coil_1$ Q_U @ 900MHz =88, C_{C2}=0.8pF, $Coil_2$ =2.14nH; $Coil_2$ Q_U @ 1.7GHz =35, C_L=100pF.

clos

Figure 11. Setup for measuring the power delivered by the GSM base station across a resistive load. The RF to DC rectifier is the circuit as presented in Figure 6 and the antenna is from Homg-Dean Chen et al. [17]. R_L is ~0.5MΩ. V_L is about 2.3V.

close

Figure 12. Using ambient RF GSM power to operate Thermo-Hygrometer sensor. The RF to DC rectifier is as presented in Figure 6.

Fig. 3. Frequency doubler: schematic (a) and prototype manufactured in paper substrate (b). All the components, except for the diode and the capacitor in the output-matching network, are implemented as distributed elements in microstrip technology, which have been folded in order to reduce the area occupation. The Schottky diode is soldered on the Cu laminate as in standard PCBs. Active area: 18 mm in length and 19 mm in width [21].

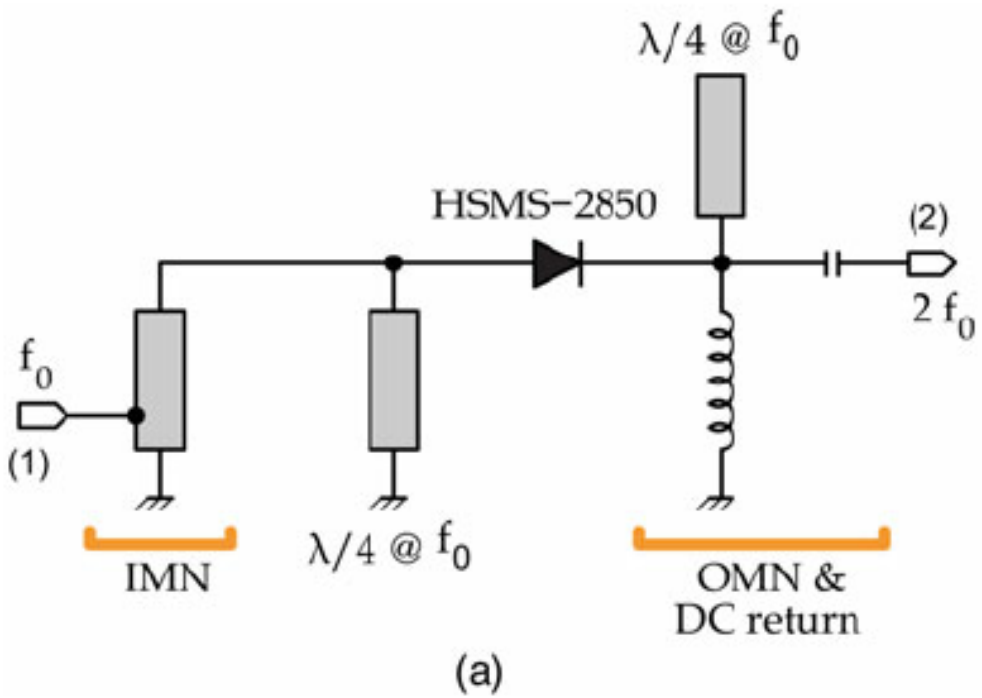

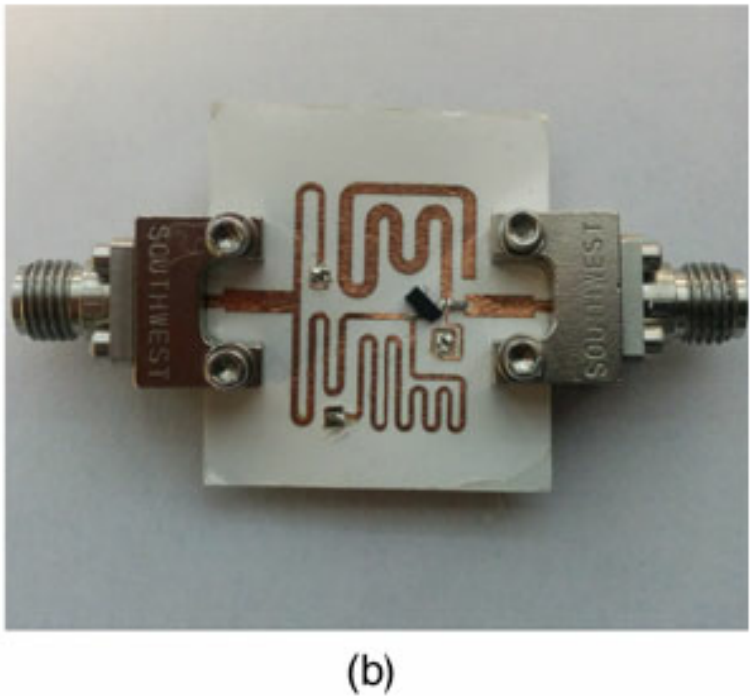

Although it may not be immediately evident, the antenna is a dipole. One half of the dipole is the white wire that protrudes to the left, and the other half of the dipole is the metal cylinder. Each half is electrically insulated from the other, and is approximately ¼ wavelength long. Similar antennas have a gain of about 2dBi, and exhibit a relatively circular radiation pattern.

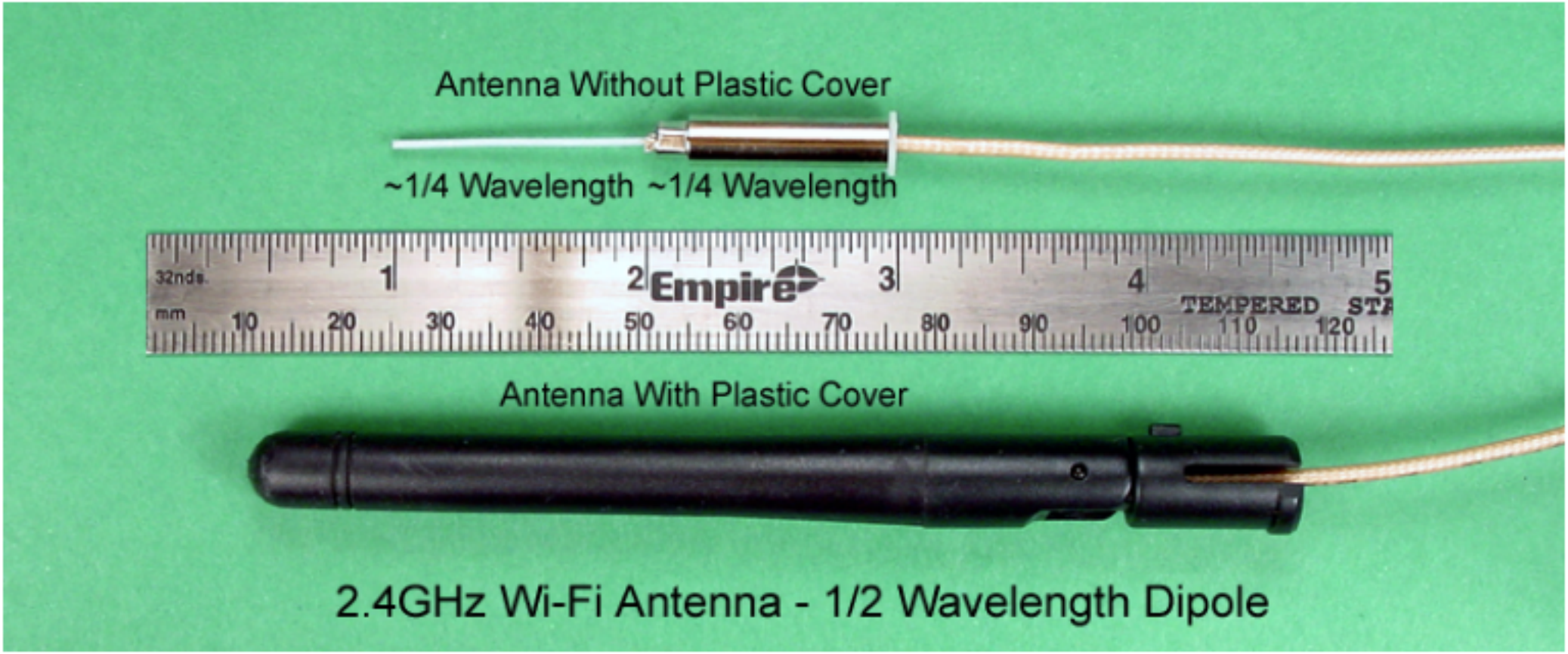

In both cases, the wire feedline exits from the bottom of the antenna to connect to the Wi-Fi radio transceiver. The feedline is a coaxial cable with an inner conductor and an outer braided shield; a clear plastic cover encases the feedline. This particular feedline is often used for Wi-Fi devices because of its small size and relatively low RF losses; it is designated RG-178. Coaxial feedlines are often referred to as "coax."

The other end of the coax is connected the router, as shown below. Note that the shields are securely soldered to the ground plane on the PCB, and the center conductors are soldered to PCB tracks that lead to the transceiver inside the gold metal box. The inset shows an alternative soldering style; sometimes connectors are soldered to the PCB and the coax is equipped with mating connectors that snap into place.

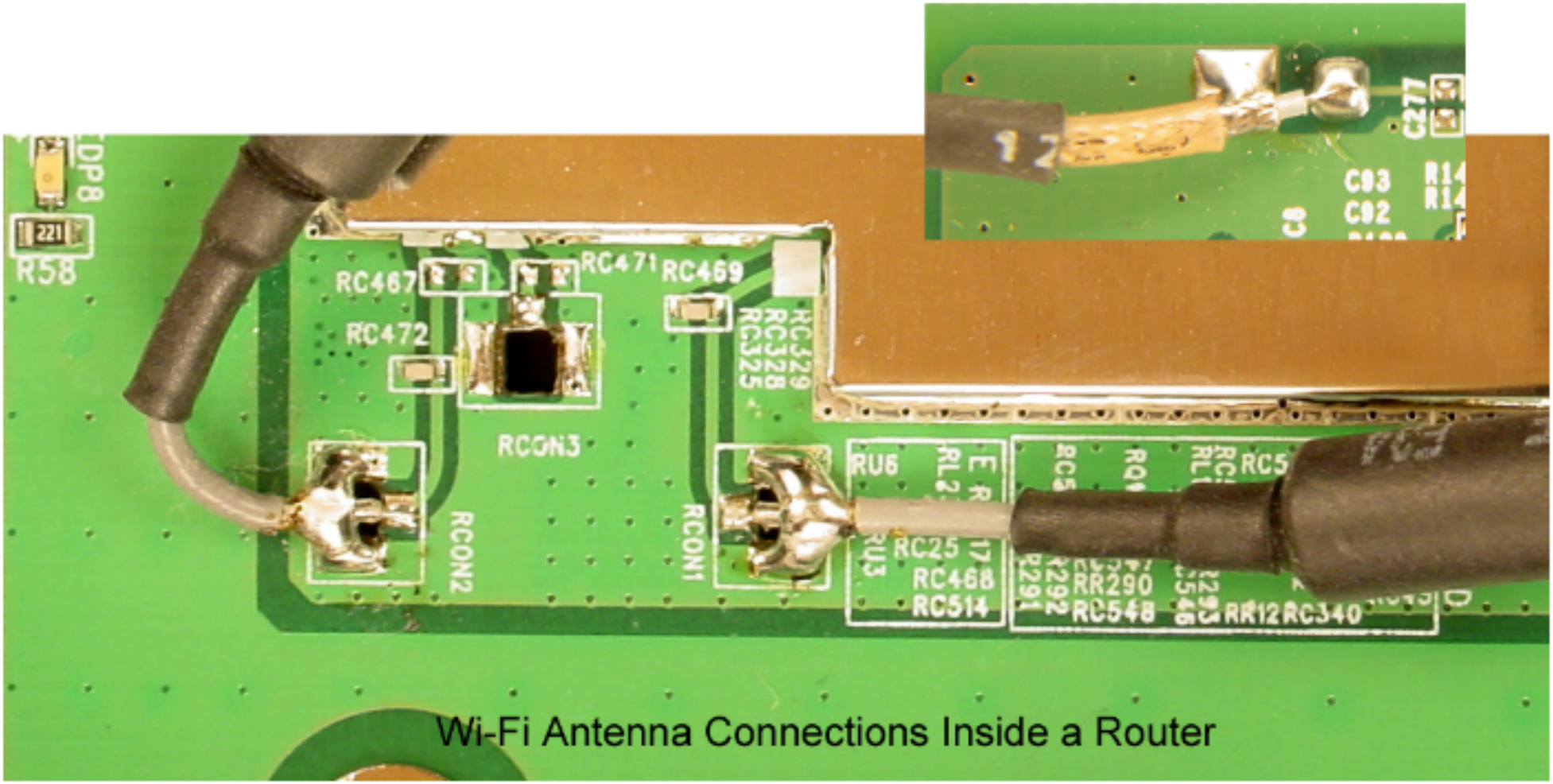

Wi-Fi Antenna Connections Inside a Router

RF energy harvesting

RF energy can be used to trickle charge or operate consumer electronics such as e-book readers or headsets, wearable medical sensors and other devices. This power source has plenty of potential because of the large and growing number of radio transmitters around the world, related to TV and radio broadcasting as well as mobile phones and other devices.

Fig. 4: Pet implant RFID chip; the rice grain indicates size – Image via Wikimedia

Radio-frequency identification (RFID) is a special form of RF energy harvesting, in which power, as well as information, is obtained from a specific source rather than random ambient RF energy. An RFID base station has a scanning antenna which transmits radio-frequency signals over a relatively short range. This communicates with a transponder built into a passive RFID tag – and provides the transponder with the energy necessary to wake up, read and communicate in response. There are active RFID tags with batteries that operate at a greater distance, but passive tags without batteries have a virtually unlimited lifespan.

Applications are widely diverse: examples include credit cards, real time location systems (RTLSs) to track worker movements or the effectiveness of a store floor plan, asset tracking, motorway tolls and pet ID implants.

What you will need:

- 1 x 470 ohm resisitor
- 1 x 100p ceramic capacitor
- 1 x 100n greencap capacitor
- 2 x 1N4148 signal diodes
- 1 x 5mm red LED
- 1 x 5cm hook-up wire
- 2 x paper clips

Build the circuit up as shown below:

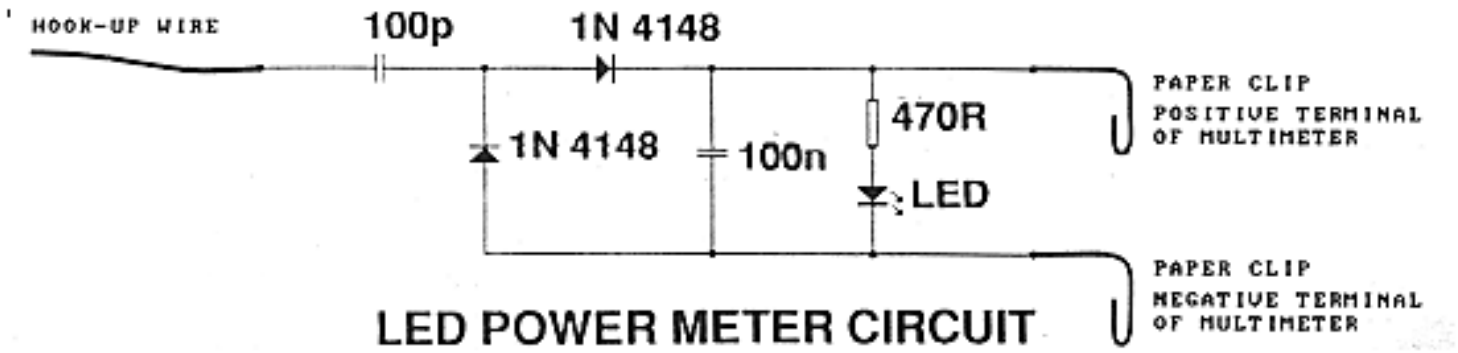

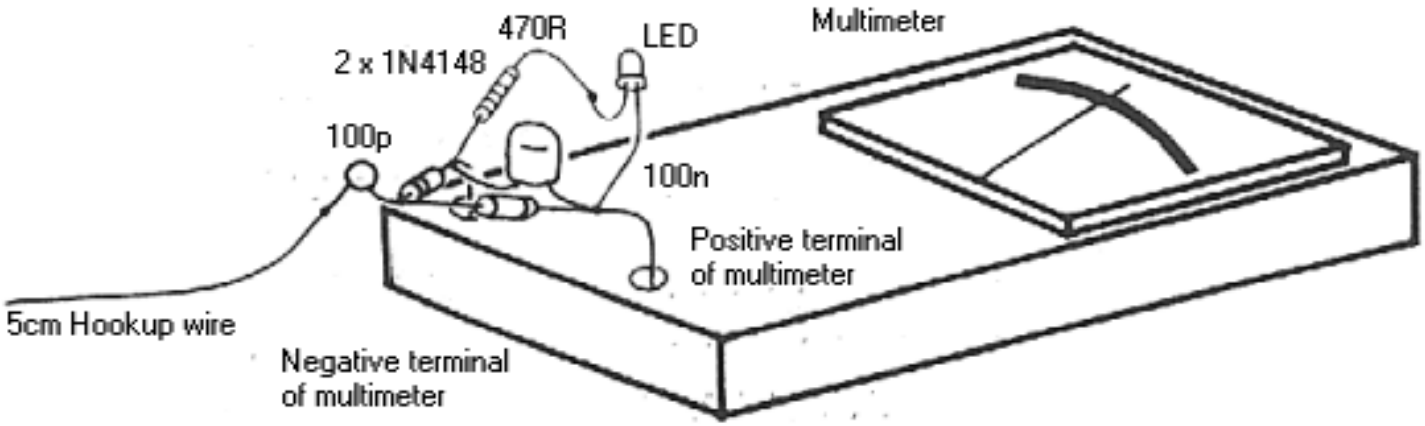

2N3904
NPN General Purpose Amplifier

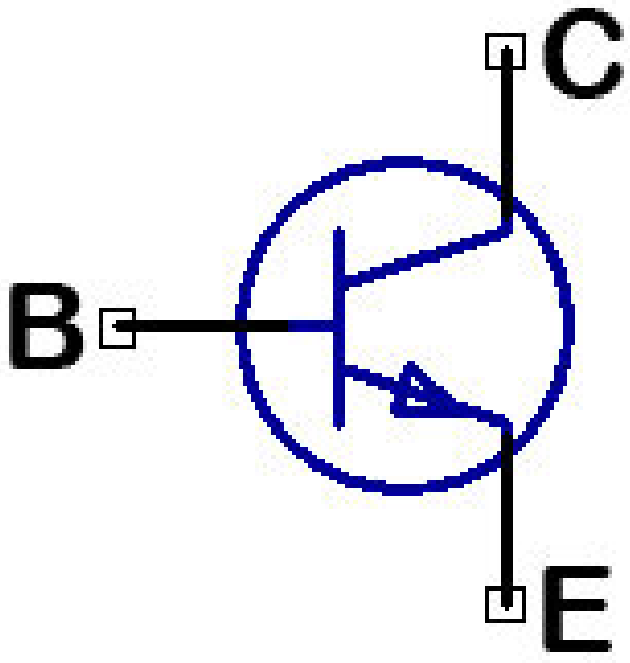

E = EMITTER
C = COLLECTOR
B = BASE


www.electronicecircuits.com

previous next image 1 of 2 Radio frequency LED Output Indicator Circuit close

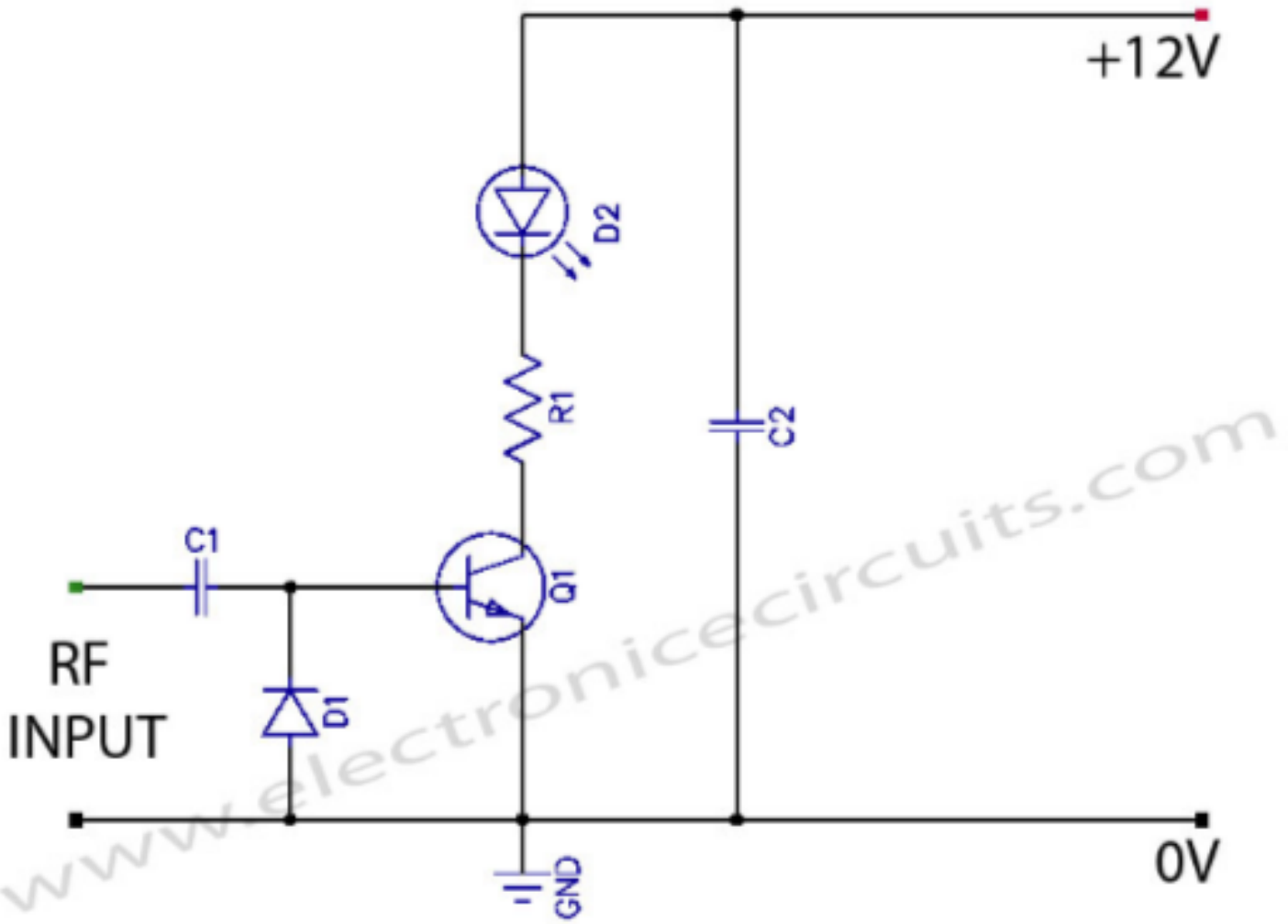

PARTS LIST	
R1	560Ω
C1	330pF
C2	0.1µF
D1	1N34 or 1N60 or ECG-109 or NET-109
D2	LED
Q1	2N3904

Parts Required:

1. 100nF & 100pF
2. n4148 Diode x(2)
3. A bright good quality LED

Circuit Diagram:

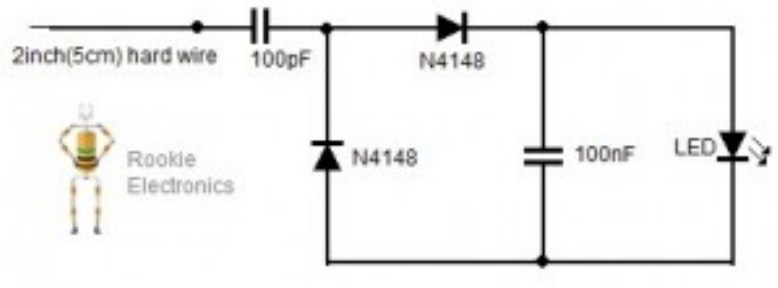

Bread board Arrangement:

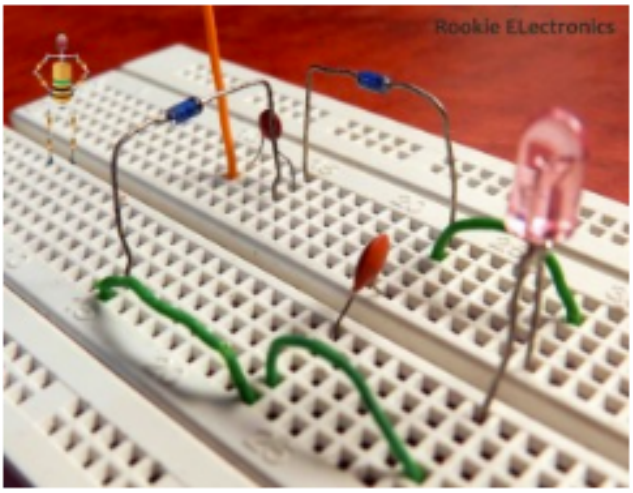

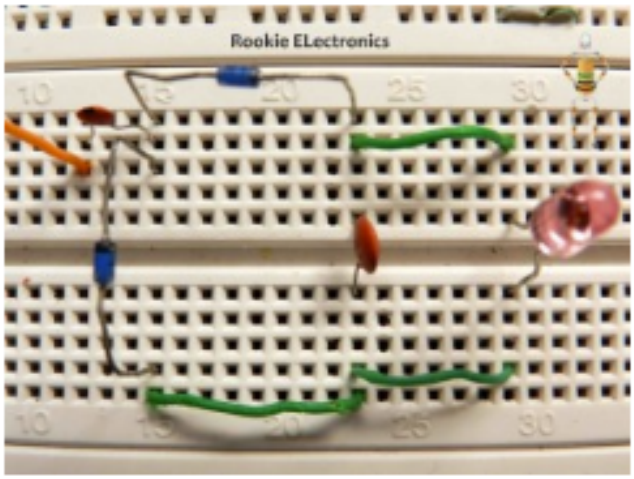

Strip Board:

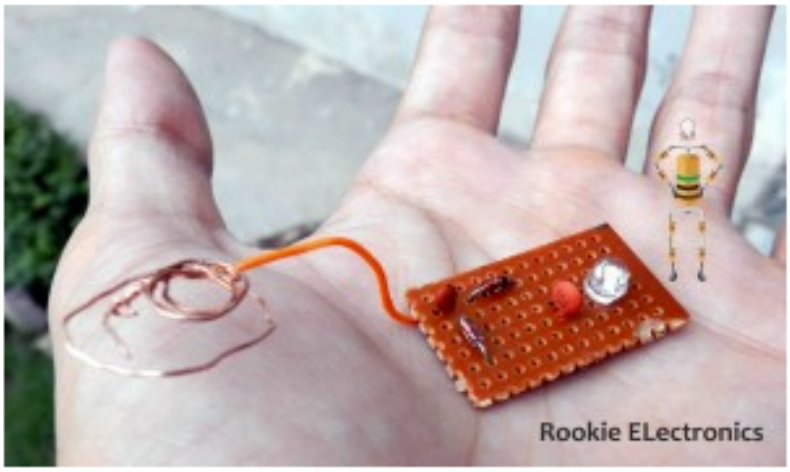

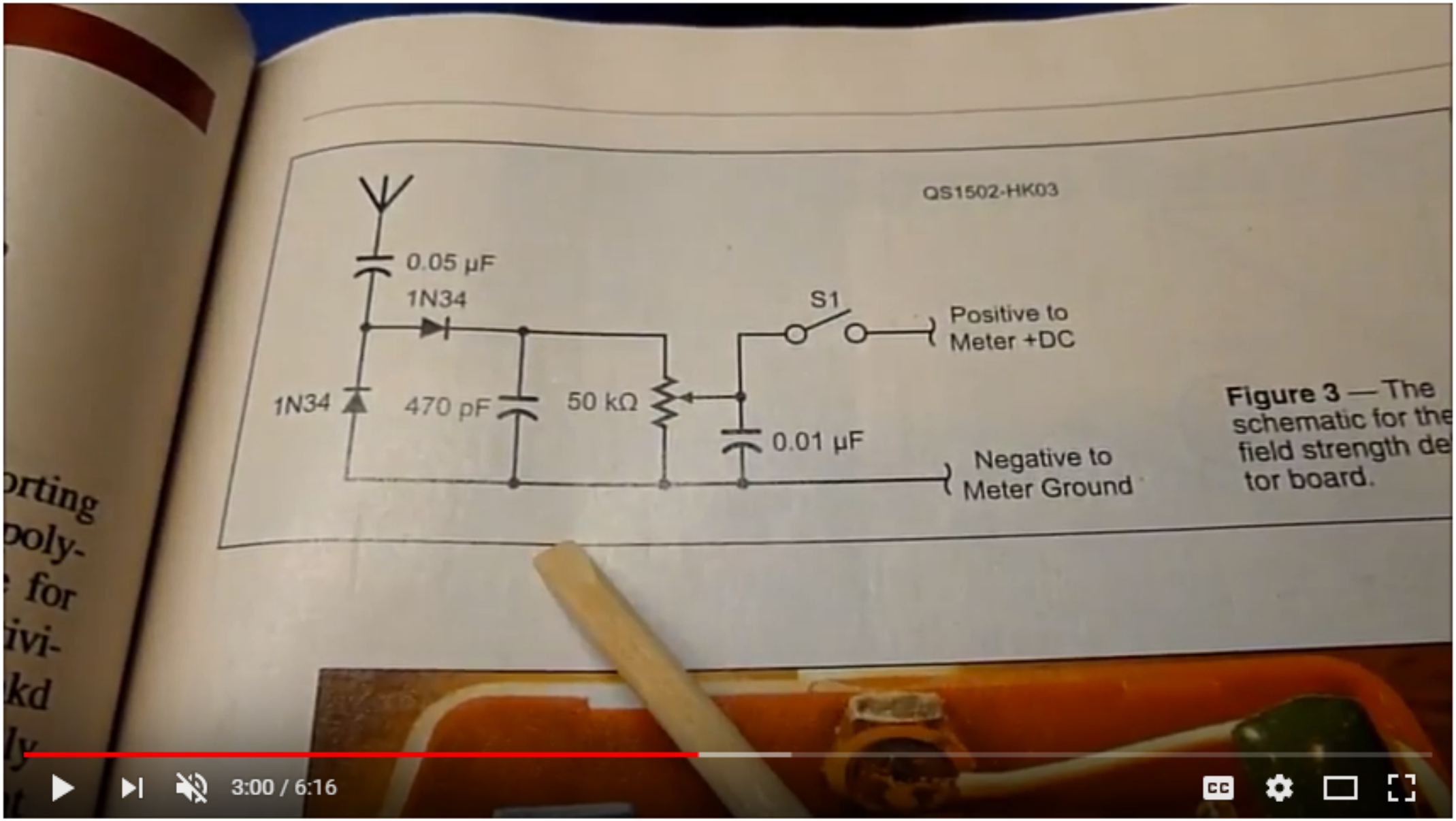

#007: Field Strength Meter

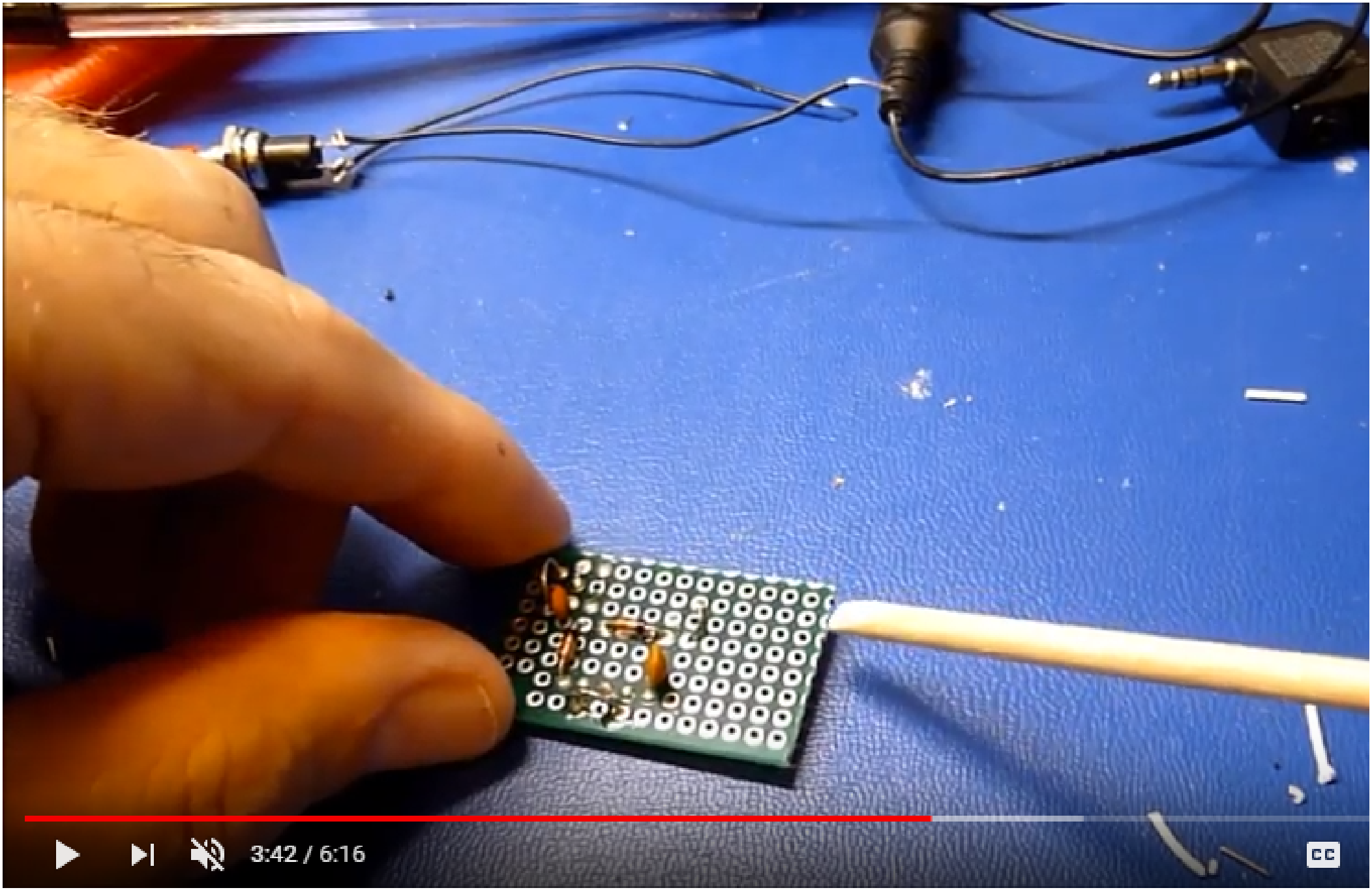

#007: Field Strength Meter

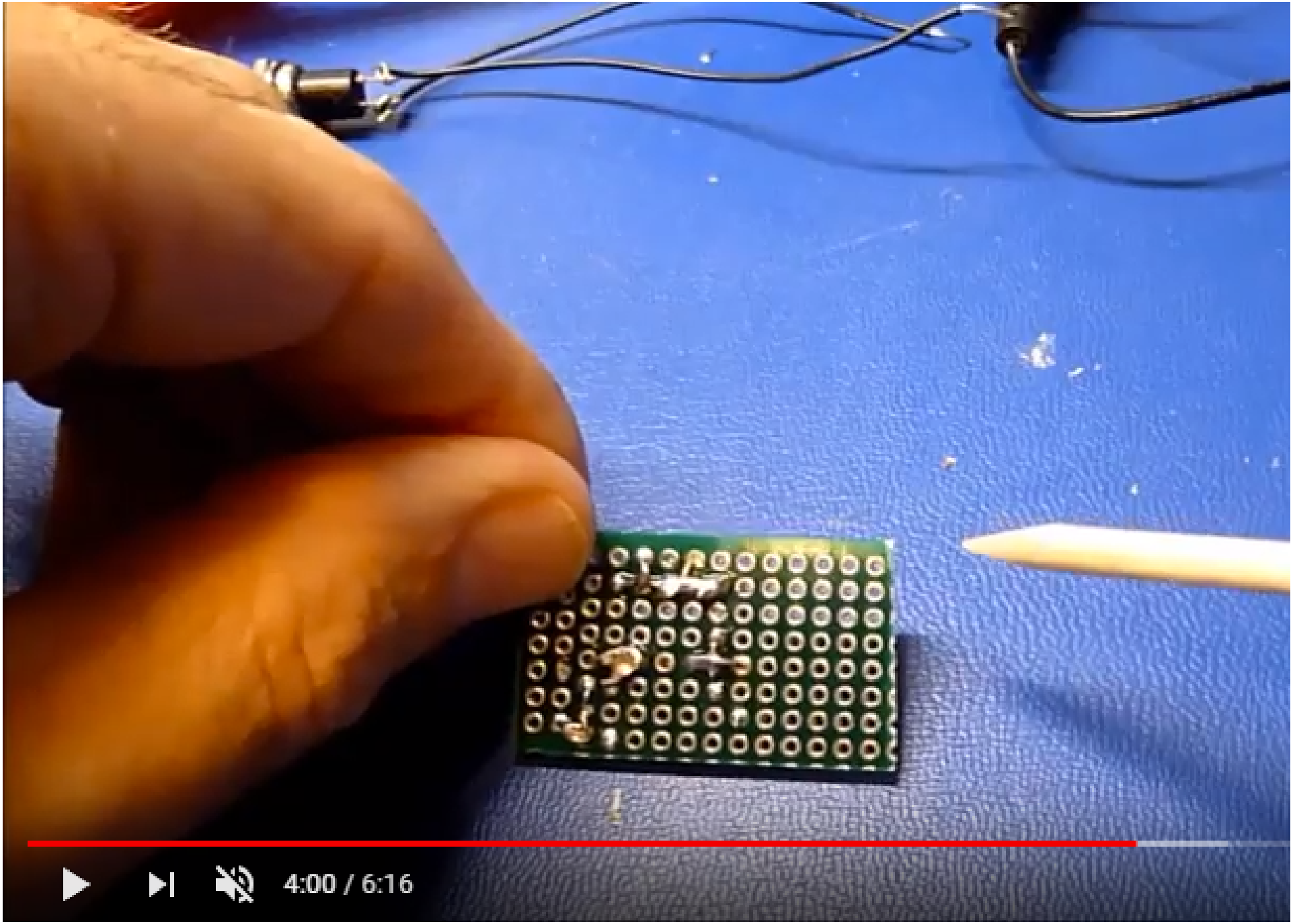

#007: Field Strength Meter

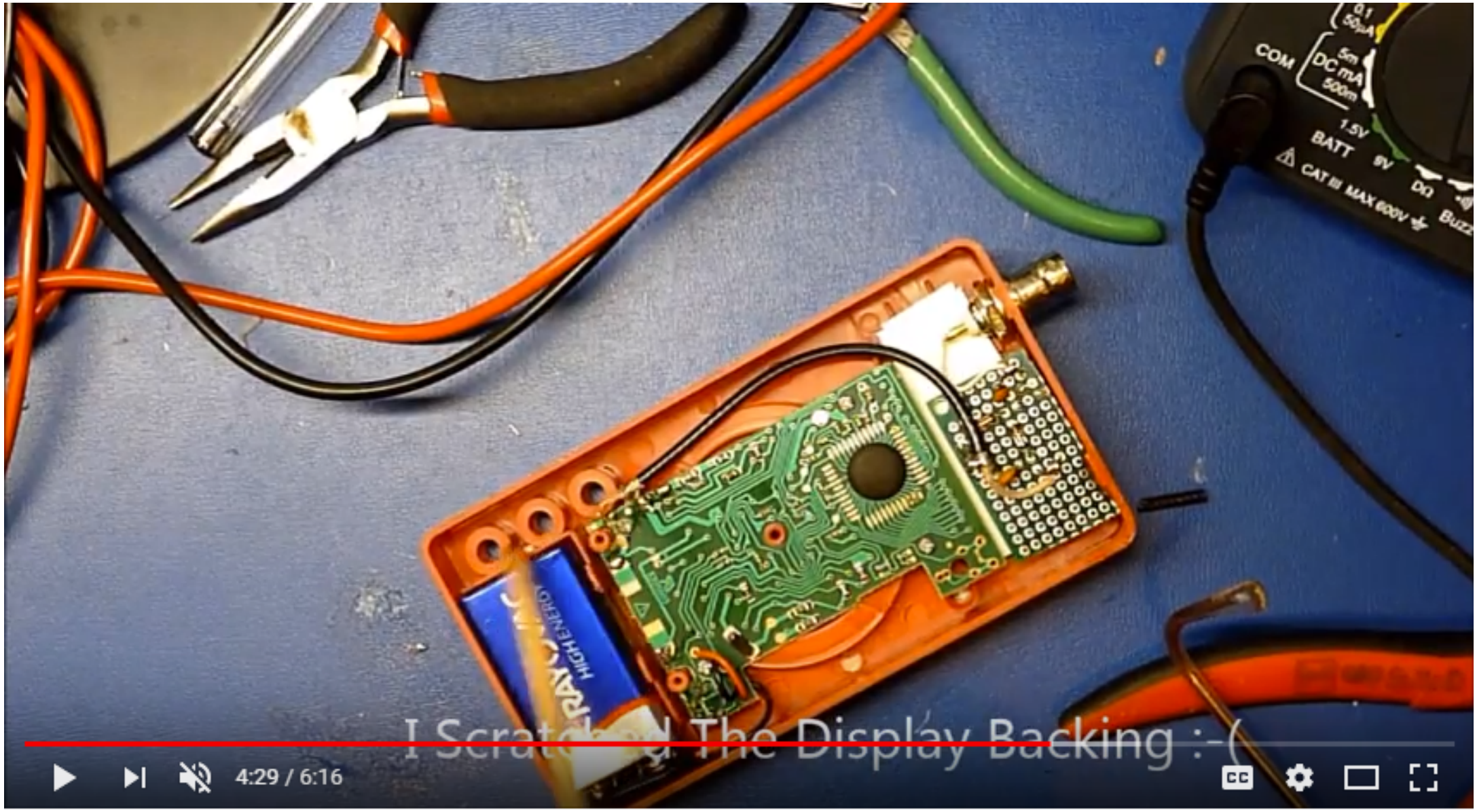

#007: Field Strength Meter

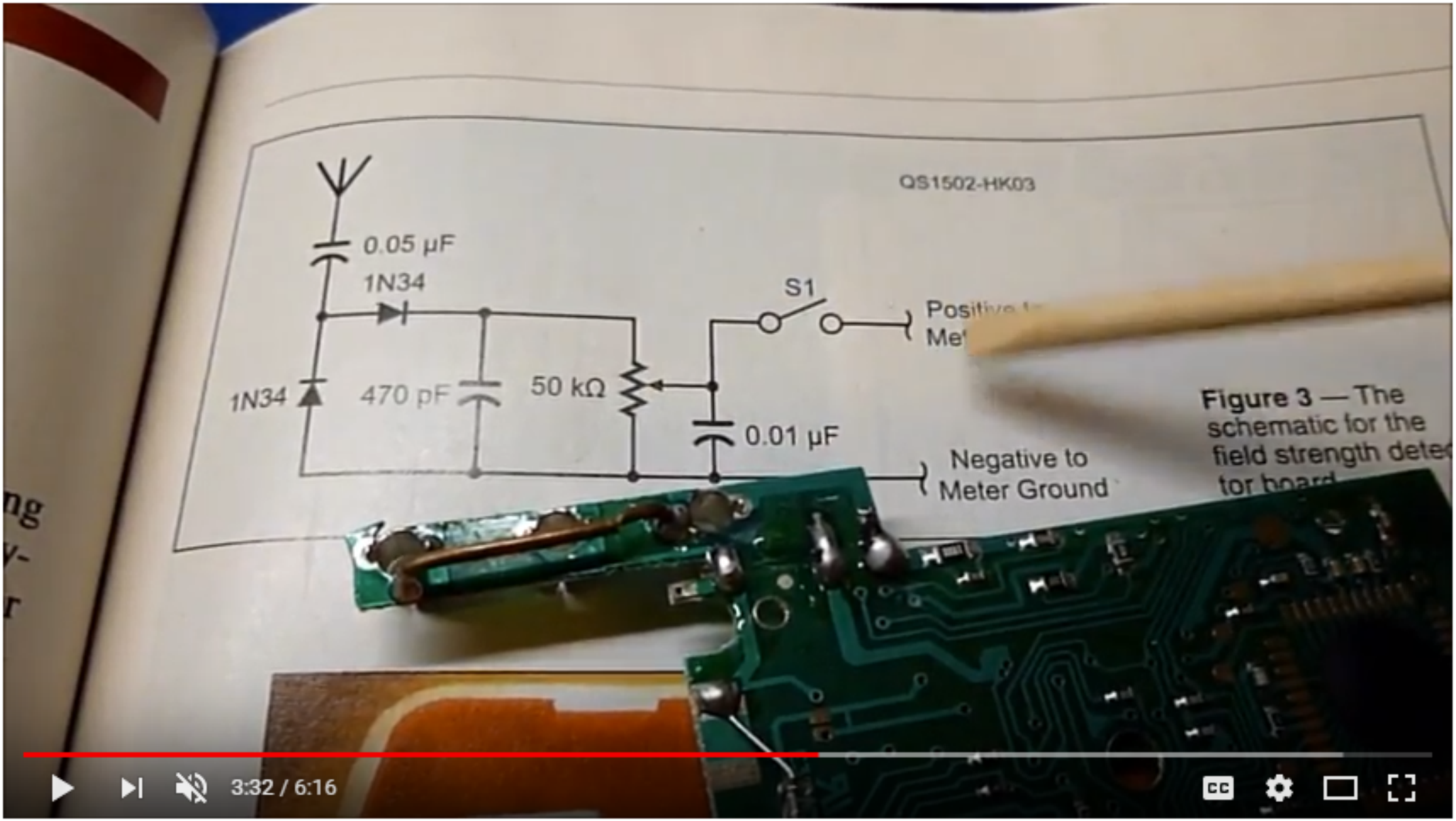

#007: Field Strength Meter

#007: Field Strength Meter

Specifications

Frequency	45-450 Hz
DC Amps	Ranges: 200µA/2000µA/20mA/200mA, 10A
Accuracy	(@200µA-200mA) 1.2%±2D; (@10A) 3%±2D
DC Voltage	Ranges: 200mV/2000mV/20/200/1000V
Accuracy	(@200mV) 0.5%±1D; (@2000mV-200V) 1.0%±1D; (@1000V) 1.0%±2D
AC Voltage	Ranges: 200/750V
Accuracy	(45-450 Hz) 1.2%±10D
Resistance	Ranges: 200/2000/20K/200K/2000K Ohm
Accuracy	(@200-200K Ohm) 0.8%±2D; (@2000K Ohm) 1.0%±2D;
Sampling Rate	2.5 times/Second
Overload Protection	Fast-Acting 500mA/250V Fuse
Operating Temperature	Range: 32° - 104° F
Display	1/2" high 3-1/2-digit LCD
Battery	One 9 V (included)
Weight	.45 lb.
Features	29-1/2" Test Leads; Transistor (NPN and PNP) Testing Function; Battery Testing Function; and Automatic Polarity and Zero Adjust

#007: Field Strength Meter

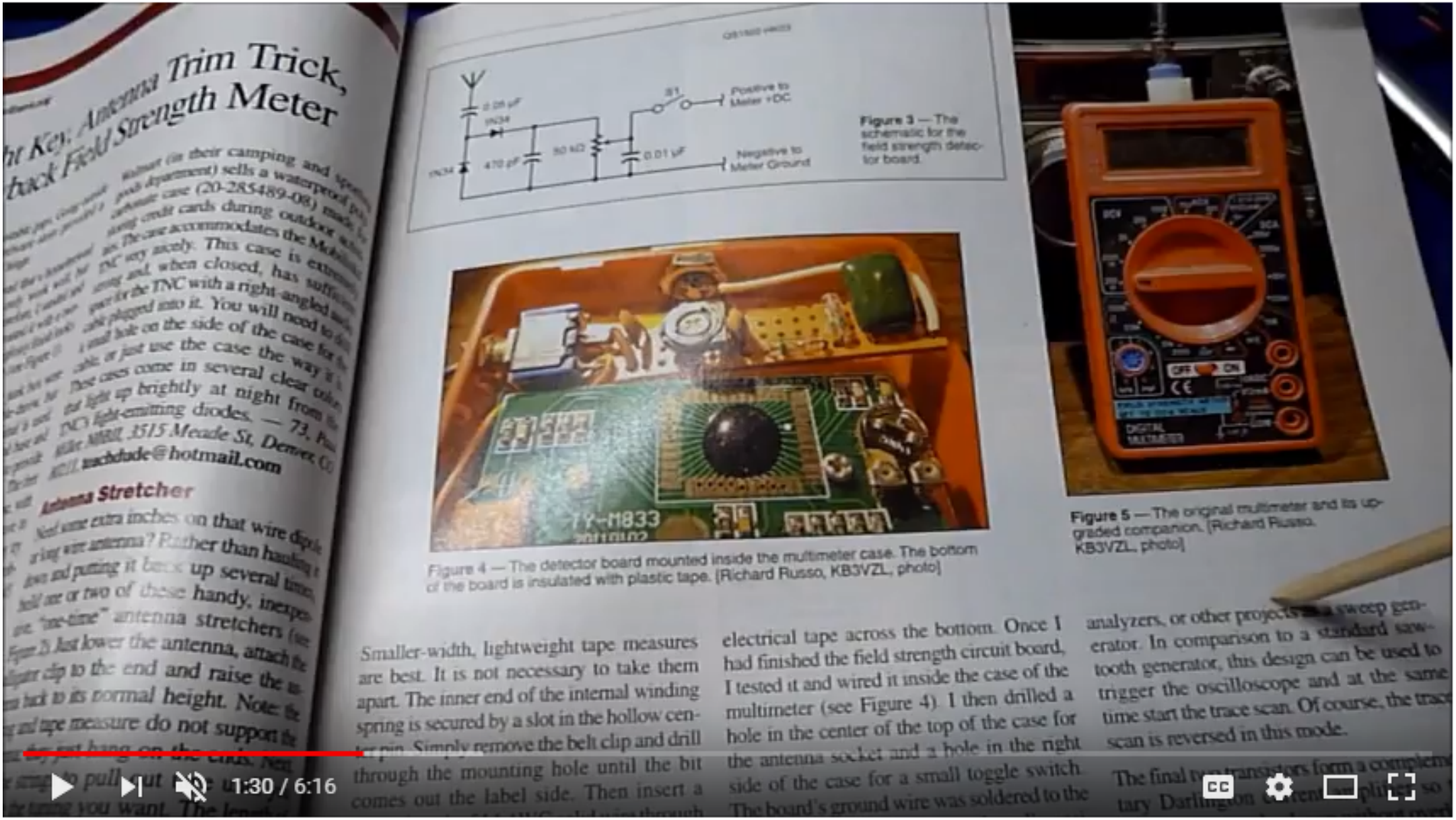

#007: Field Strength Meter

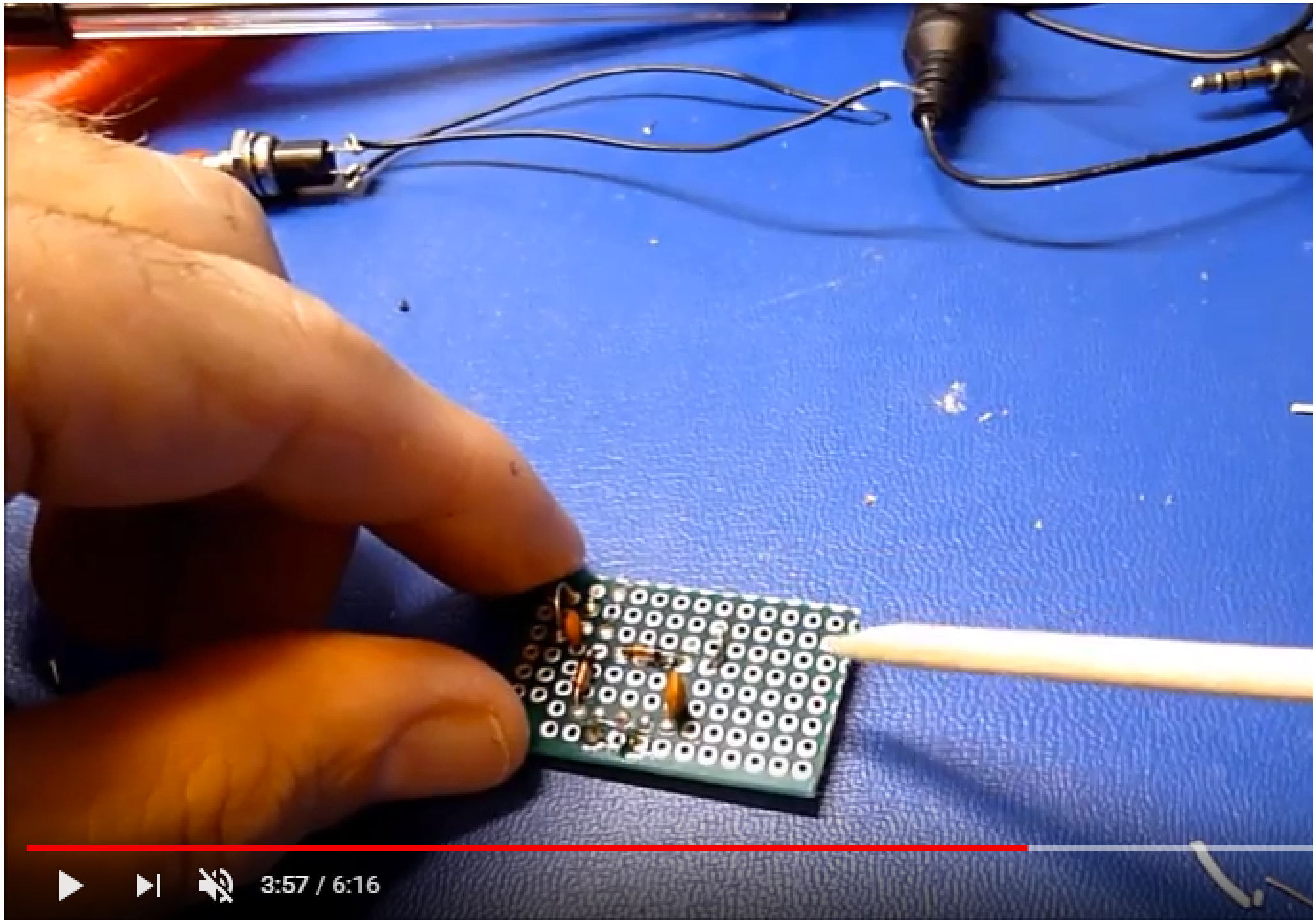
3:57 / 6:16

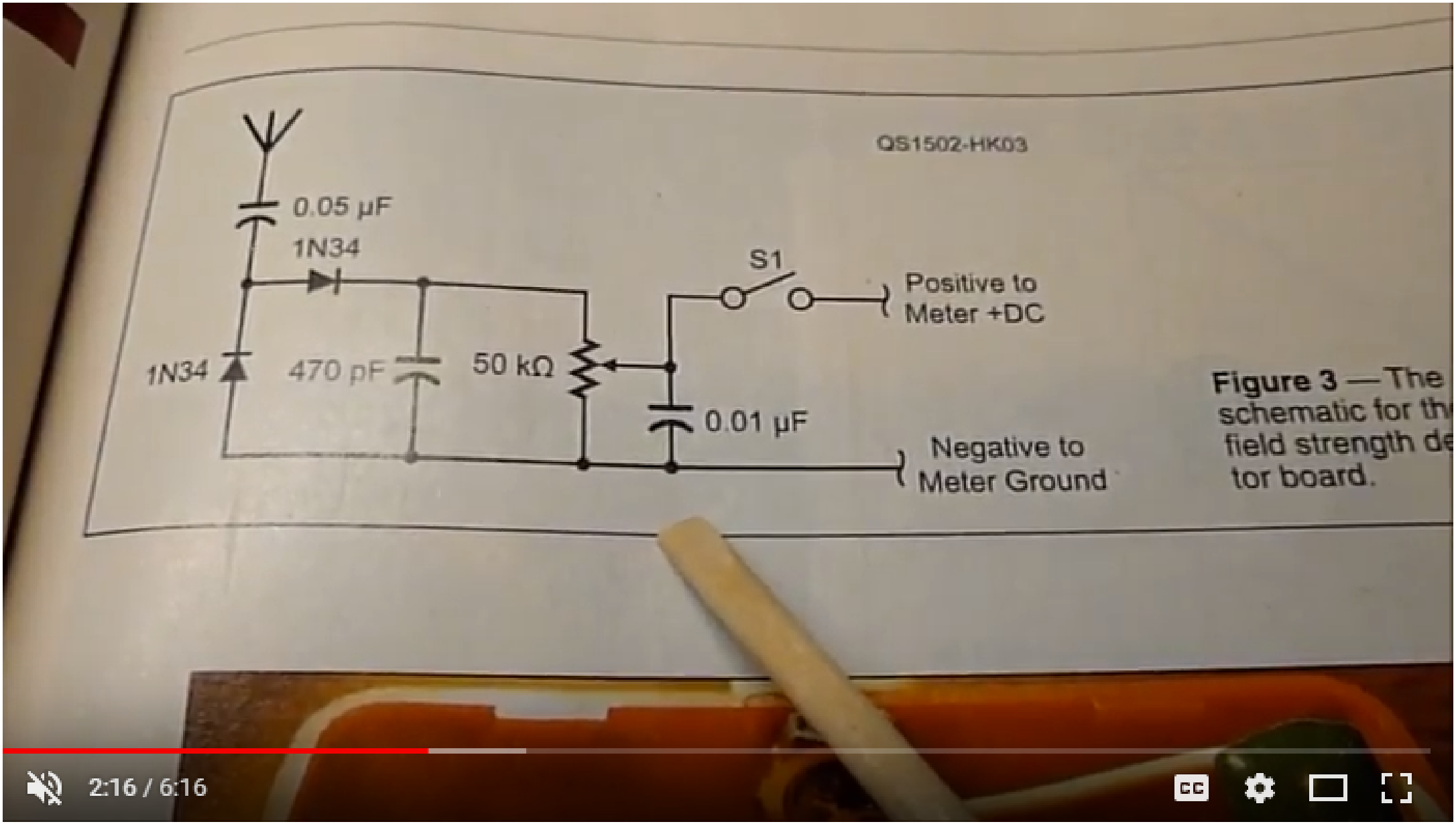
QS1502-HK03
0.05 µF
1N34
S1
Positive to
Meter +DC
1N34
470 pF
50 kΩ
0.01 µF
Negative to
Meter Ground
Figure 3 — The
schematic for th
field strength de
tor board.
2:16 / 6:16

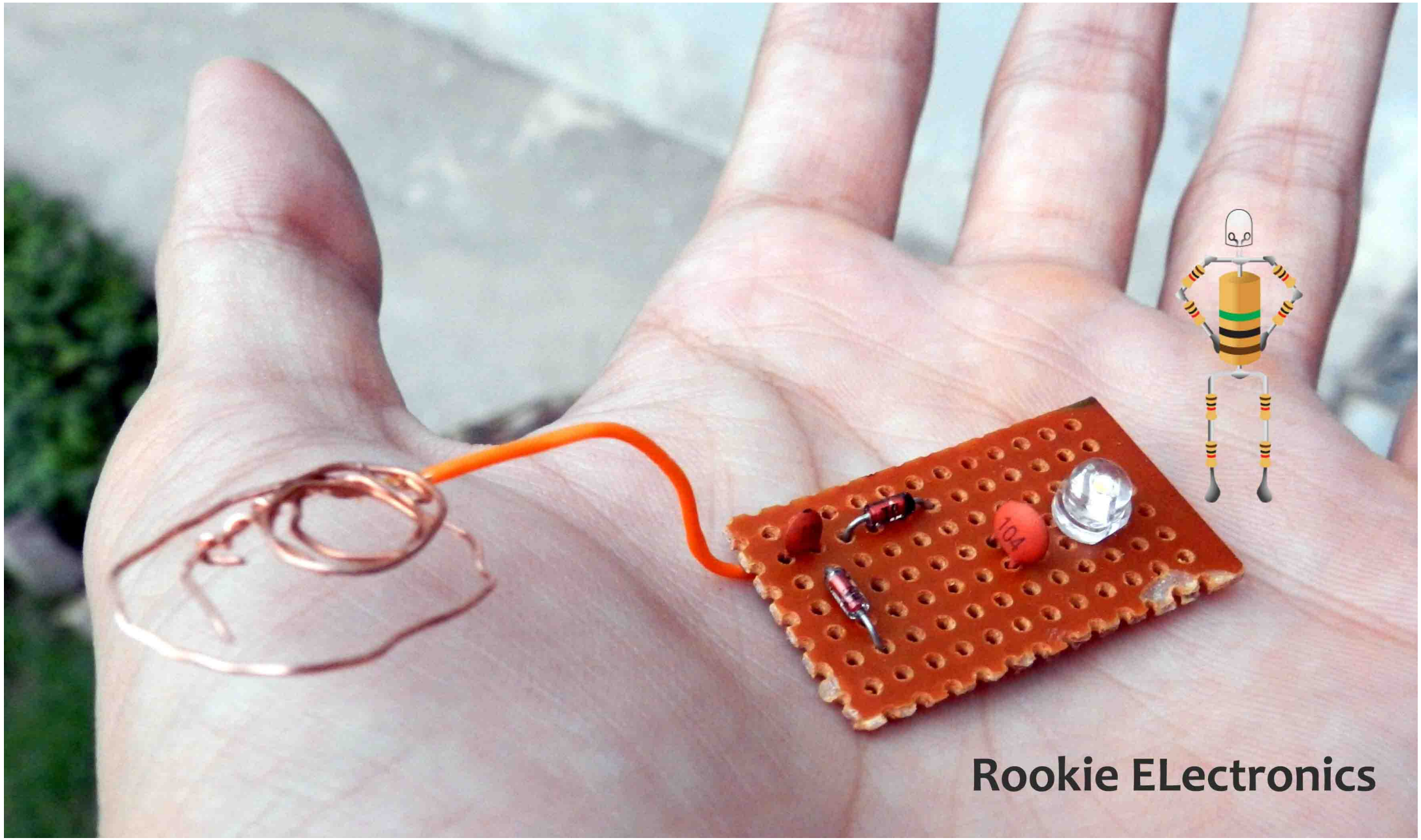
104
Rookie ELectronics

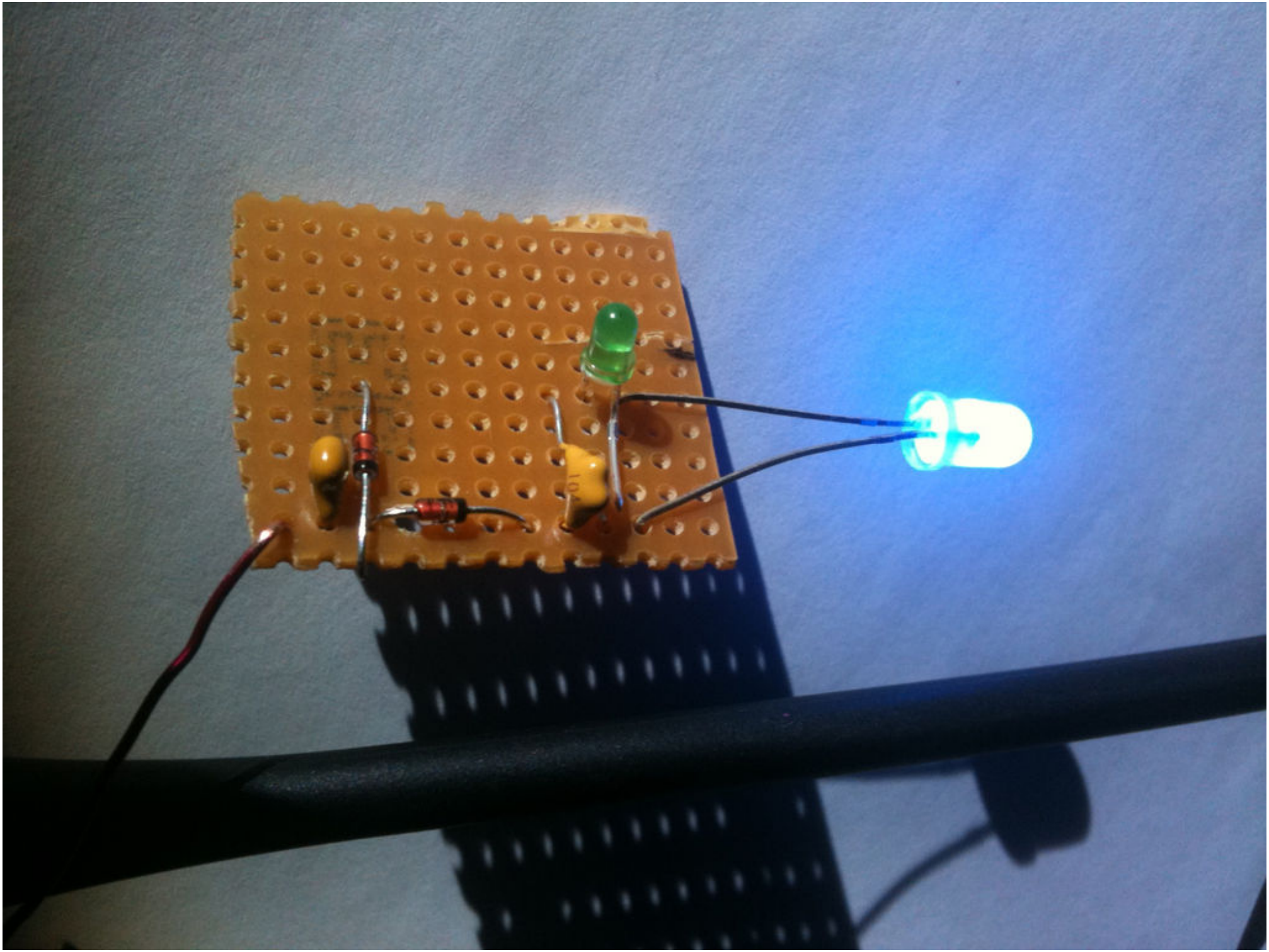

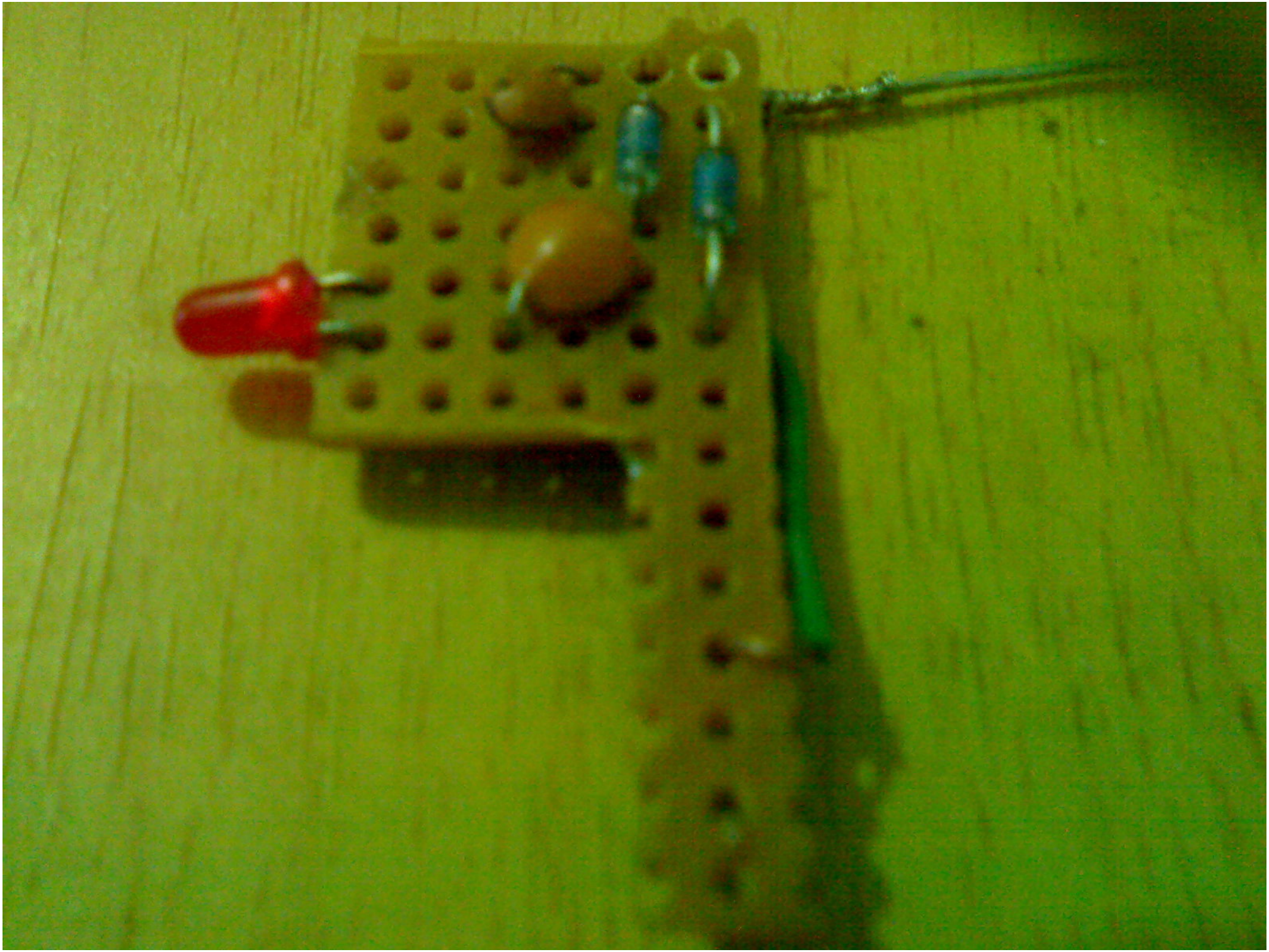

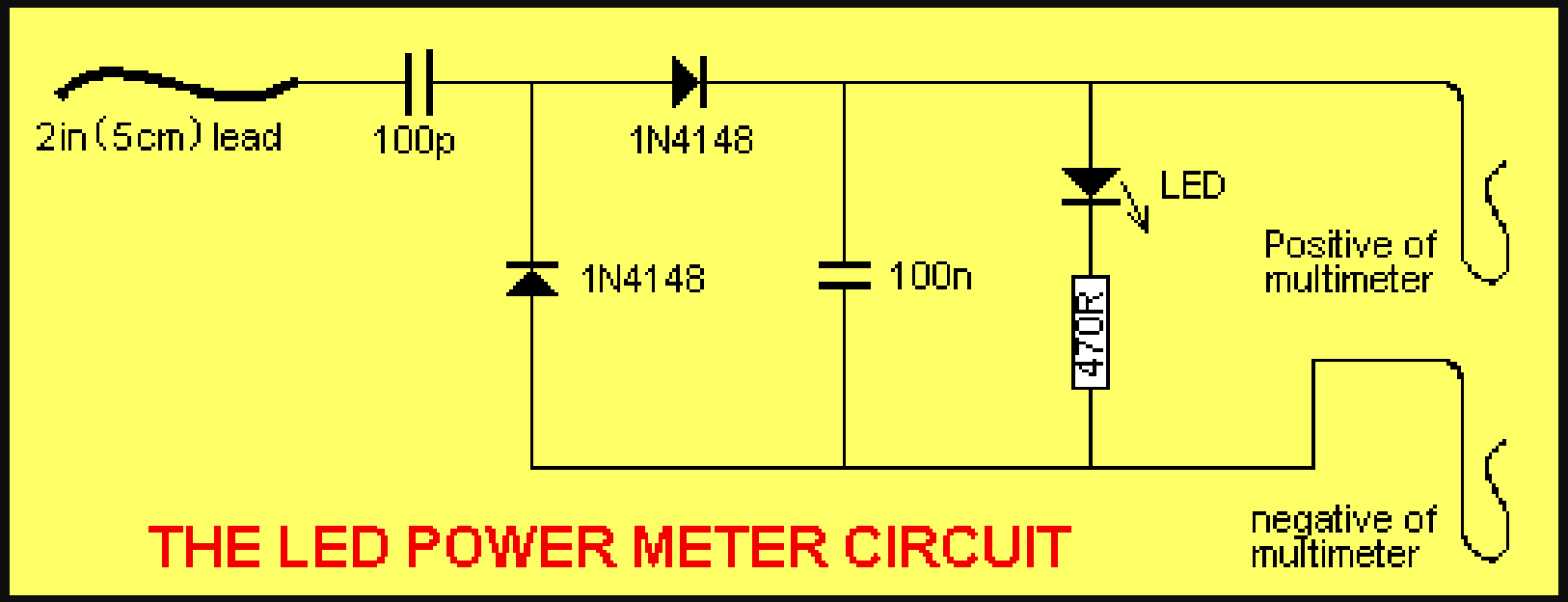
2in (5cm) lead
100p
1N4148
LED
1N4148
100n
470R
Positive of multimeter
negative of multimeter
THE LED POWER METER CIRCUIT

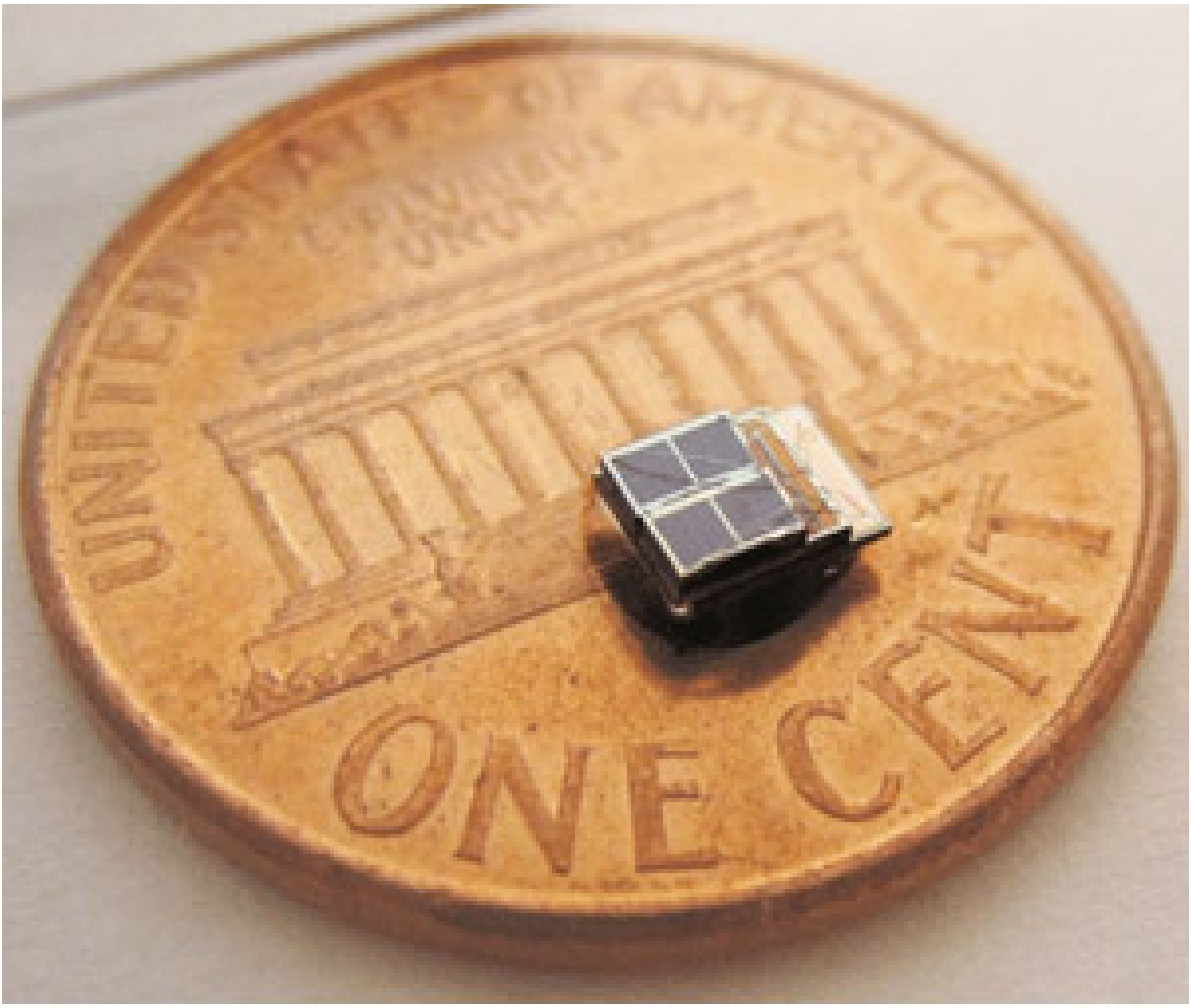

Figure 1. A Cymbet EnerChip placed on a penny shows the relative size of the energy-storage and -management circuits available now for energy-harvesting devices.

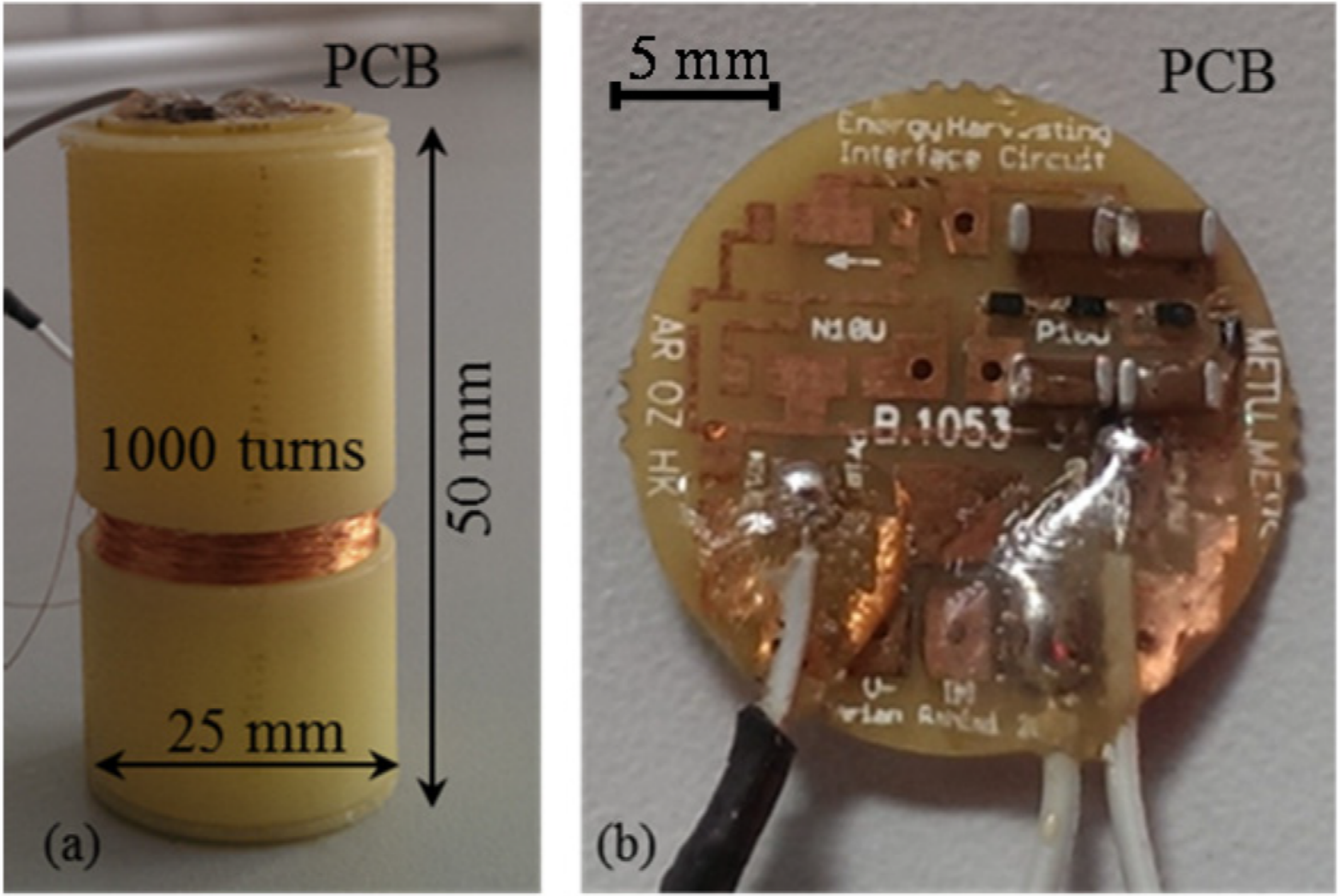
PCB
1000 turns
50 mm
25 mm
(a)
5 mm
PCB
Energy Harvesting
Interface Circuit
B.1053
(b)

metamaterial devices and applications

back to focus areas ↘

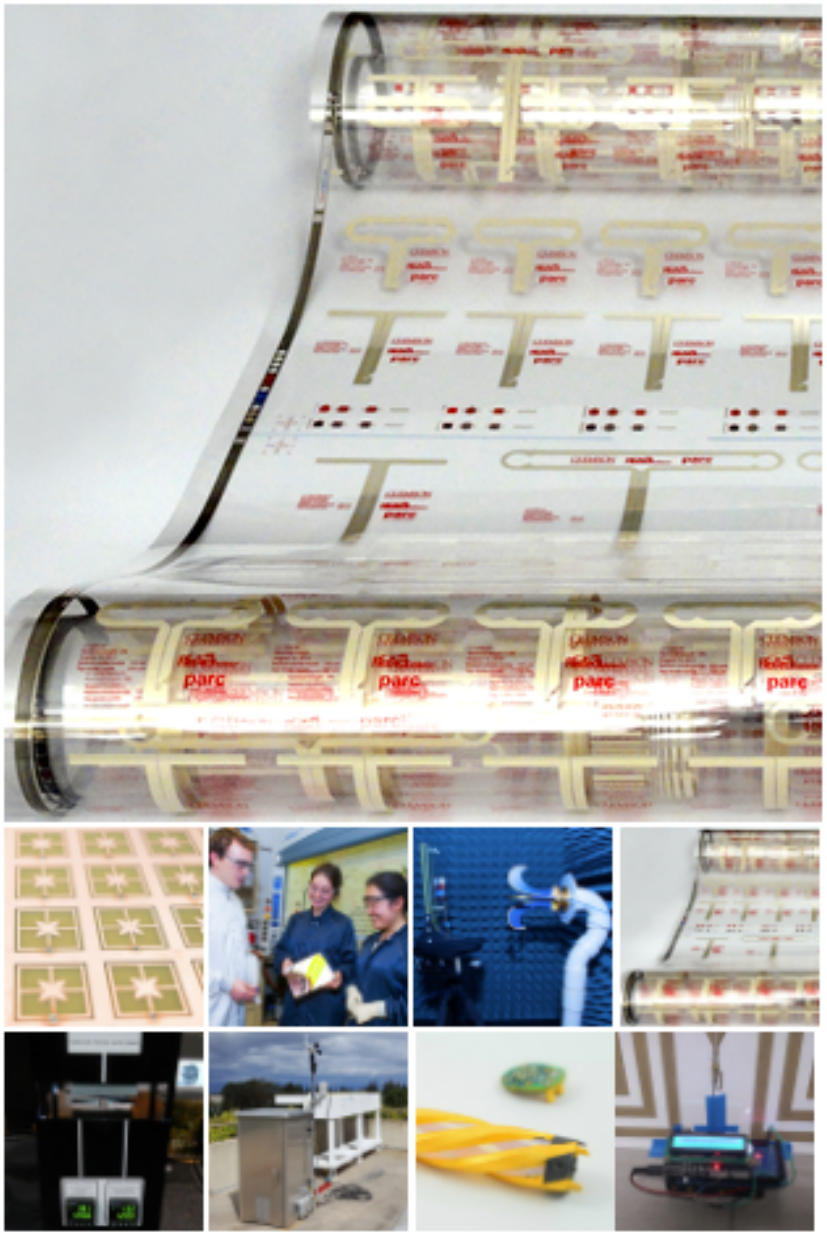

Accelerating innovation by leveraging metamaterials

Metamaterials (i.e., engineered electromagnetic structures), are poised to disrupt industries, create entirely new markets, and change society. The ability to design and fabricate materials with new functionalities opens the door to a new world of possibilities — it is now possible to realize Harry Potter's invisibility cloak and optical black holes, which we once thought was impossible. Beyond the realms of science fiction, metamaterials can be tailored to either augment the functionality of existing devices or create new devices with superior performances.

PARC has been developing a broad array of exciting and impactful metamaterial technology platforms. Today, the metamaterials team is engaged in developing passive radiative cooling (self-cooling films) for buildings and power plant cooling; electronically scanned array platform for drones and self-driving cars; smart metamaterial antennas for 5G networks and satellites; metasurfaces for molding the flow of light; thermal barriers for energy-efficient single pane windows; RF energy harvesting platform for IoT; peripheral nerves/brain focused magnetic stimulation (FMS) technologies; thermophotovoltaics devices; multispectral imaging chemical sensor; defense applications; and a state-of-the-art computational electromagnetics simulation platform.

***Top row** (left to right): Metamaterial electronically scanned array (MESA); Researchers in the lab; Snapshot of the state-of-the-art applied electromagnetic lab; printed metamaterials RF energy harvesters.*
***Bottom row** (left to right): Demonstration of passive radiative cooling indoor; Rooftop measurements setup at PARC; Antennas for cubesats; Arduino device interacting with metamaterial antennas.*

Key Technology Platforms

Metamaterials Electronically Scanned Array (MESA)

A low-cost, high-performance RF beam steering module that can be adapted for a broad range of applications, including: collision avoidance system for self-driving cars or drones, broadband satellite internet/radio, hypothermia treatment, wireless communications, etc. The key performance feature of PARC's MESA is its capability to maintain a high signal-to-noise ratio and high-resolution, simultaneously.

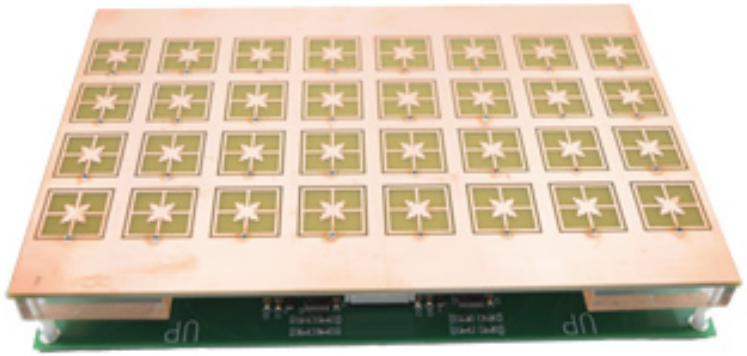

Smart Metamaterial Antennas

Highly reconfigurable metamaterial antennas are a natural evolution of the MESA architecture. They are tailored for 4G LTE/5G bay stations and for satellite communications.

RF Energy Harvesting Platform

An RF energy harvesting platform that converts Wi-Fi and other RF bands to electricity, to power IoT sensors. It consists of a metamaterial-inspired antenna and a custom rectifying circuit. There are two classes of prototypes that we have demonstrated: hybrid (printed antenna with integrated silicon chips) and all-printed devices. The performance and bandwidth of the RF energy harvesters exceed by at least an order of magnitude that of the state of the art.

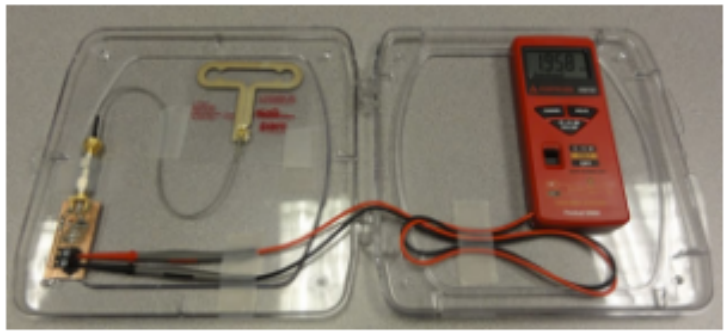

Focus Magnetic Stimulation (FMS)

In FMS, the magnetic fields are dynamically shaped by injecting phase and amplitude-controlled currents in an array of three-dimensional micron-scale coils. The FMS scheme enables more localized stimulation (enhanced focusing), better depth control, and complex stimulation patterns (beamshaping and beamsteering), as compared to current magnetic/electric stimulation methods. Tailored stimulations can be obtained with appropriate coil array designs, by selecting the optimal number of elements, array configuration, driving circuits, and current distribution in the coils.

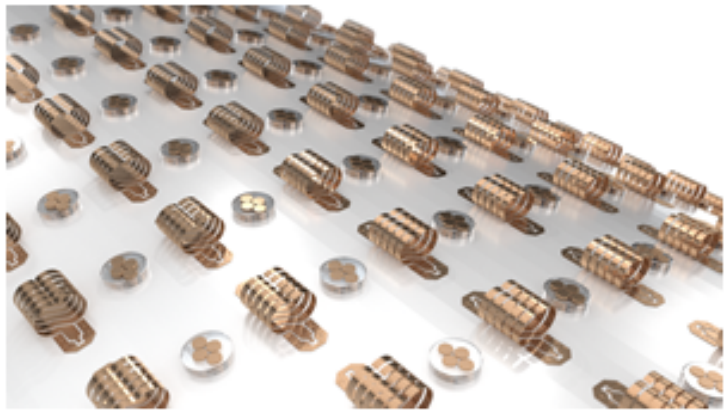

The w
BMW
team,
Autor
the w
consu

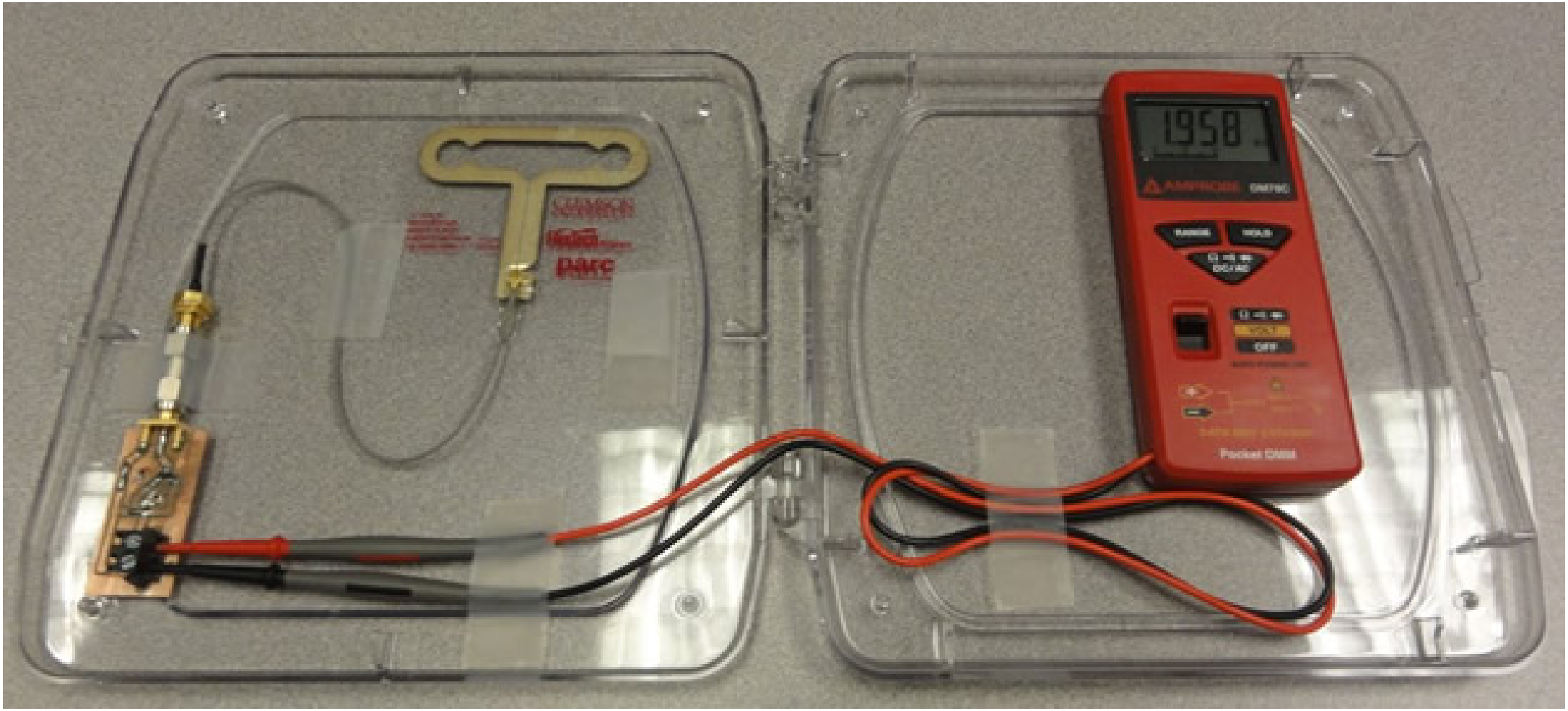
1958
Pocket DMM

3. RF/Microwave Circuits, Components, and Systems

Our research in this field covers the following topics: Design of compact, broadband, and multi-band passive components; Microwave power amplifiers such as Doherty power amplifiers; High power and high performance microwave filters/multiplexers for satellite and base-station applications; Compact, tunable, reconfigurable, and multi-band microwave filters design; Synthesis of advanced filter networks.

3.1 High-power, Compact, Tunable and Reconfigurable Microwave Filters / Multiplexers: Microwave bandpass filters / multiplexers are the key components for the modern RF/microwave systems. They provide the isolations between the receiver and the transmitter circuits, which enables the integrations of these two systems in one chip. Throughout Hualiang's research, he had design microwave filters and multiplexers (e.g. duplexers, triplexers) with high-power handling, high selectivity, compact size, tunability and reconfigurability.

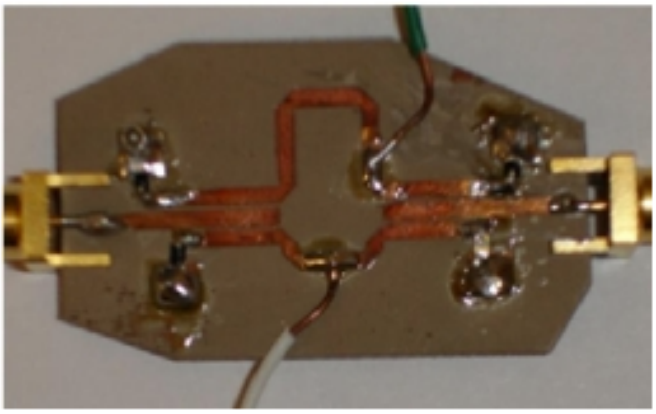

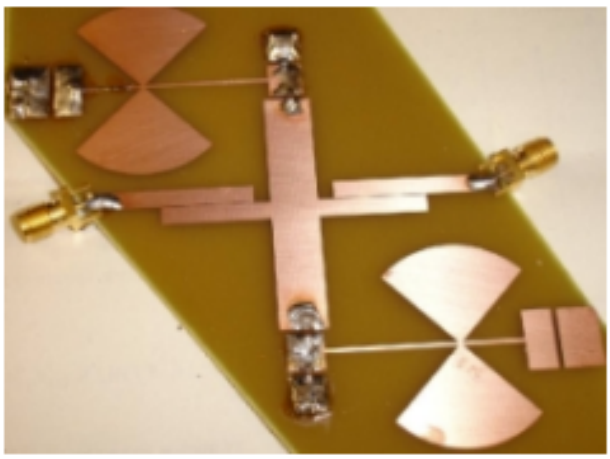

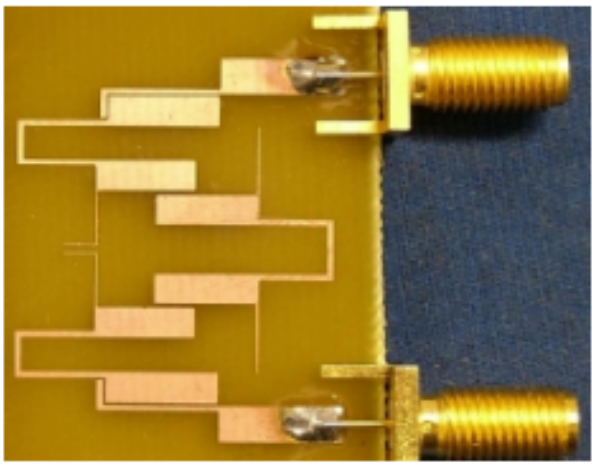

3.2 Multi-Functional RF / Microwave Circuits: Rapid developments in modern communication systems have imposed requirements such as wide bandwidth, small size and multi-band operation for RF / microwave components. Among them, the multi-band operation is of special interest. Normally, to support multi-band operations, multiple sets of single band circuits were needed, which were large in size and expensive in cost. Alternatively, by replacing the original bulky circuits with the multi-band circuits, both the size and the cost of the whole system could be reduced, which is attractive.

3.2 Multi-Functional RF / Microwave Circuits: Rapid developments in modern communication systems have imposed requirements such as wide bandwidth, small size and multi-band operation for RF / microwave components. Among them, the multi-band operation is of special interest. Normally, to support multi-band operations, multiple sets of single band circuits were needed, which were large in size and expensive in cost. Alternatively, by replacing the original bulky circuits with the multi-band circuits, both the size and the cost of the whole system could be reduced, which is attractive.

To achieve the multi-band operation of the RF / microwave system, various microwave components need to be re-designed. Different topologies and design theories need to be developed for this purpose. So far, our effort in this area has led to several new designs of microwave baluns, couplers and Wilkinson power dividers, all of which are essential components in the microwave systems. In the future, we are going to design microwave power amplifiers for dual-band operation.

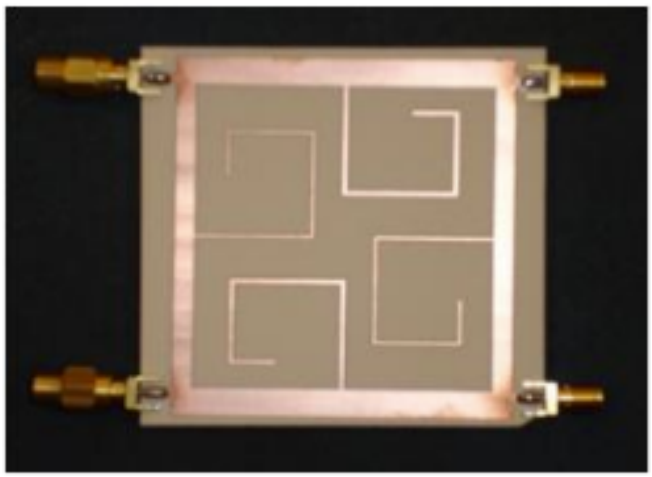

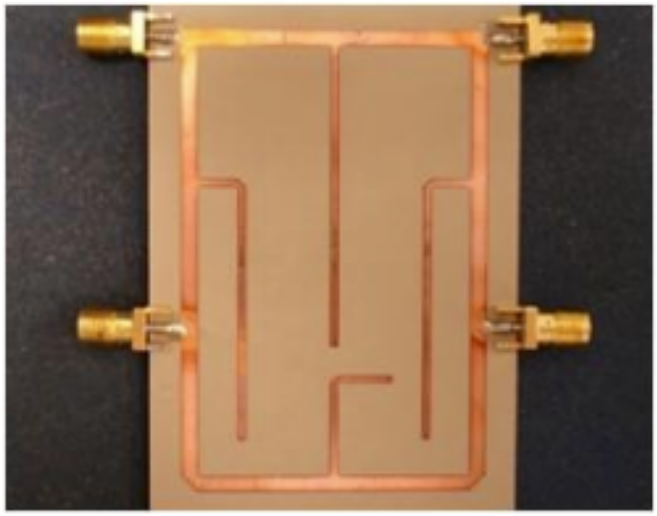

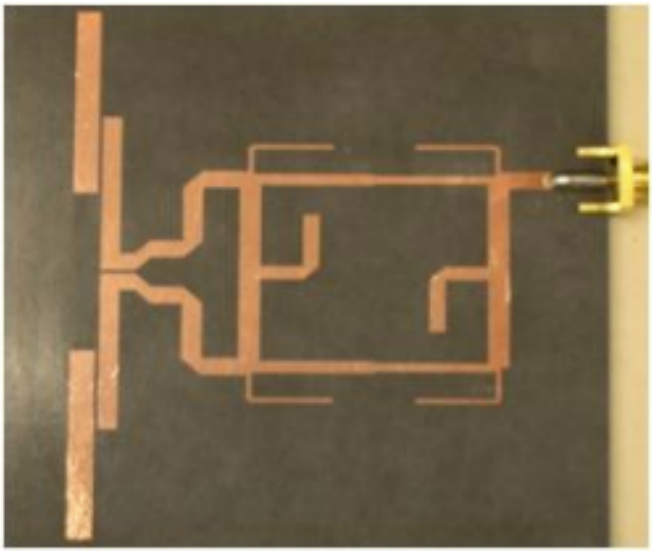

3.3 Broadband Doherty Power Amplifiers and Other Microwave Systems

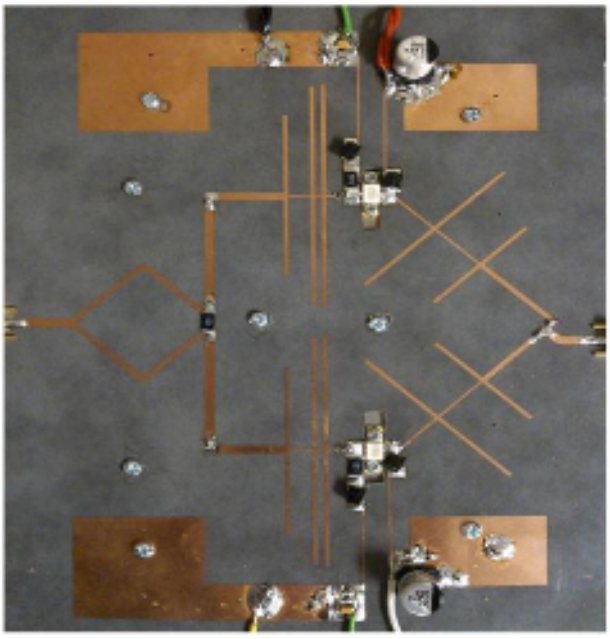

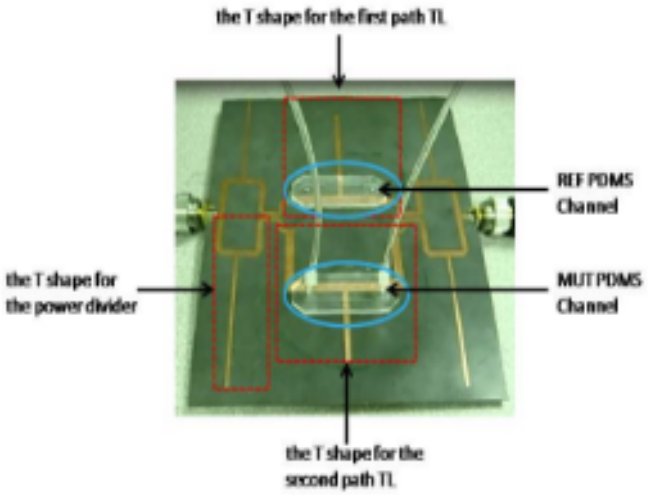

4. Antennas

Antenna as an imperative component for wireless communication system is very important. It exists in every wireless modules. According to different systems, antennas with different characteristics are required. Our research in this field has focused on the following topics: Phased-array antennas and their applications; Beam-forming networks; Reconfigurable UWB antennas; Conformal antennas; Electrically small antenna.

UWB and On-Chip Antennas

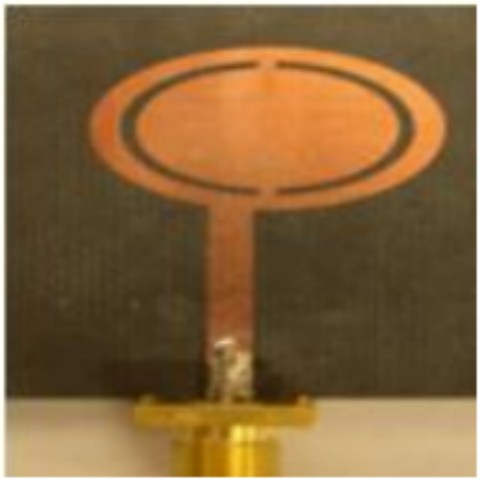

Dual-Band Beam-Forming Networks and Antenna Arrays

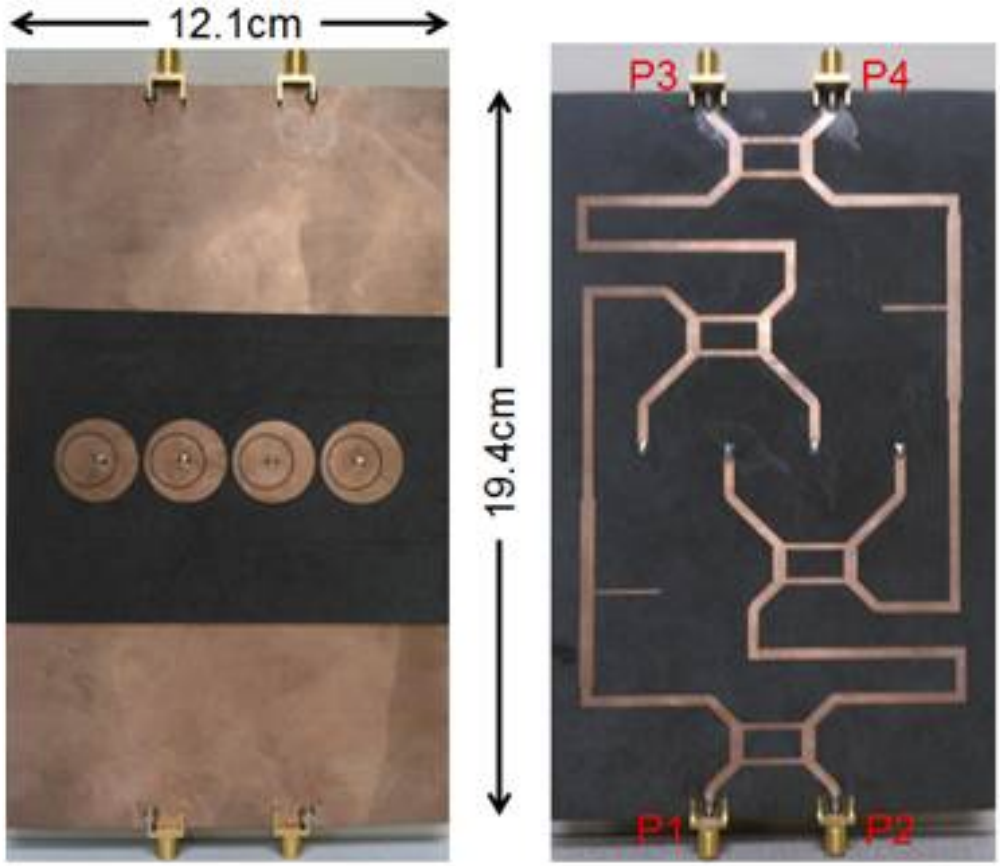

5. Transformation Optics-Based Electromagnetic Devices

Transformation optics (TO) is an emerging research and engineering field that addresses the inverse engineering problem of electromagnetism with respect to how an engineered structure will perform a requested functionality. It can prescribe the path of electromagnetic waves at will, by controlling the index of refraction as a function of position, potentially to any desired profile . Transformation optics is driven by coordinate transformation and providing a profile of permittivity and permeability together with anisotropy in the transformed media. It allows for the mathematical mapping of desired distortions of space onto an actual distribution of optical material properties in normal Cartesian space. Our research in this field has relied on transformation optics techniques such as coordinate transformation, quasi-conformal mapping, and inverse quasi-conformal mapping.

Cloaking Devices

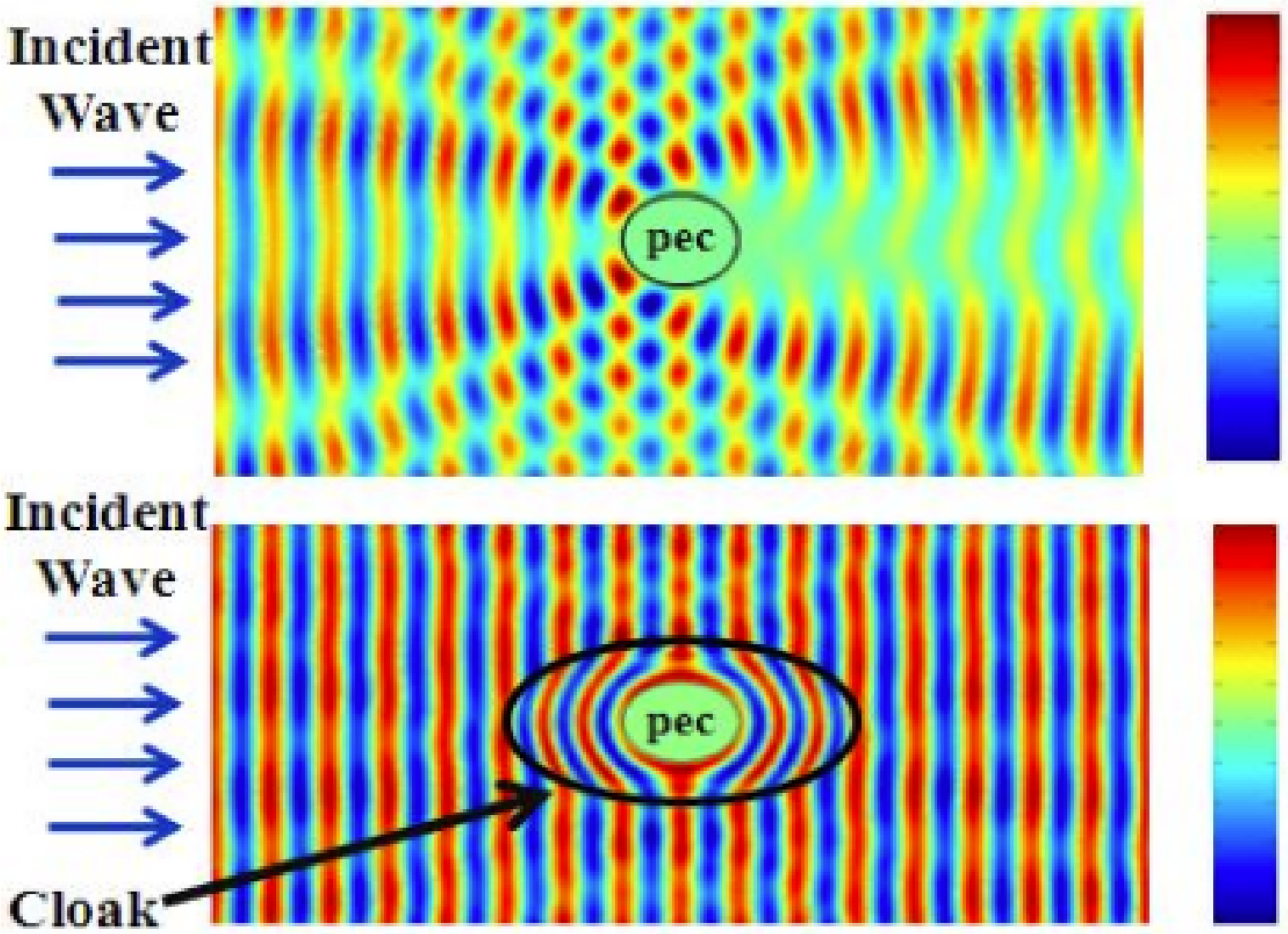

Transformation Optics-Based Reconfigurable SPP Wave Adapter (*Optics Express*, 13789, 2012)

Wireless device converts ‘lost’ microwave energy into electric power

November 8, 2013

Using inexpensive materials configured and tuned to capture microwave signals, researchers at Duke University’s Pratt School of Engineering have designed a power-harvesting device with efficiency similar to that of modern solar panels.

The device wirelessly converts a microwave signal to direct current voltage that is capable of recharging a cell phone battery or other small electronic device.

It operates on a principle similar to that of solar panels, which convert light energy into electrical current. But this versatile energy harvester could be tuned to harvest the signal from other energy sources, including Wi-Fi signals, satellite signals, or even sound signals, the researchers say.

The key to the power harvester lies in its application of metamaterials, engineered structures that can capture various forms of wave energy and tune them for useful applications.

[+]

Prototype power harvester resonant at 900MHz (a GSM cell-phone frequency) (credit: Allen M. Hawkes at al./Applied Physics Letters)

Three-dimensional micro-fabricated microwave and millimeter-wave circuits and antennas

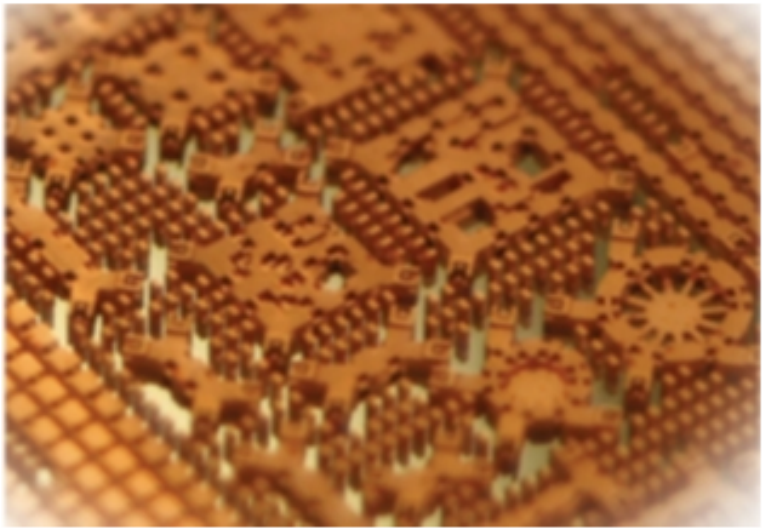

Another active area of research has been in collaboration with Nuvotronics LLC (DAPRA and NASA) in the area of wafer-scale microfabricated coaxial lines and passive and active coaxial-based components. The advantages of these lines, fabricated by Nuvotronics, is extremely low loss into the millimeter-wave range, extremely good isolation of neighboring lines enabling high density circuits, broad bandwidth and low dispersion, and amenability for integration with passive and active surface-mount components. Our research goals are focused on design of completely new components in this technology, in order to push the bandwidth, power handling and flexibility for various communications and sensing applications. Some results include 22:1 bandwidth impedance transformers and 22:1 bandwidth power divider networks which operate up to millimeter-wave frequencies.

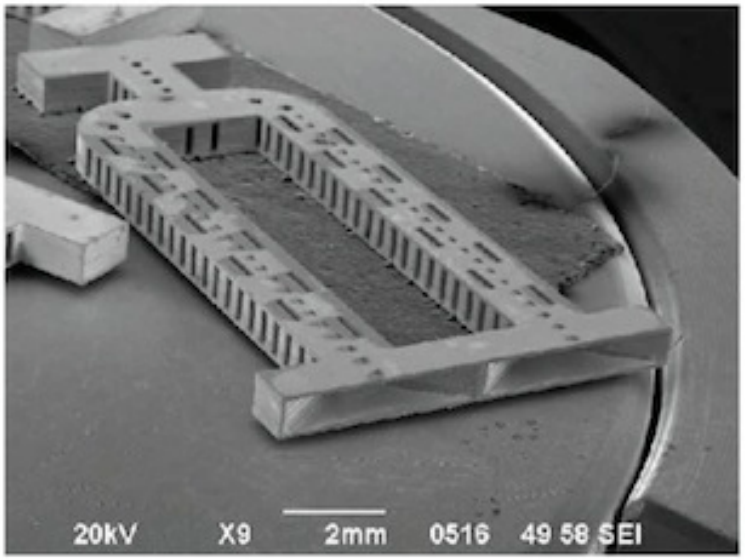

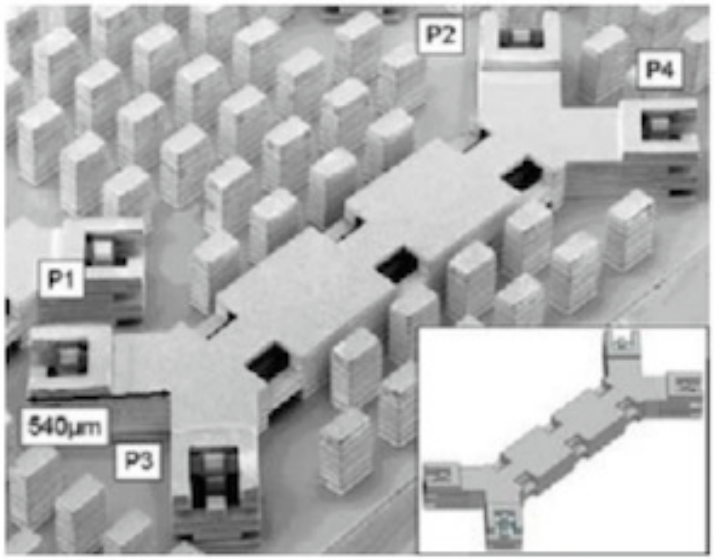

Wireless powering for battery-less sensors

An area in which we have promising initial results, as well as a best paper award, is in RF energy harvesting and wireless powering of wireless sensors. This is an area with a strong collaboration with the Colorado Power Electronics Center (CoPEC), with strengths in low-power management design. The work resulted in a comprehensive patent application and licensing of the IP by several companies, e.g. Cymbet. The applications are for low-maintenance batteryless sensors for manufacturing environments, structural monitoring, and healthcare. We have shown that broadband statistically varying randomly polarized background microwave radiation can be efficiently rectified and the stray energy stored over time for useful electronic applications. We have also shown that FCC-compliant low-power transmitters can be strategically placed to enable constant very low power density energy delivery and storage. Our goals related to this research are to improve the integration of our current hybrid demonstrations, and to expand the circuit-antenna library so that we can address many concrete applications with the best-suited architecture.

- *Reconfigurable antennas*

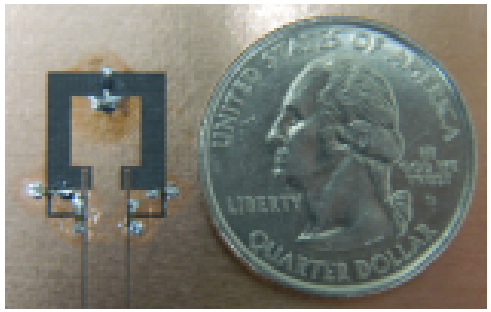

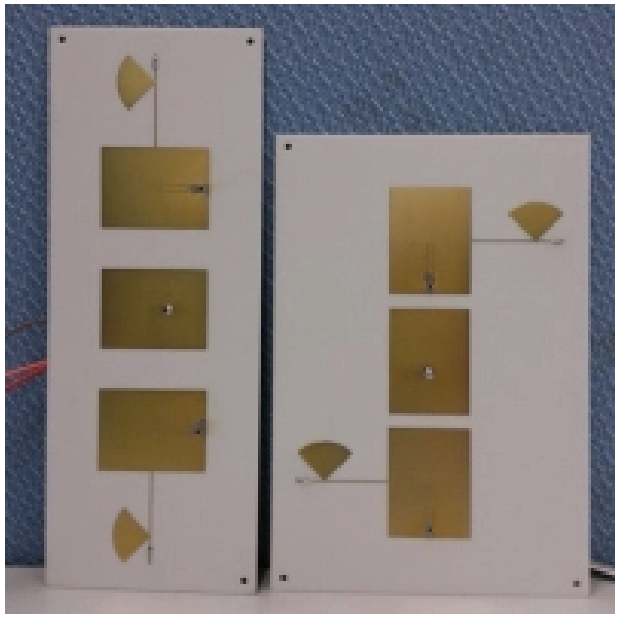

- *RF energy harvesting*

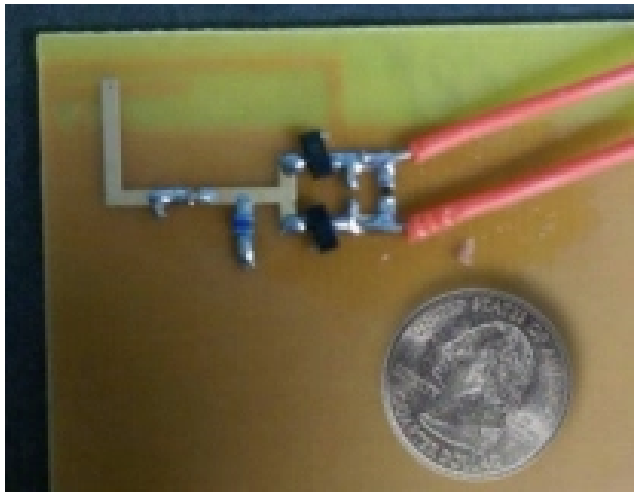

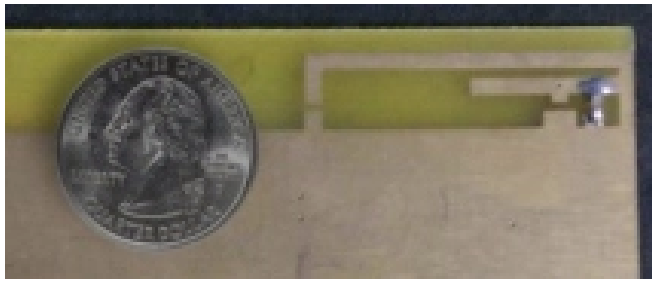

Rectifier Circuit

A RF-to-DC rectifier circuit converts collected RF energy to DC electricity. The designed circuit is a half wave voltage doubler circuit with a impedance matching network that matches the rectifier's input impedance to 50Ohms for maximum power transfer or minimum power reflection.

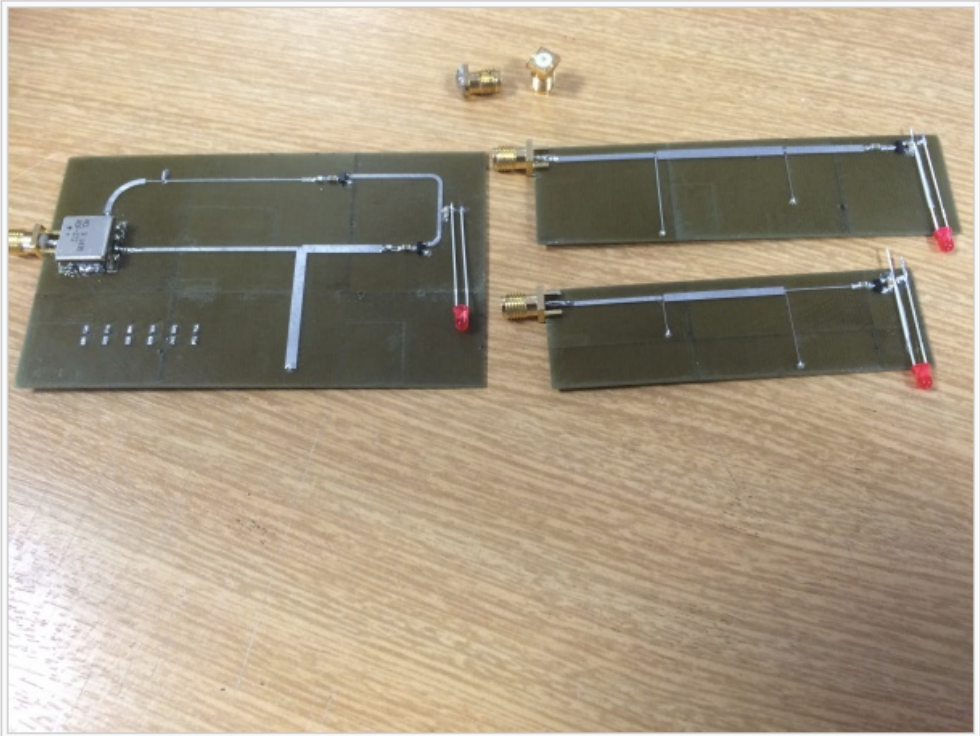

3 prototypes of rectifier circuit

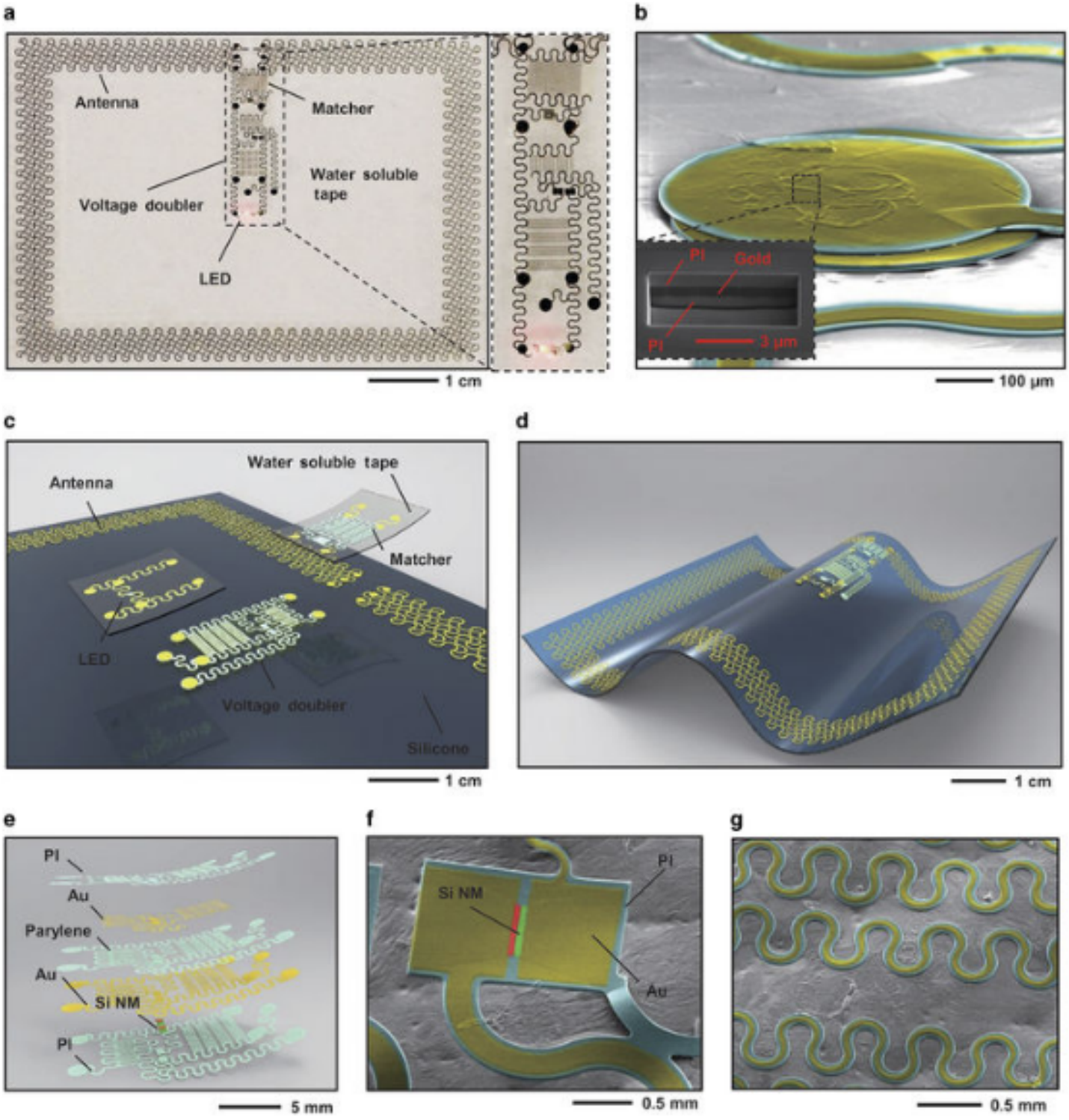

Schematic illustration and implementation of a modularized epidermal RF system for wireless power transfer. (**a**) Image of device while operating an integrated LED via power delivered by a remote RF source (15 W, 1.5 m). The loop antenna, formed with serpentine conductive traces in a square layout, spans the perimeter. The inset on the right highlights the collection of active components. (**b**) Top view SEM image of aligned gold pads whose

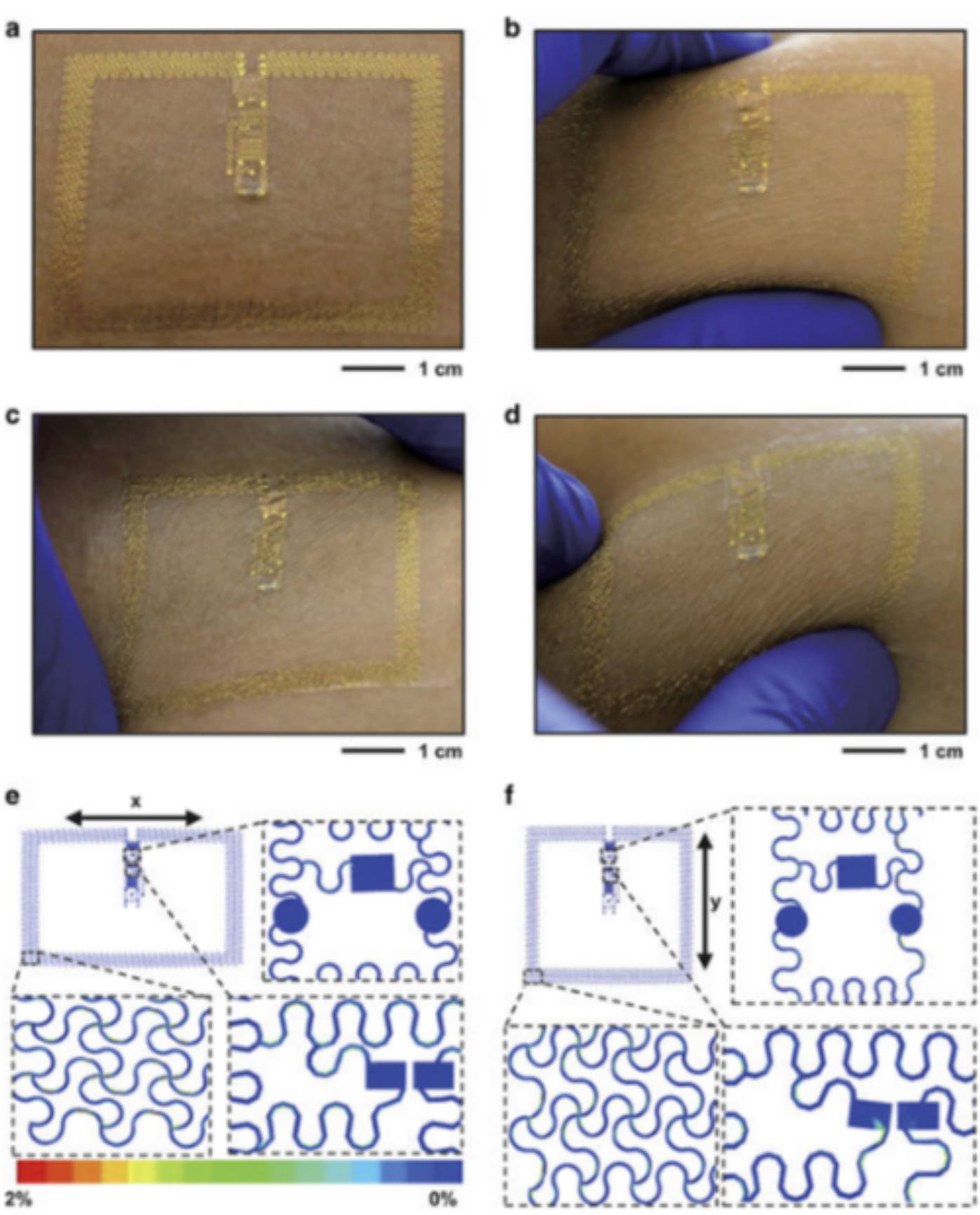

Mechanics of an epidermal RF system. Pictures of an epidermal RF system integrated on the skin (**a**) in its native state, (**b**) during compression by pinching (**c**) under uniaxial stretch and

Figure 5

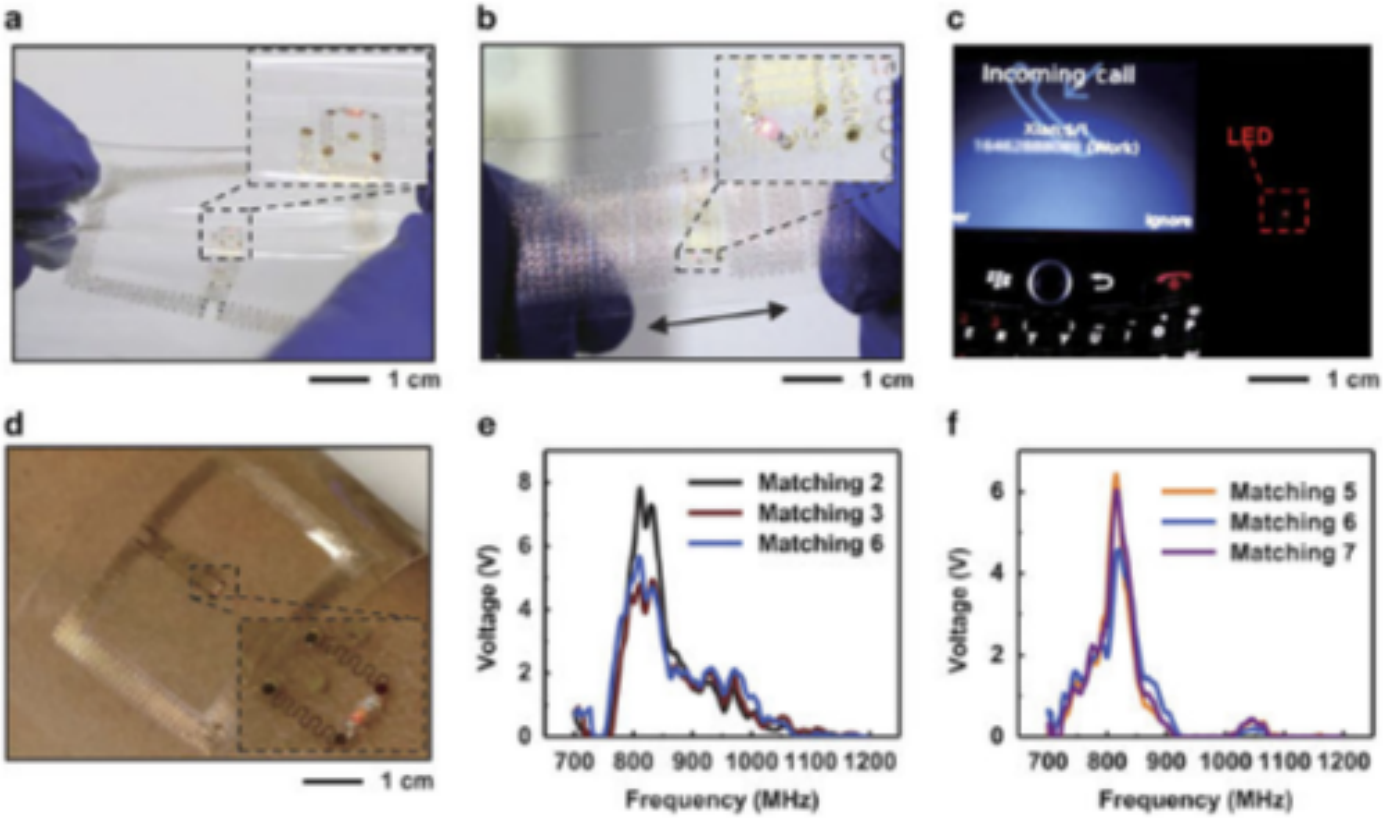

Demonstration of RF wireless power transfer. Epidermal RF system operating while (**a**) twisted and (**b**) repeatedly stretched. (**c**) Demonstration of the use of an epidermal RF system to capture RF output from a cell phone to supply power to an LED. (**d**) Epidermal RF system powering a red LED while on the skin using RF transmitted by a remote source (15 W, 1.5 m, 700 MHz–1.5 GHz). Open-circuit voltage output (**e**) in air and (**f**) on skin when implemented with different matching components.

Full size image »

stretchable electronic systems.

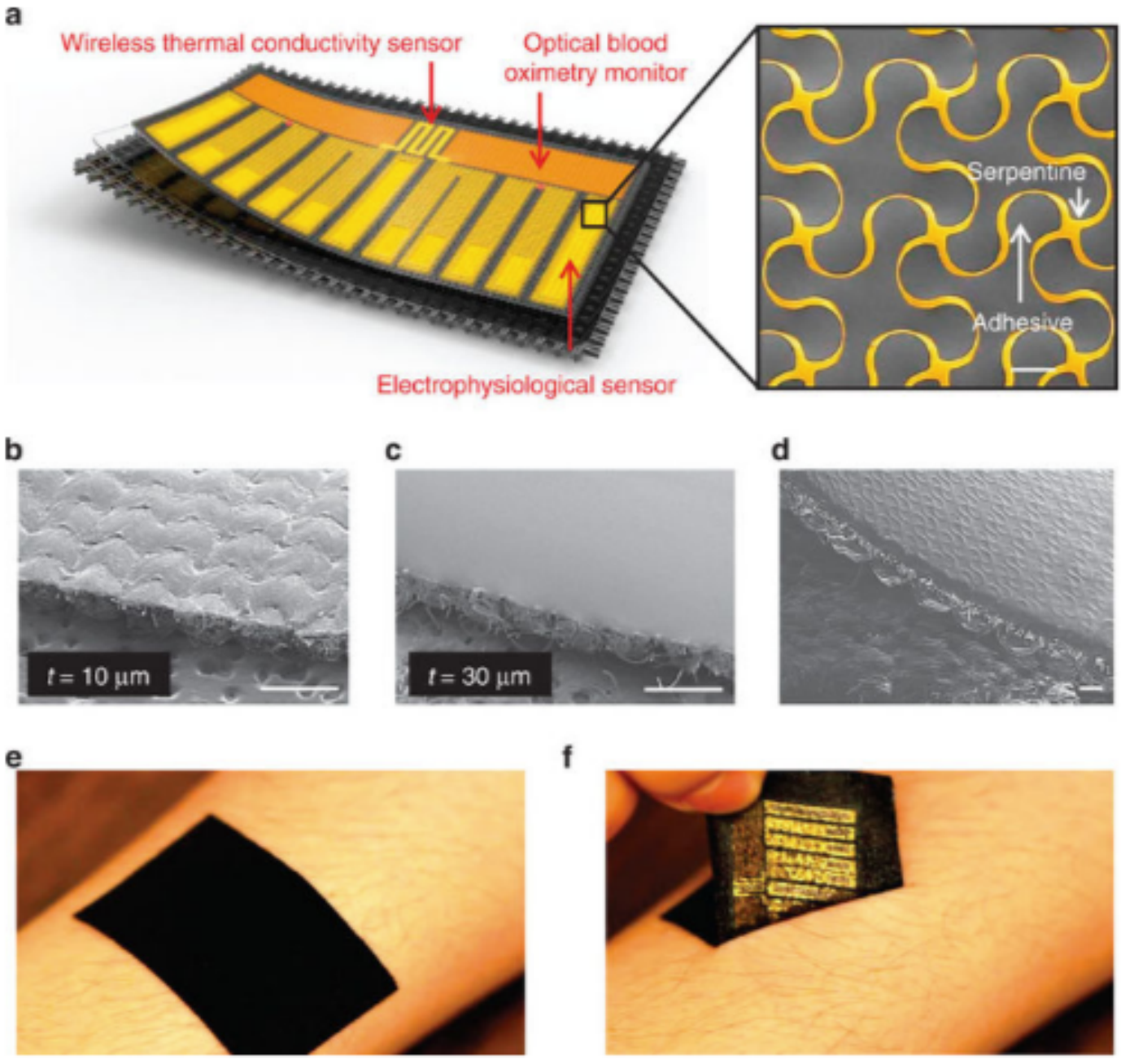

(**a**) Illustrations of the various layers in a representative system, including the active electronics (~5 μm thick), an ultralow modulus elastomer coating (~100 μm thick) and a stretchable fabric (~1 mm thick; 90% nylon, 10% spandex). The active electronics layer includes a wireless thermal conductivity sensor, a blood flow monitor and an EP sensor. The magnified view shows the FS structure of part of an EP sensor, as a coloured scanning electron micrograph (SEM; gold corresponds to the conducting traces, scale bar, 100 μm).

Figure 2: Capabilities for applying device to the skin with hairs and washing.

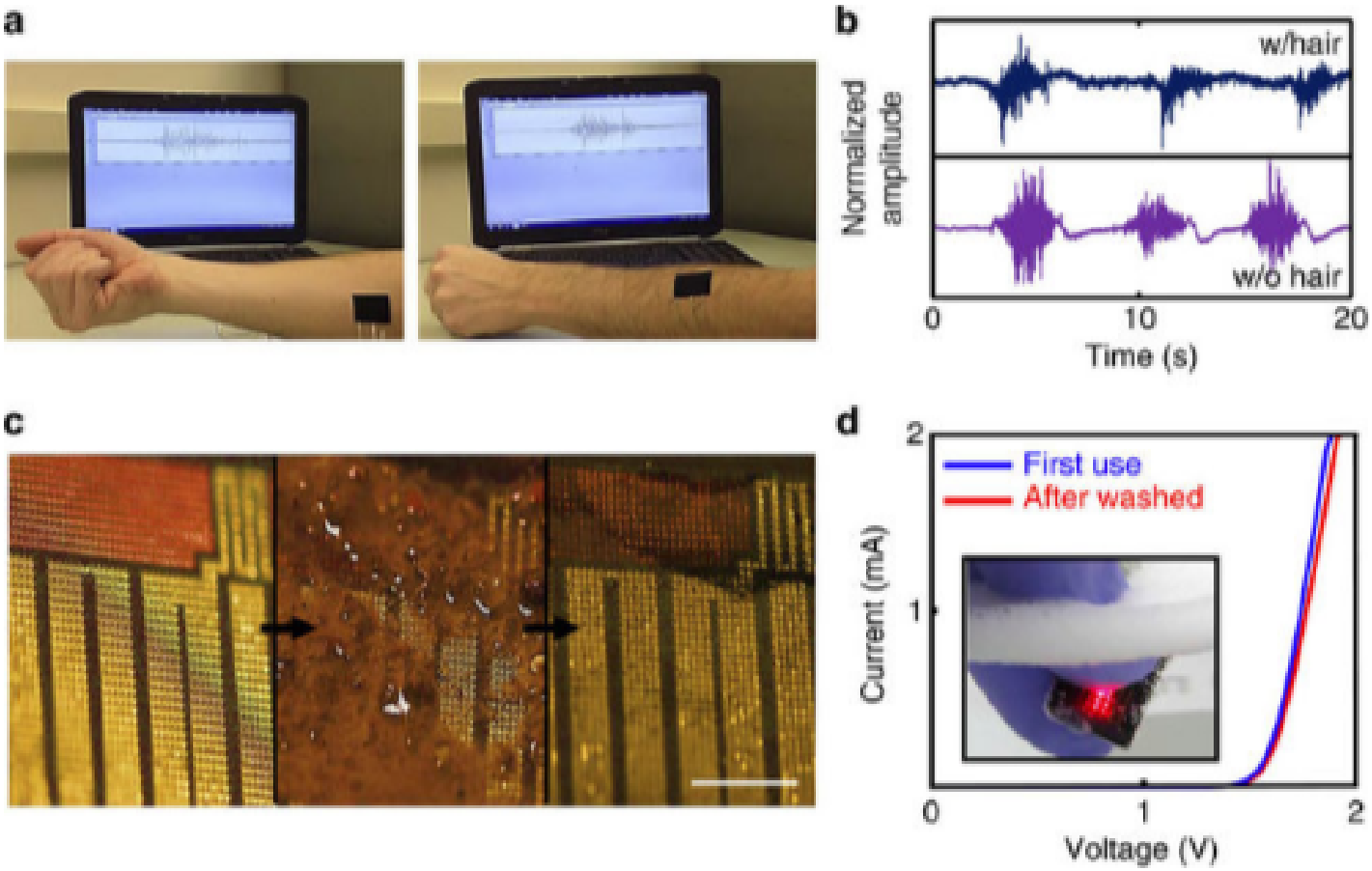

EMG measurement setup (**a**) and data (**b**) from inside (w/o hair) and outside of the forearm (w/hair). (**c**) Optical images (scale bar, 1 mm) of cleaning with soap and water: as-fabricated device (left), after contamination with dirt (center) and after washing with soap and water (right). (**d**) Current–voltage characteristics of an AlInGaP microscale inorganic LED module associated with the blood flow monitoring after first use and after washing. The image in the inset shows the device immersed in soapy water.

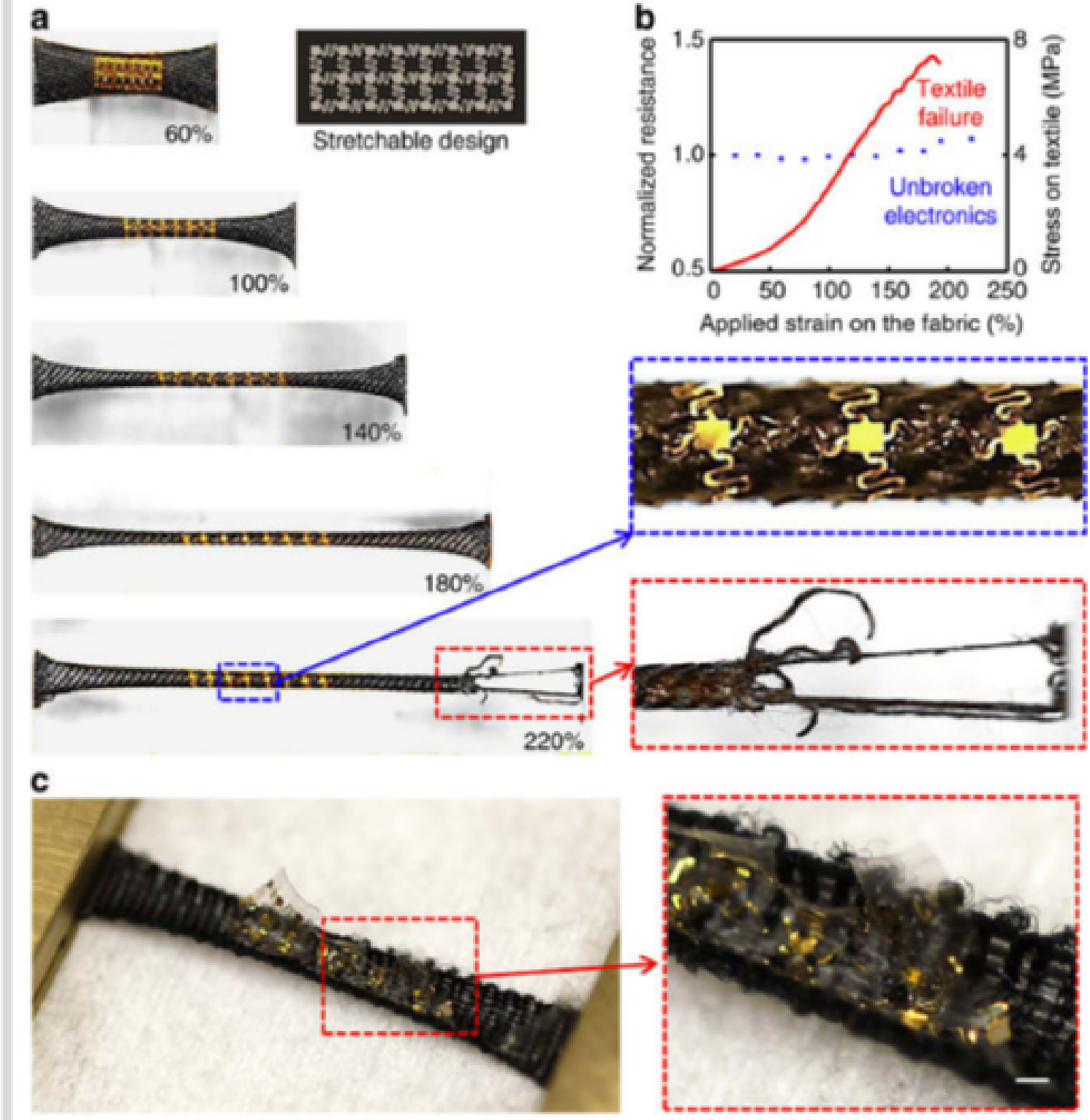

(**a**) Device integration with UL-Sil coating (*E*=3 kPa), Optical images of a stretchable electronic test structure (thickness ~2 µm) at increasing levels of uniaxial stretching. Magnified views of unbroken electronics (blue dotted box) and torn fabric (red dotted box) observed at an applied strain of 220%. (**b**) Normalized electrical resistance (left *y* axis) and

Figure 6: Functional demonstration of cerebral oximetry.

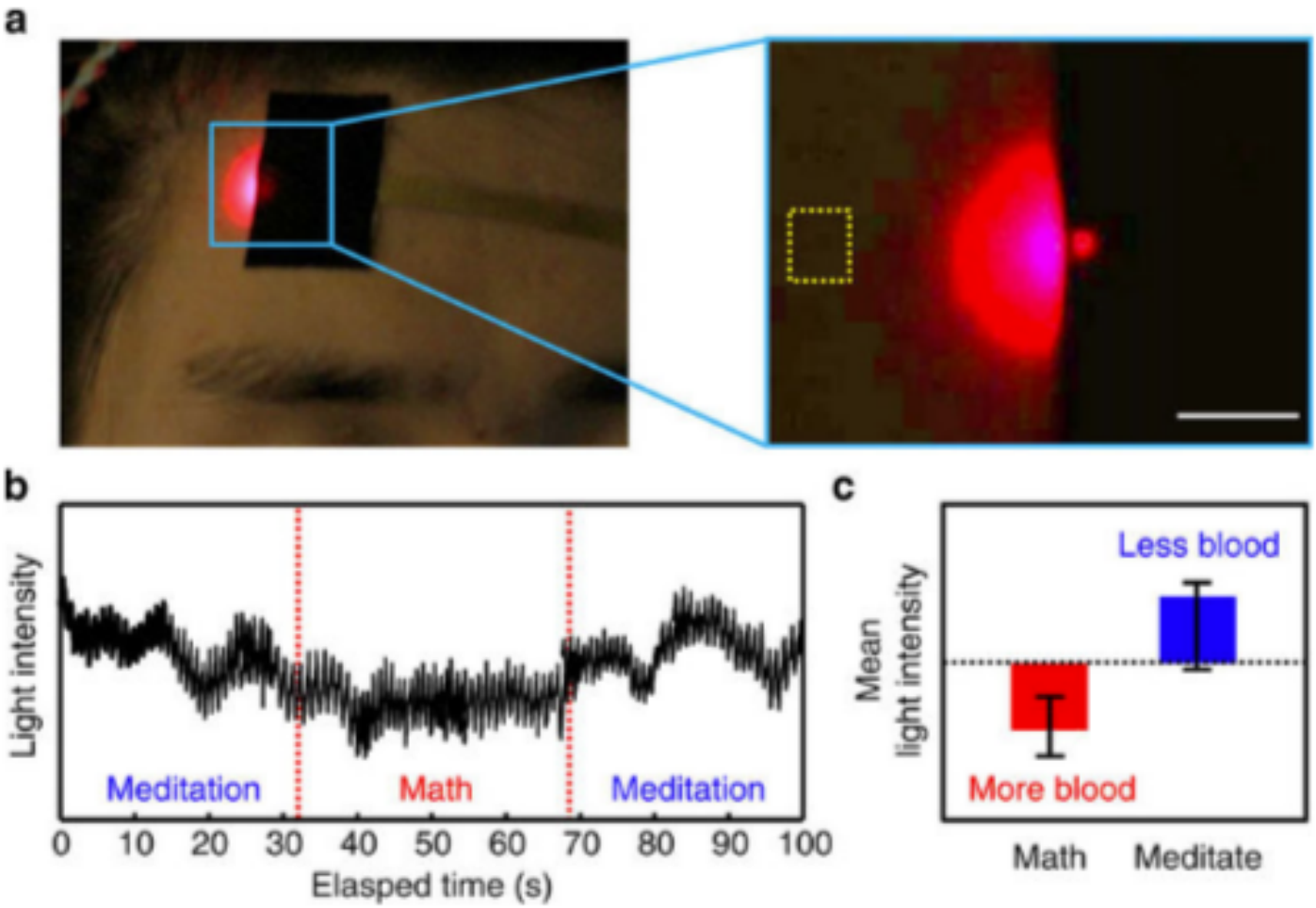

(**a**) Image of a device laminated on the skin of the forehead, with an operating μ-ILED (wavelength 650 nm) under room light illumination and in the dark. Scale bar, 1 cm. Light intensity integrated over the region indicated by the yellow dotted box of the right frame of (**a**), plotted as a function of time (**b**). (**c**) Scattered light intensity during mental math and rest, mean centred, smoothed with a moving window and averaged over time for each condition. Error bars denote +/−1 s.d. of the signal over time in each condition. Reduced intensity during mental activity is consistent with increased light absorption induced by additional blood flow in the cerebral cortex.

Figure 7: Wireless evaluation of skin thermal properties.

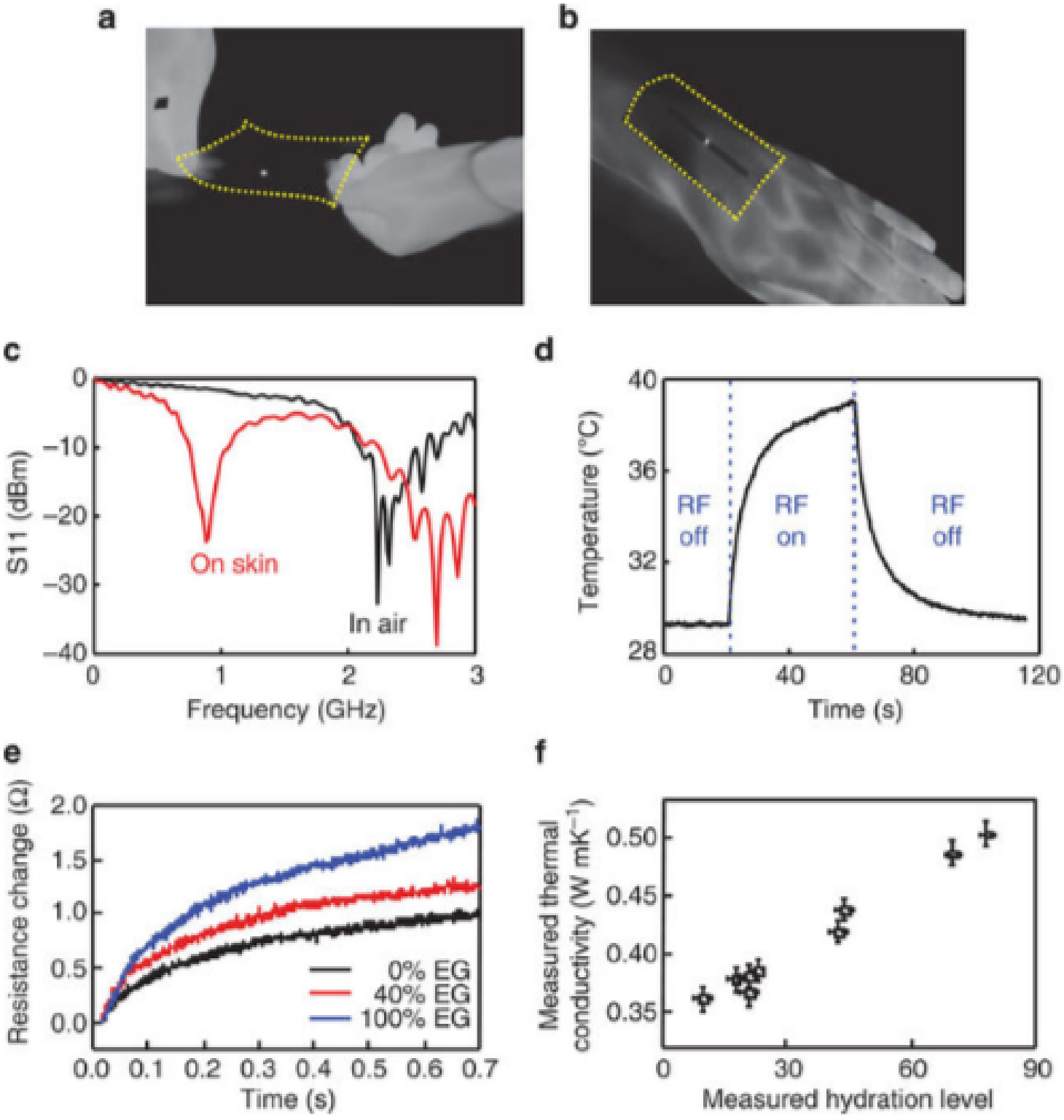

IR images of a wireless heating device, collected during exposure to RF energy, in a free-standing state (**a**) and mounted on the wrist area (**b**). (**c**) S_{11} coefficient measured from the wireless heating element, evaluated in air and on human skin. (**d**) Transient control of temperature on the skin using the wireless heating element, and measured using an IR

Figure 8: EP monitoring of a human subject in a driving simulator.

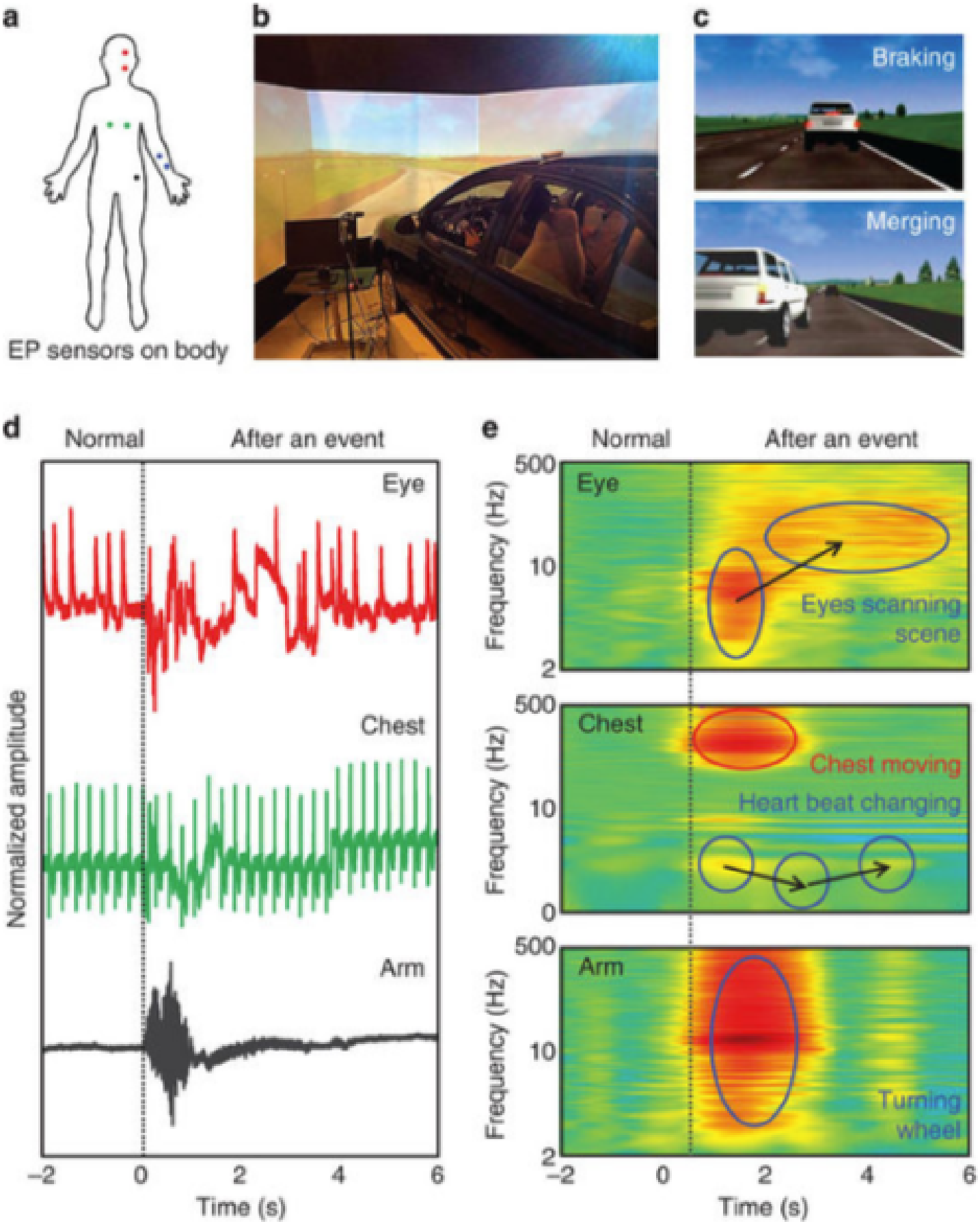

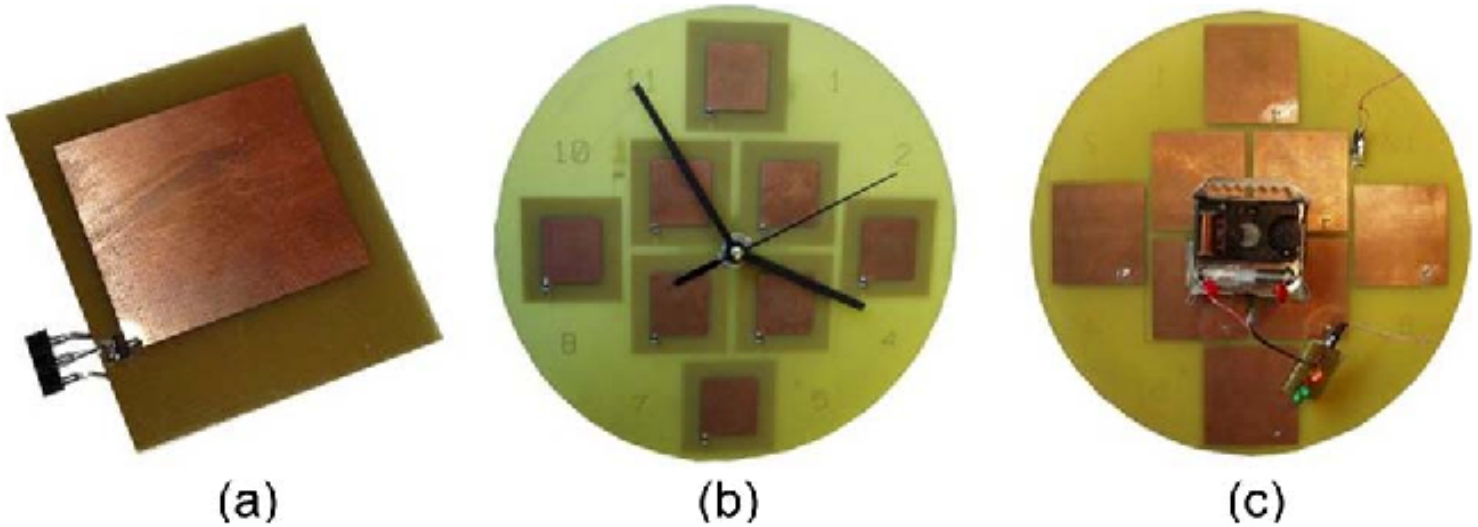

Fig. 16. Wirelessly RF powered wall clock. (a) Rectenna element. (b) Front view of the clock with eight rectenna elements. (c) Back view of the clock showing the separate rectenna element's ground planes.

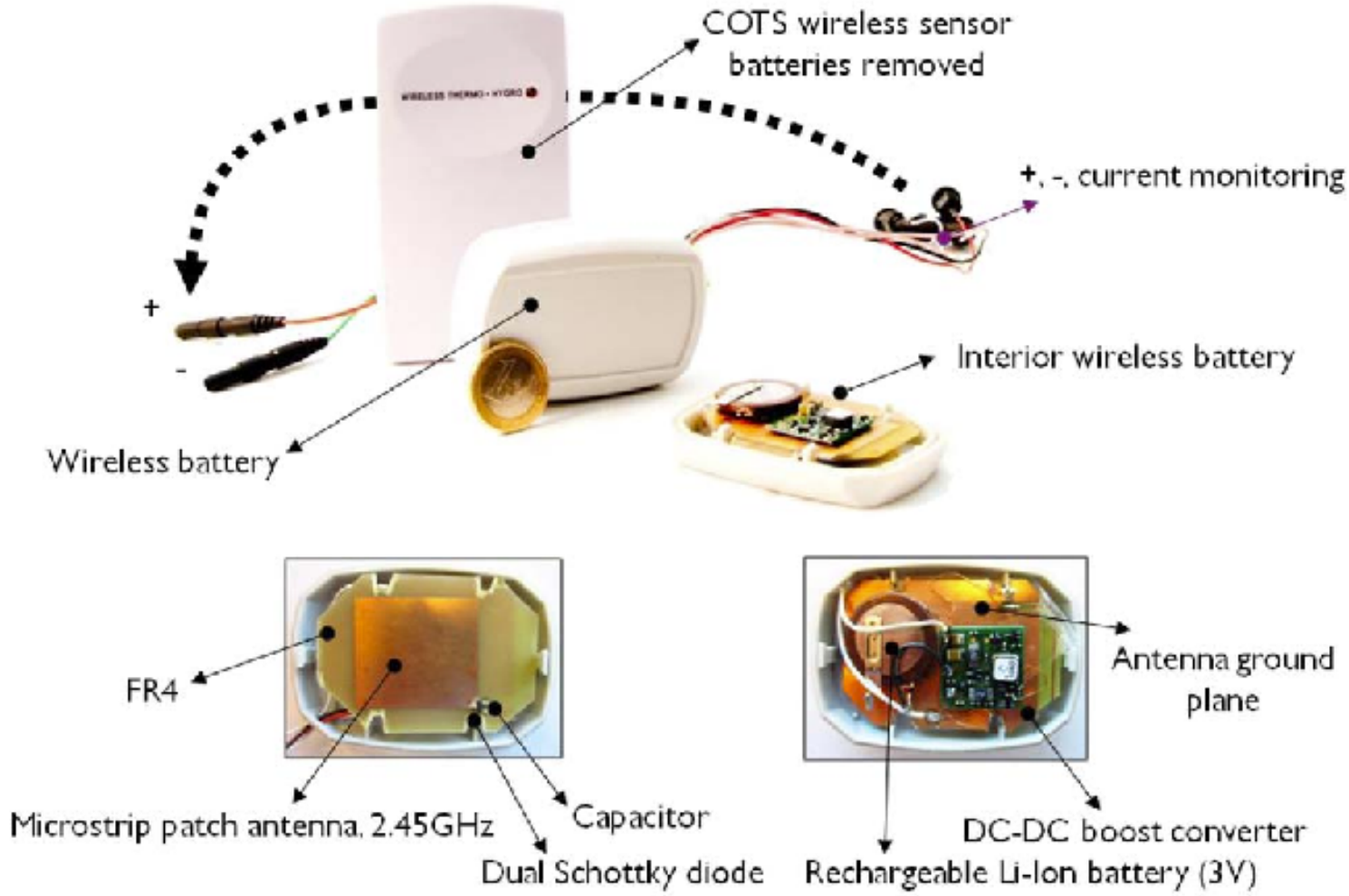

Fig. 20. Packaged 2.45-GHz remote RF battery charger and COTS 433-MHz temperature and humidity sensor. 433-MHz base station not shown.

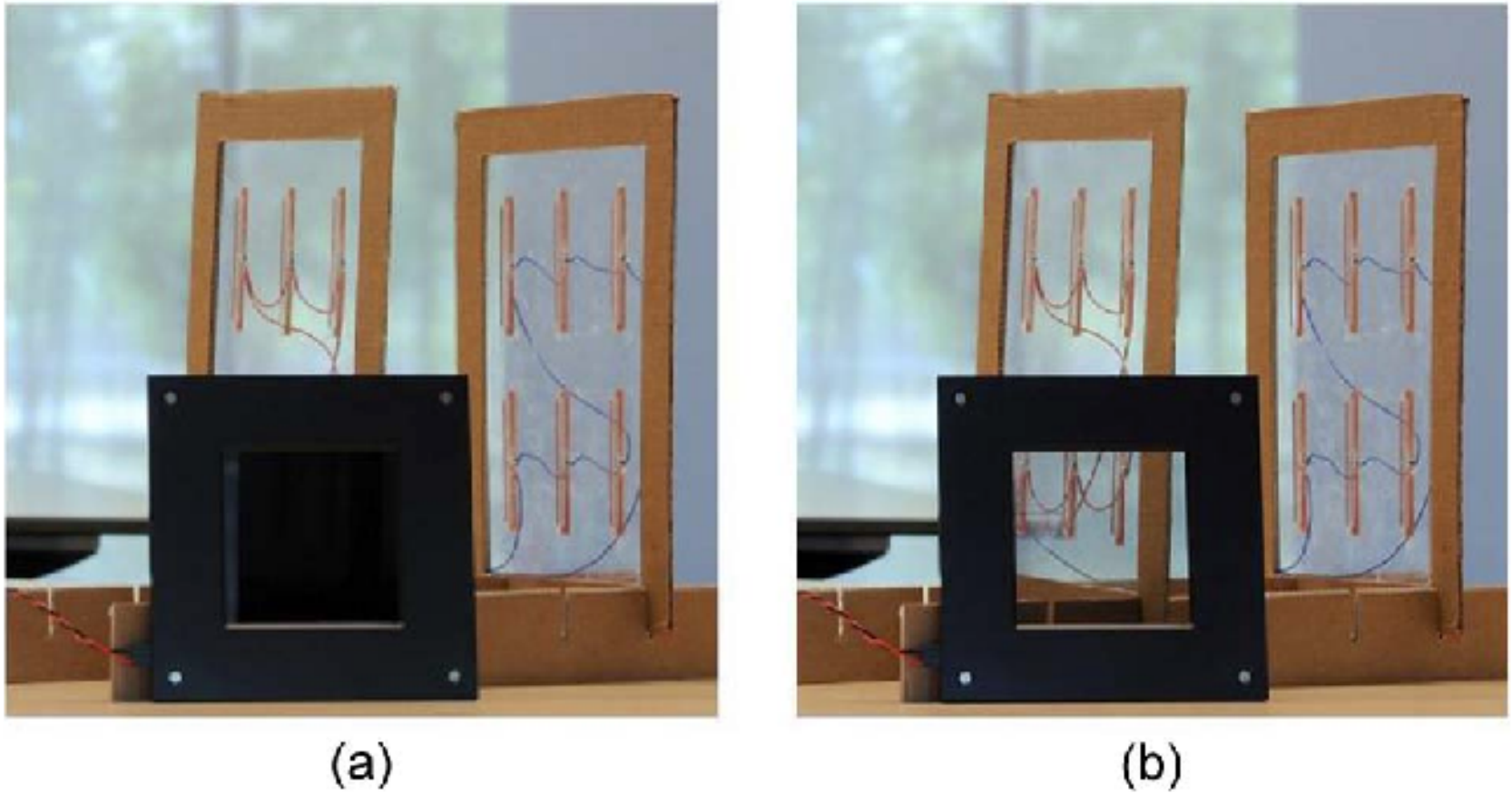

Fig. 17. E-skin. (a) No voltage supplied: E-skin panel is opaque. (b) Voltage supplied: E-skin panel is optically transparent.

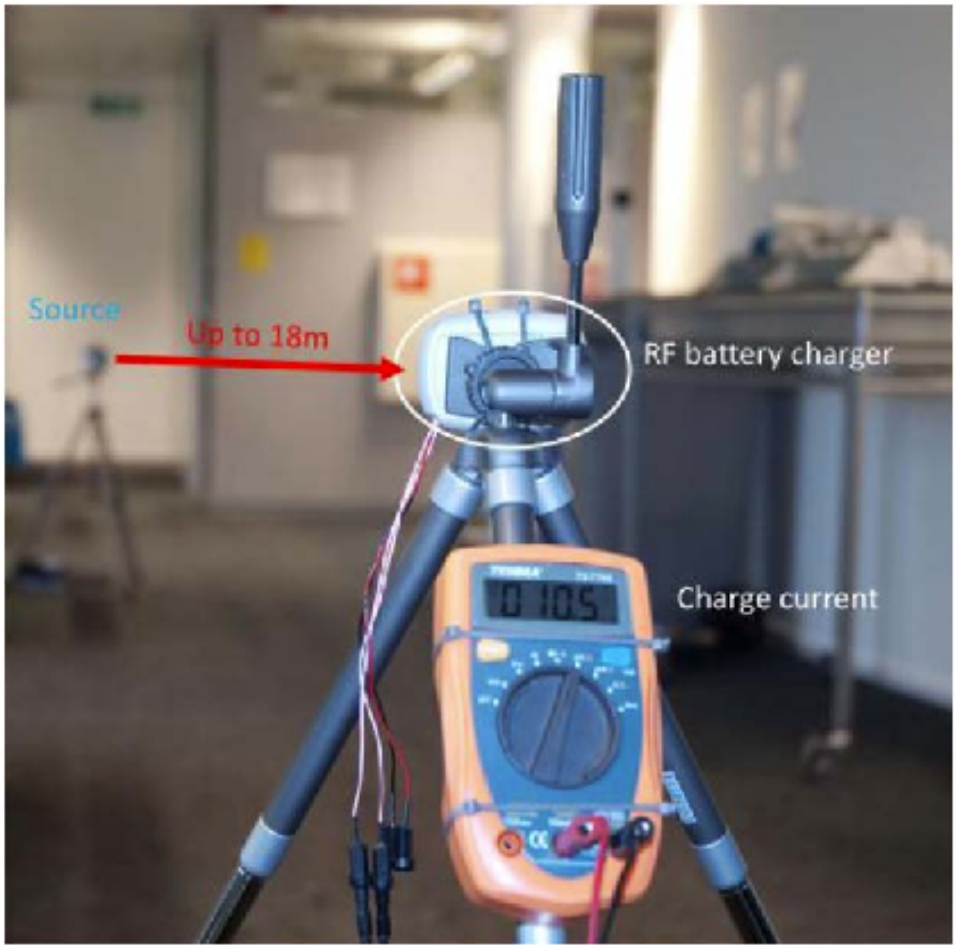

Fig. 21. Wireless energy transport measurement setup. By optimizing the receiver location, a battery may be charged up to 18 m from the source.

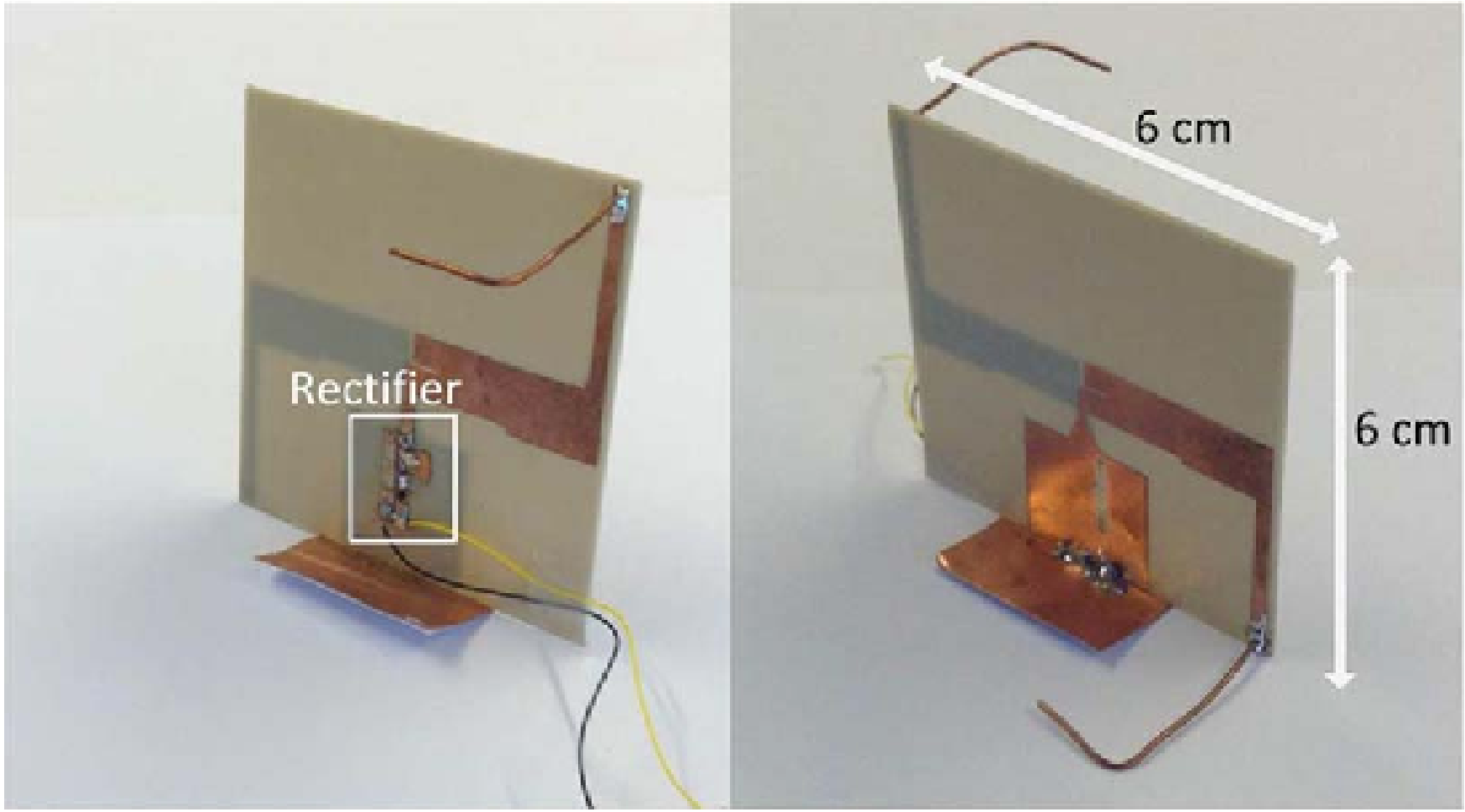

Fig. 16. Fabricated dual-band rectenna prototype [17].

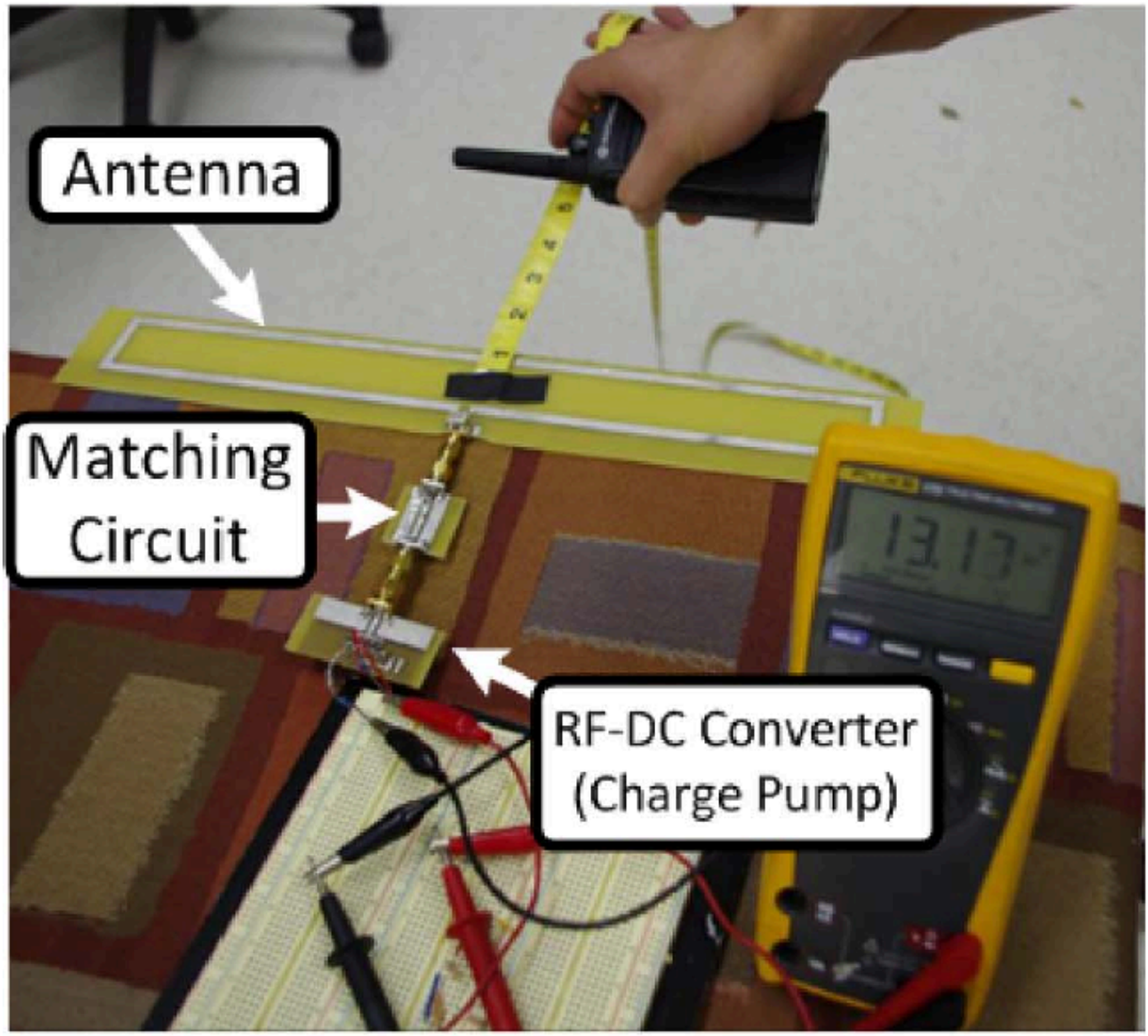
Antenna
Matching Circuit
RF-DC Converter (Charge Pump)

(a)

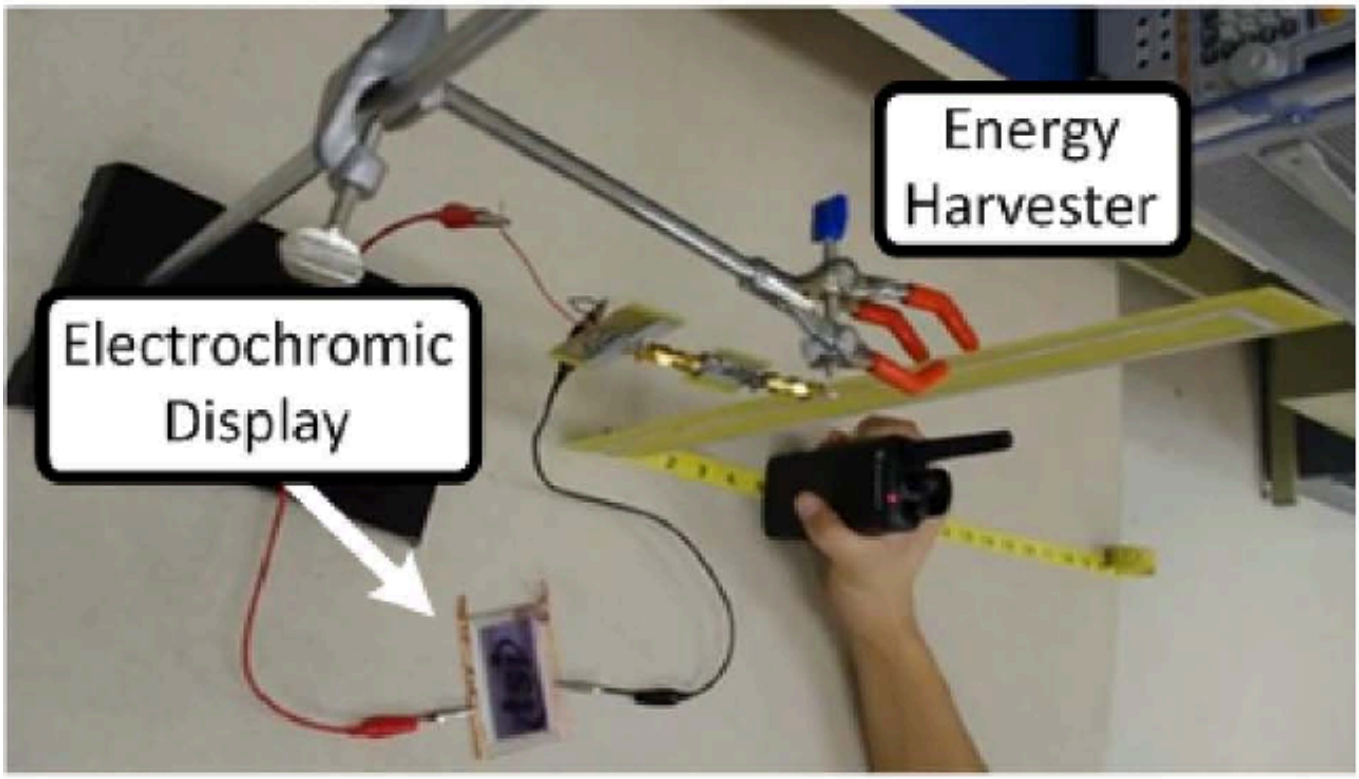
Energy Harvester
Electrochromic Display

(b)

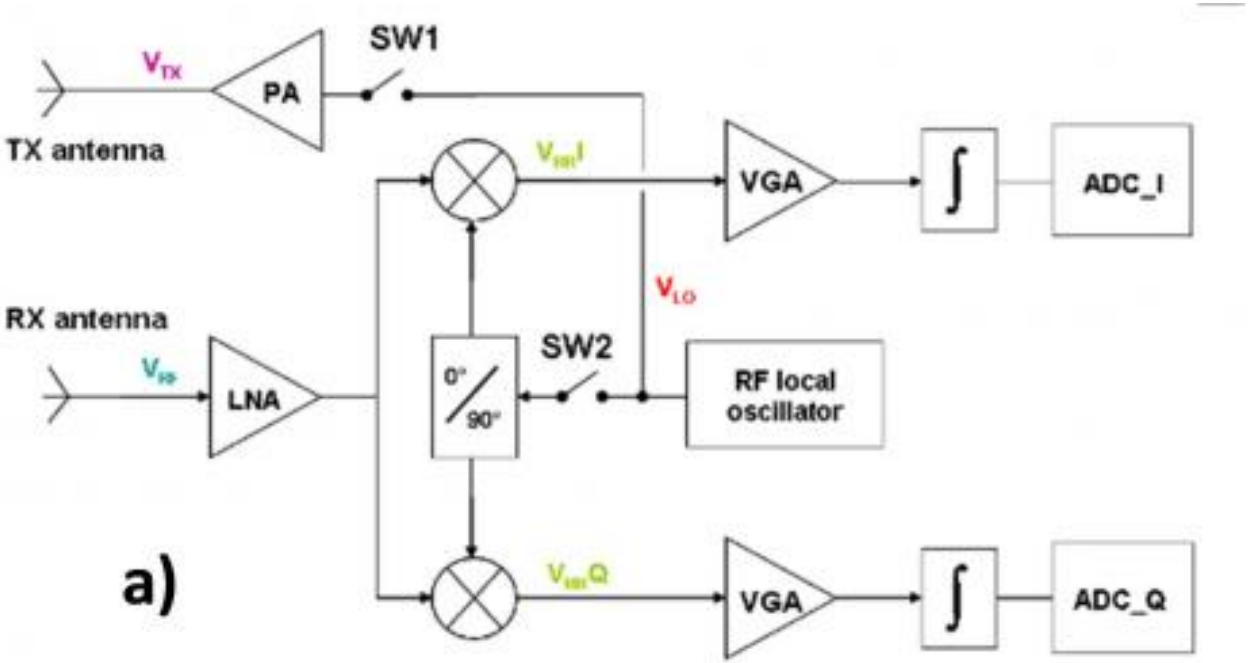
SW1
V_{TX}
PA
TX antenna
$V_{int}I$
VGA
∫
ADC_I
V_{LO}
RX antenna
V_{RX}
LNA
0°
90°
SW2
RF local oscillator
$V_{int}Q$
VGA
∫
ADC_Q
a)

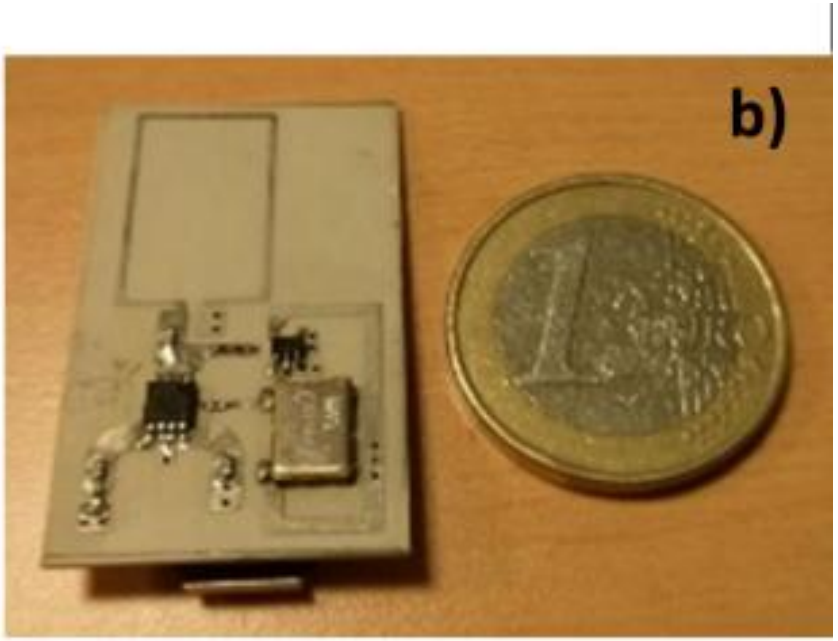
b)

Arrays can be built by connecting in series like regular batteries large numbers of single-element harvesters. These have the advantage that they have a larger effective area and can harvest greater amounts of energy. Pictured bellow is such an array, near a single element harvester.

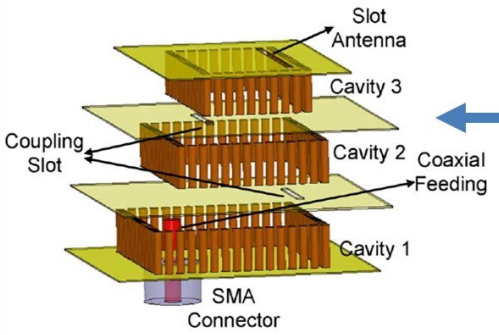

Filter/Slot antenna Integration

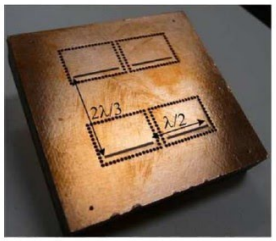

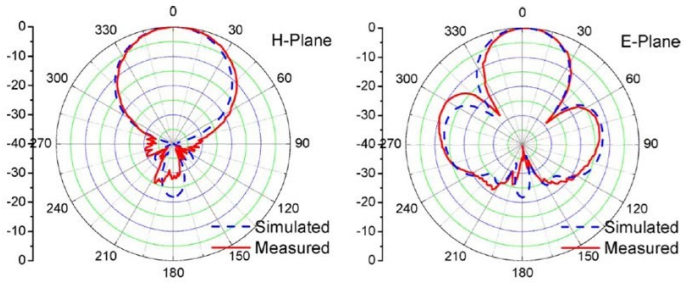

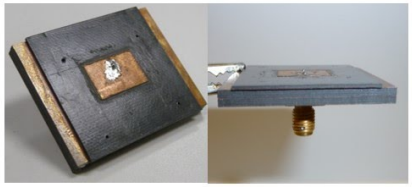

Goal:

Reduced size, high-Q and high-efficiency RF front-ends

Highlights:

No 50-Ohm transmission line transitions

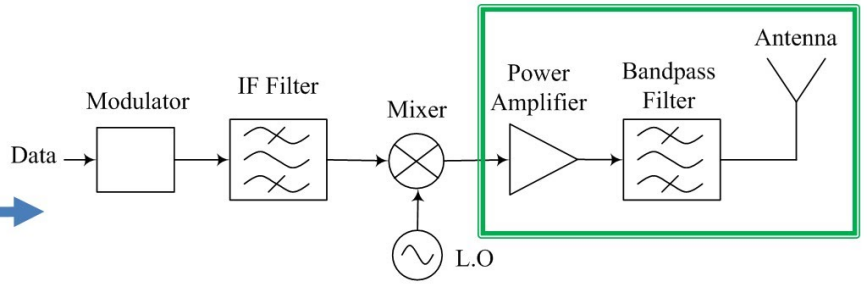

Great potential for high-level integrated and tunable RF front-ends

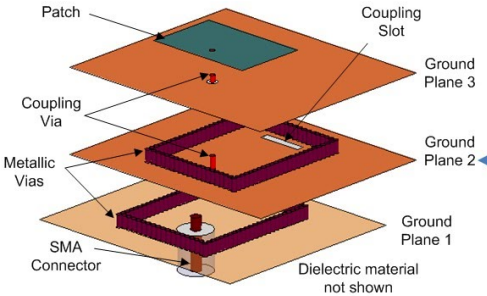

Filter/Patch antenna Integration

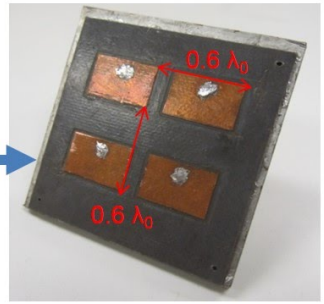

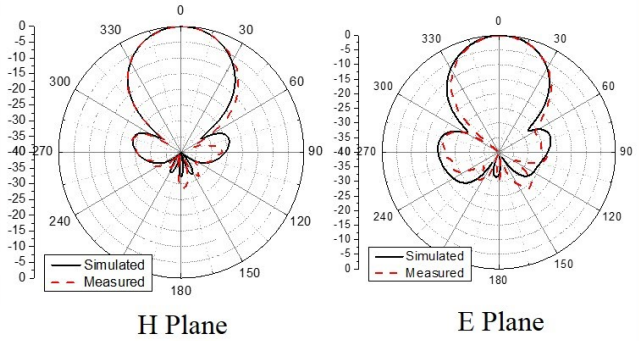

Recent Collaboration In Computational Nanophotonics at Purdue and Beyond

Chiral Metasurfaces for Optical Activity (the Shalaev group)

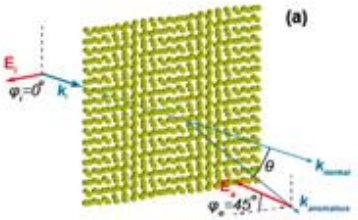

Compact Cavities and Waveguides using Reflecting Metasurfaces (the Shalaev group)

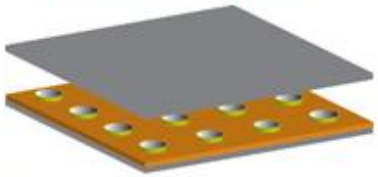

High temperature thermal emitter for thermo-photovoltaics (the Shalaev, Shakouri, Sands, and Bermel groups)

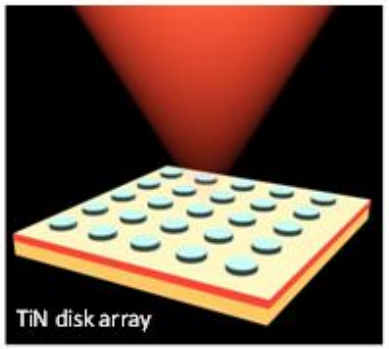

Nano-imaging and Nanoscope
Narimanov (Purdue)
Pendry (Imperal College)
Zhang (UC Berkeley)
Liu, UCSD

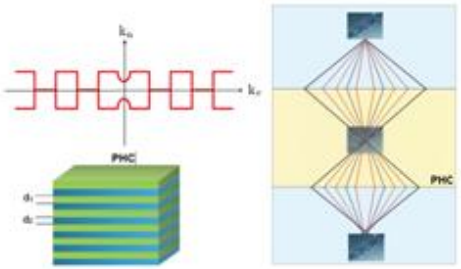

Hybrid Electro-Plasmonic Tweezers (the Wereley and Boltasseva groups)

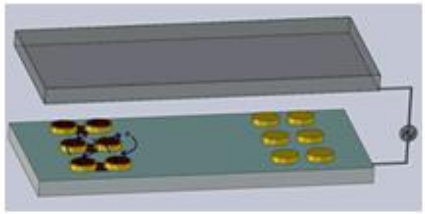

Ag nanowires-graphene transparent conducting electrodes (the Janes group)

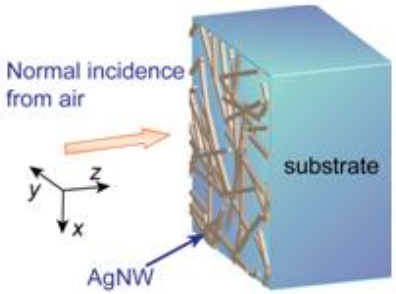

Optics of Branched Silver Nanowires (the Janes group)

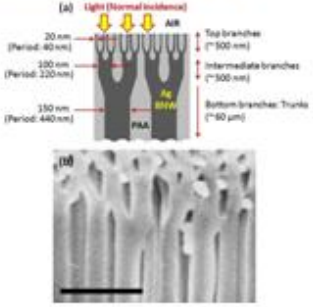

Au Nanorod Plasmonics (the Wei group)

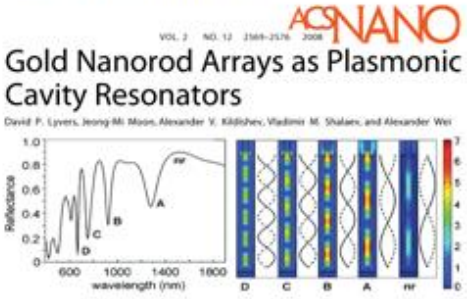

Enhanced single-photon sources based on NV centers and metamaterials (the Shalaev group)

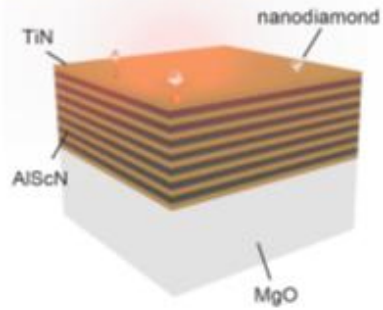

Dynamic Plasmonics with Graphene (the Yong Chen group, the Boltasseva group)

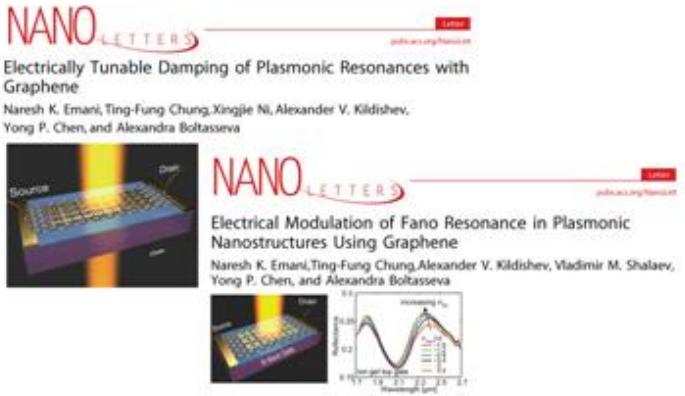

Dynamic Metamaterials and Devices (the Boltasseva group)

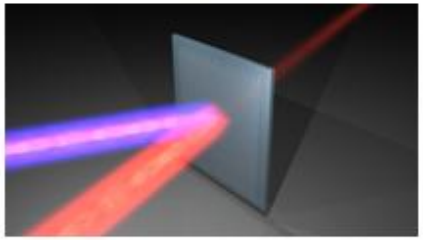

Nonlinear Optical Properties of Alternative Plasmonic Materials Bonner, Gavrilenko (NSU) with the Boltasseva and Shalaev groups

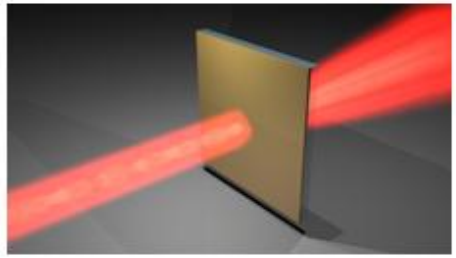


Tego Power Harvest Technology
Passive LED
P60143
Tego Power Harvest Technology
Passive LED
P60143
Tego Power Harvest Technology
Passive LED
P60143
127.0.0.1
6:02
Stop Reading
Tag Events
NONE
EPC ID
Ant
Ct
E2817023DD20120319EEA404
1
491
E2817023DD20120319EEA405
1
492
E2817023DD20120319EEA401
1
492
Total
Read

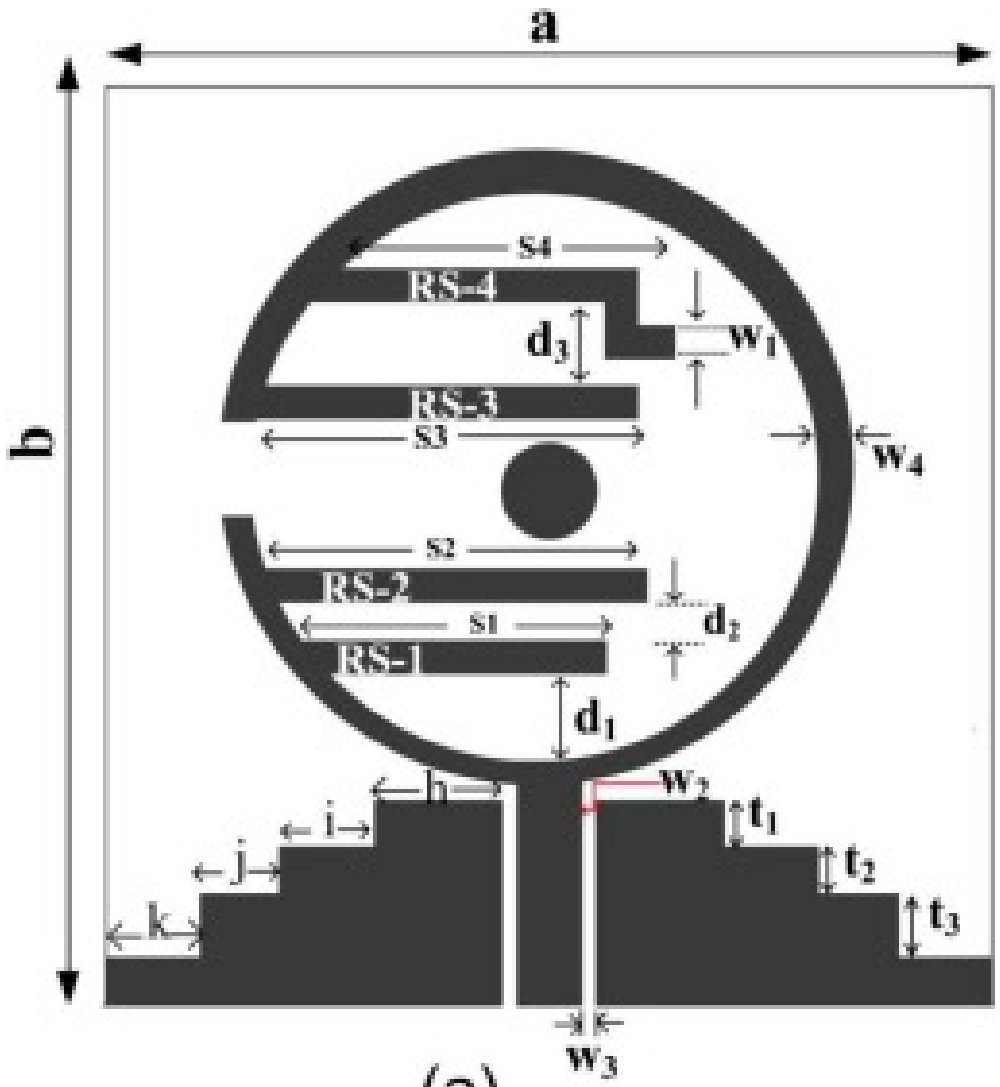
a
b
S4
RS-4
d3
w1
RS-3
S3
w4
S2
RS-2
d2
S1
RS-1
d1
h
w2
i
t1
j
t2
k
t3
w3

(a)

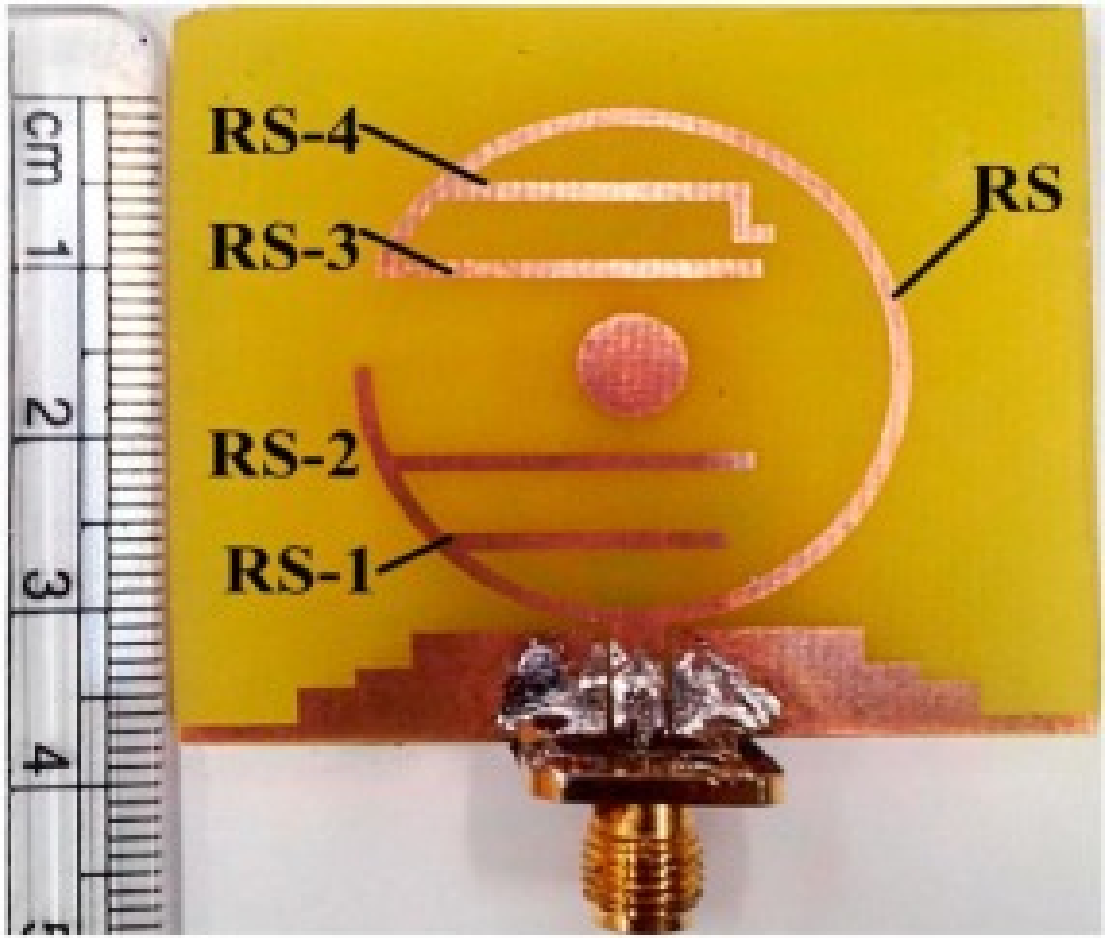
RS-4
RS-3
RS
RS-2
RS-1
cm
1
2
3
4

(b)


Wisent protocol makes batteryless computers like WISP a whole...
TU Delft TV
MORE VIDEOS
SUB SCRIBE

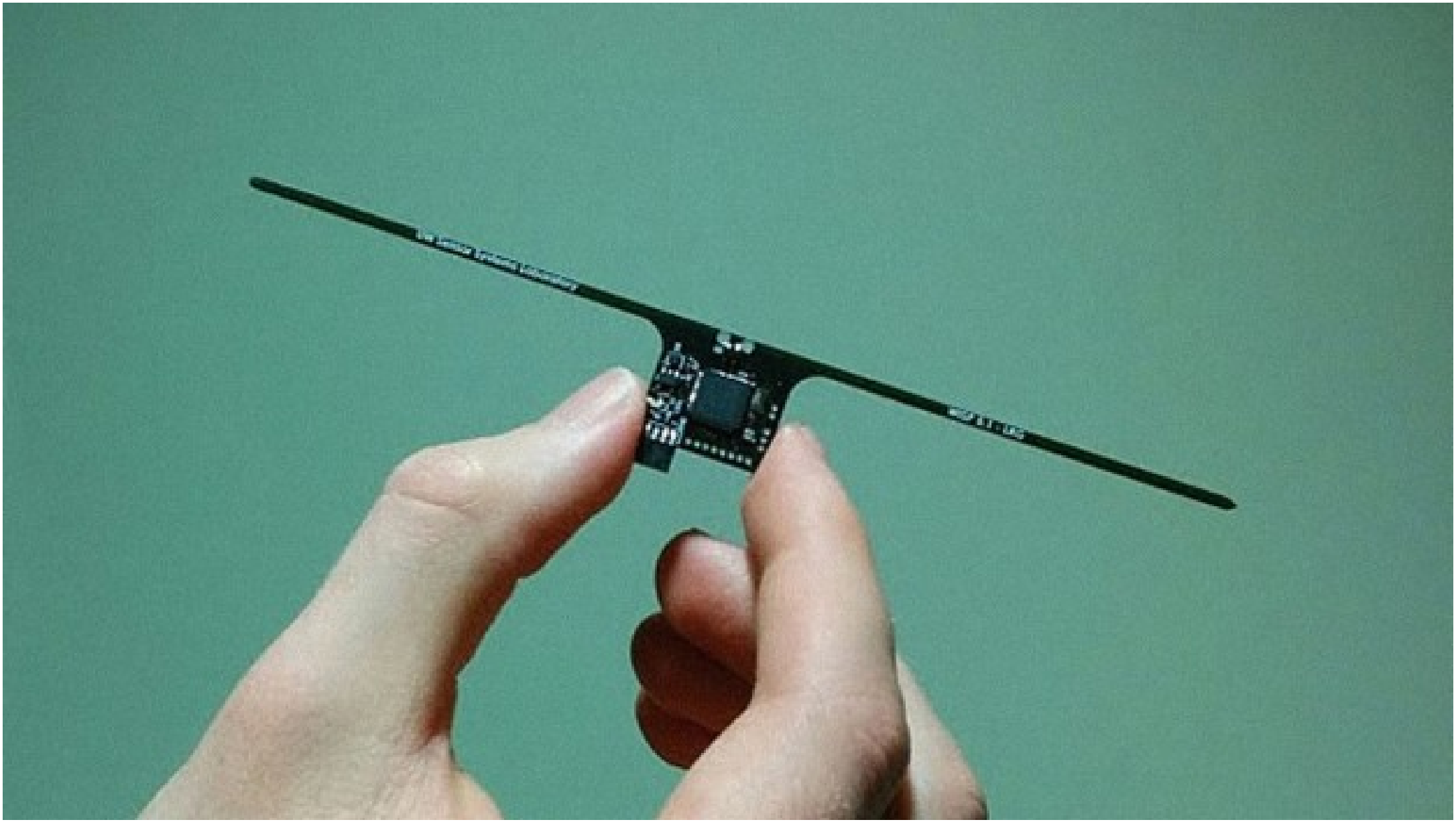

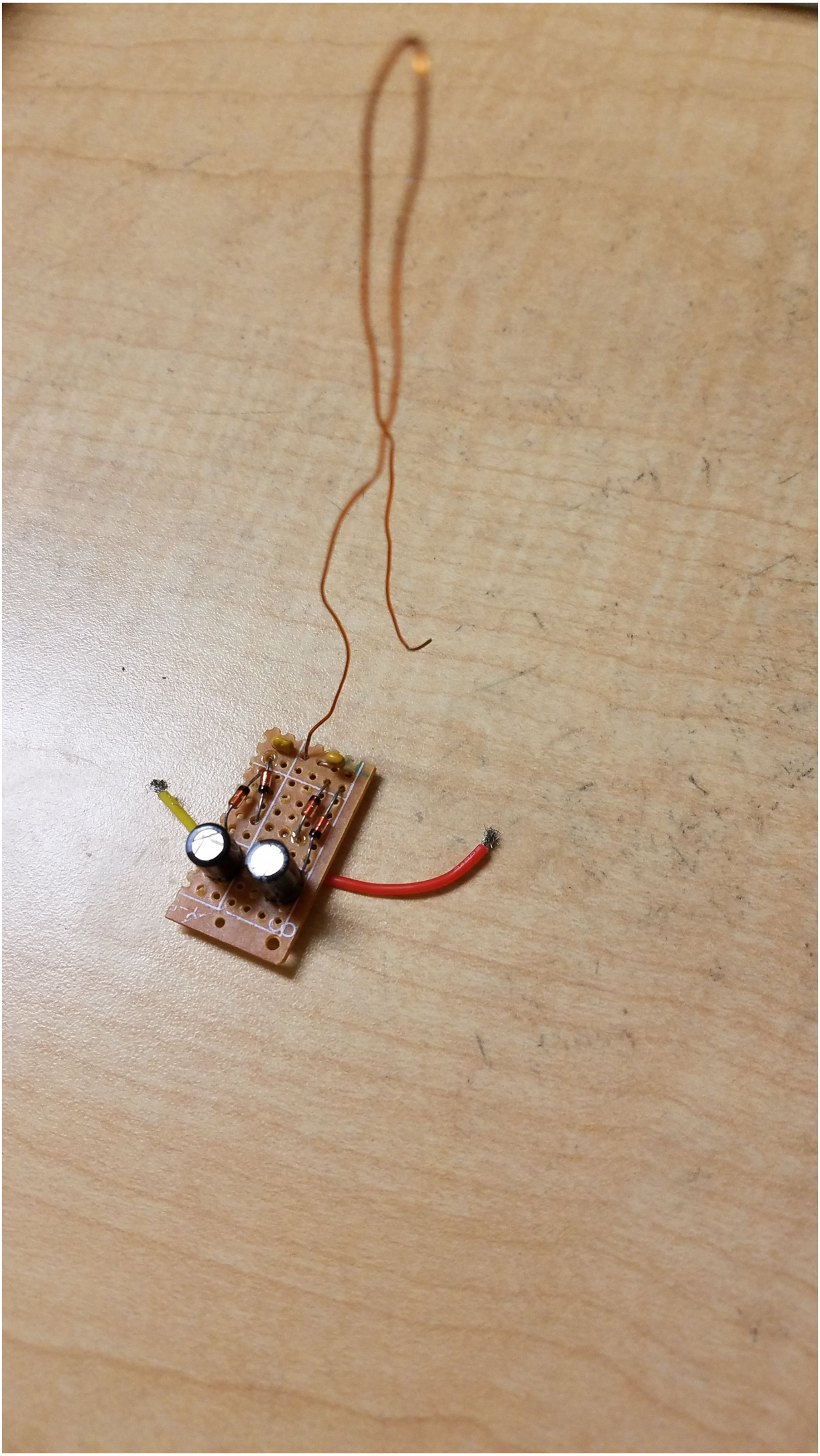

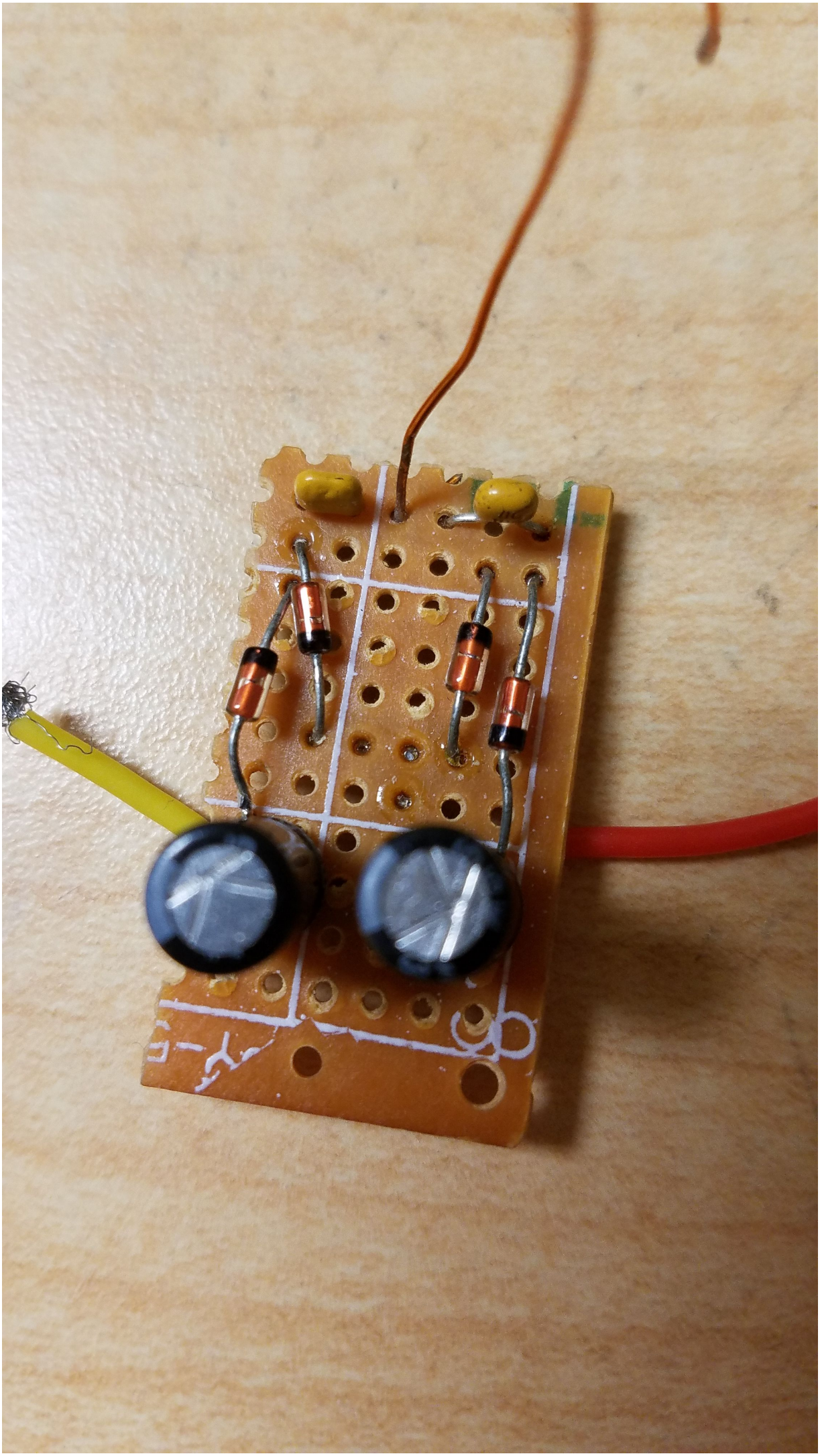

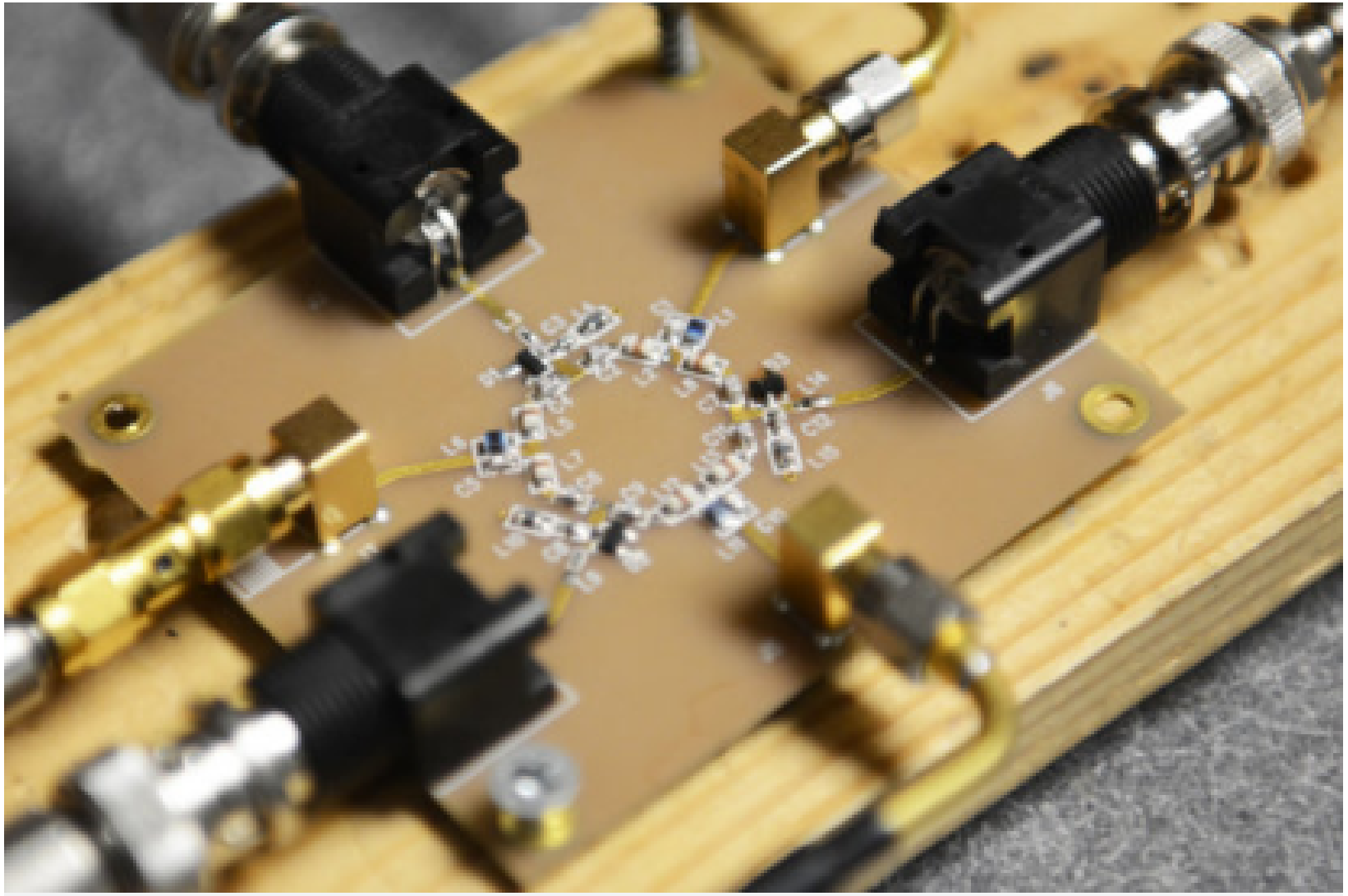

Radio wave circulator developed by researchers at the Cockrell School of Engineering.

Credit: Image courtesy of University of Texas at Austin

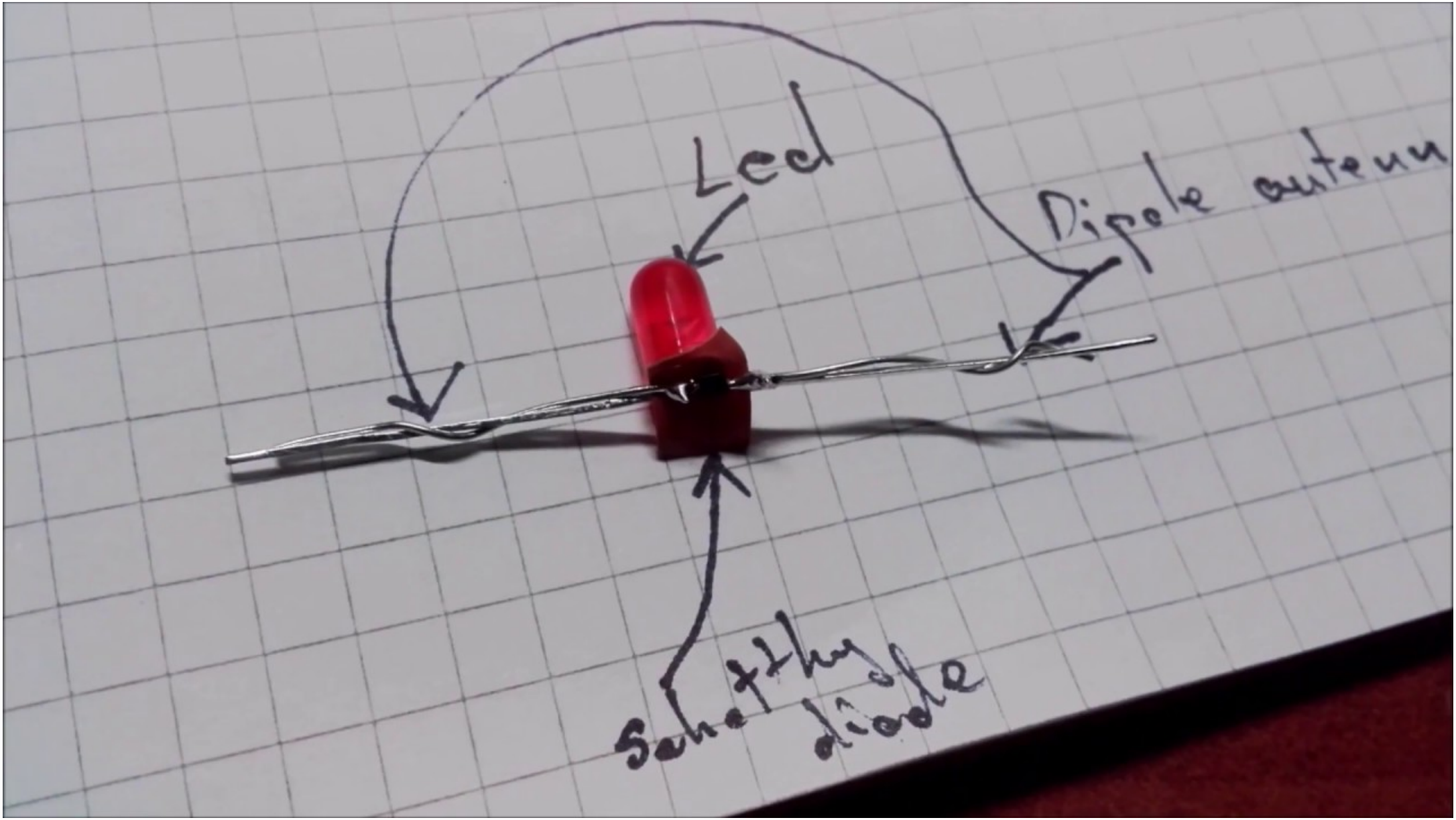
Led
Dipole antenn
Schottky
diode

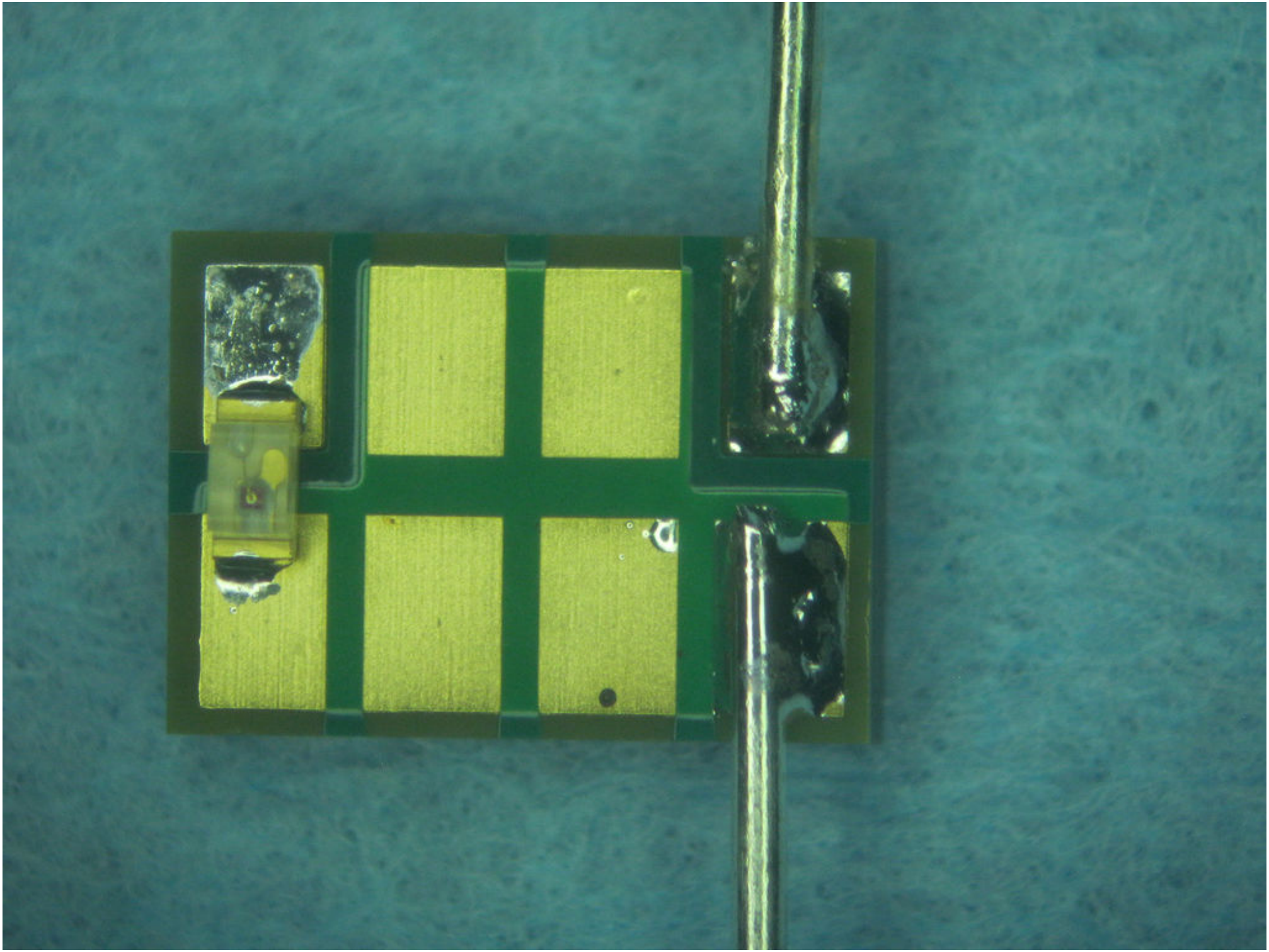

Step 1: Assembly Instructions

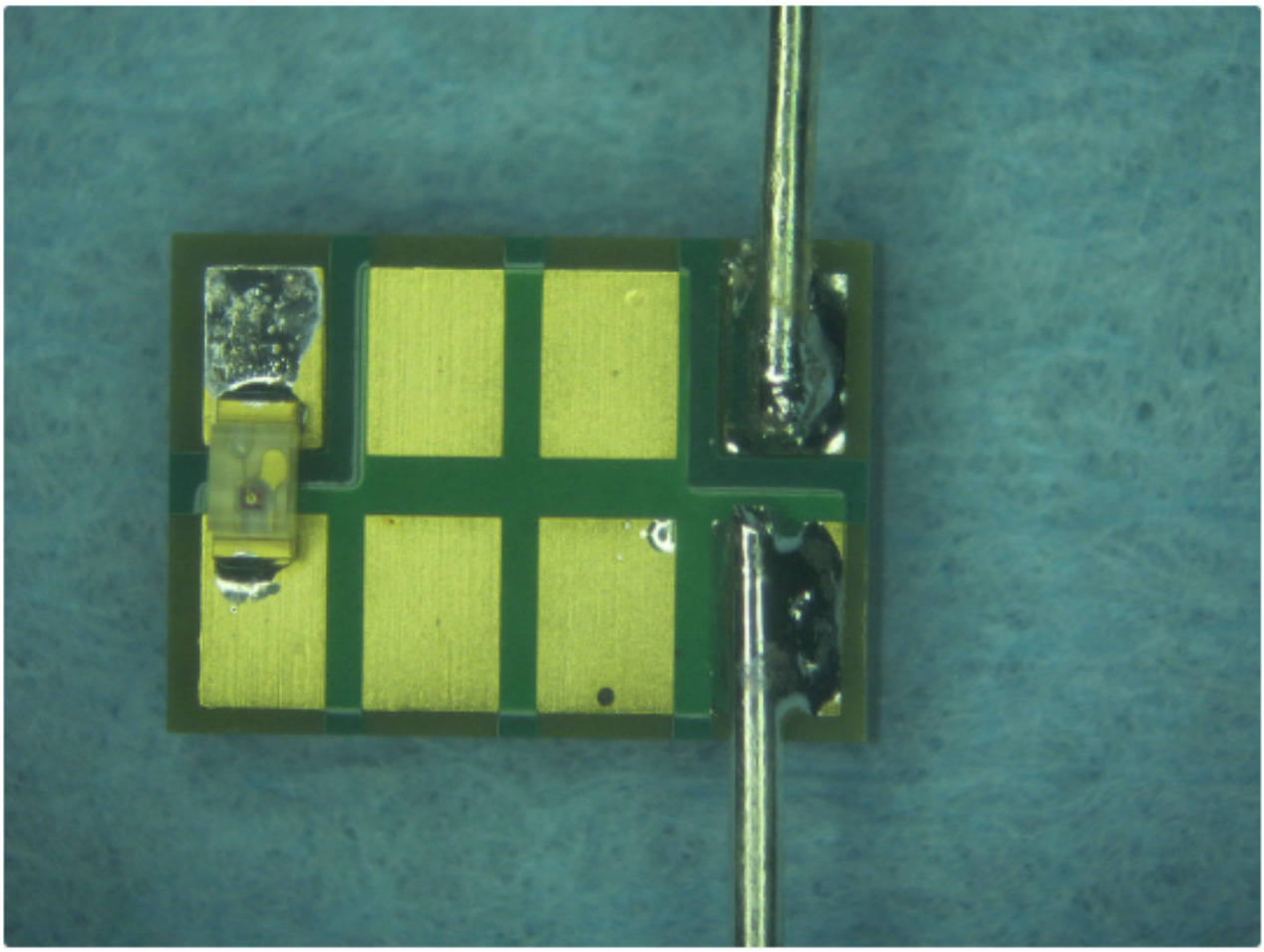

Cut the resistor wires off next to the resistor. These are just the right size at 1 1/8" long for a 2.5GHz dipole. Throw away the resistor and keep the wires.

Put solder paste on the module at pins 1 & 8 and at pins 4 and 5.Place the wires on pins 4 and 5 and solder carefully using tweezers to hold the wires (it will burn you otherwise). Solder at the lowest soldering temperature possible to avoid damaging the module. If the iron is too hot then you may damage the internal connections inside the module. Use a minimum of time for soldering (<10secs). The wires work as a dipole antenna to collect the 2.5GHz energy into the RF (Radio Frequency) Input of the module.

Place the LED with the anode (positive side) onto pin 1 and the cathode (negative side) on pin 8 and solder carefully. For those not familiar with LEDs, the triangle symbol of the diode should point to the ground pin of the module (pin 8). Your final microwave harvester should look like figure 2

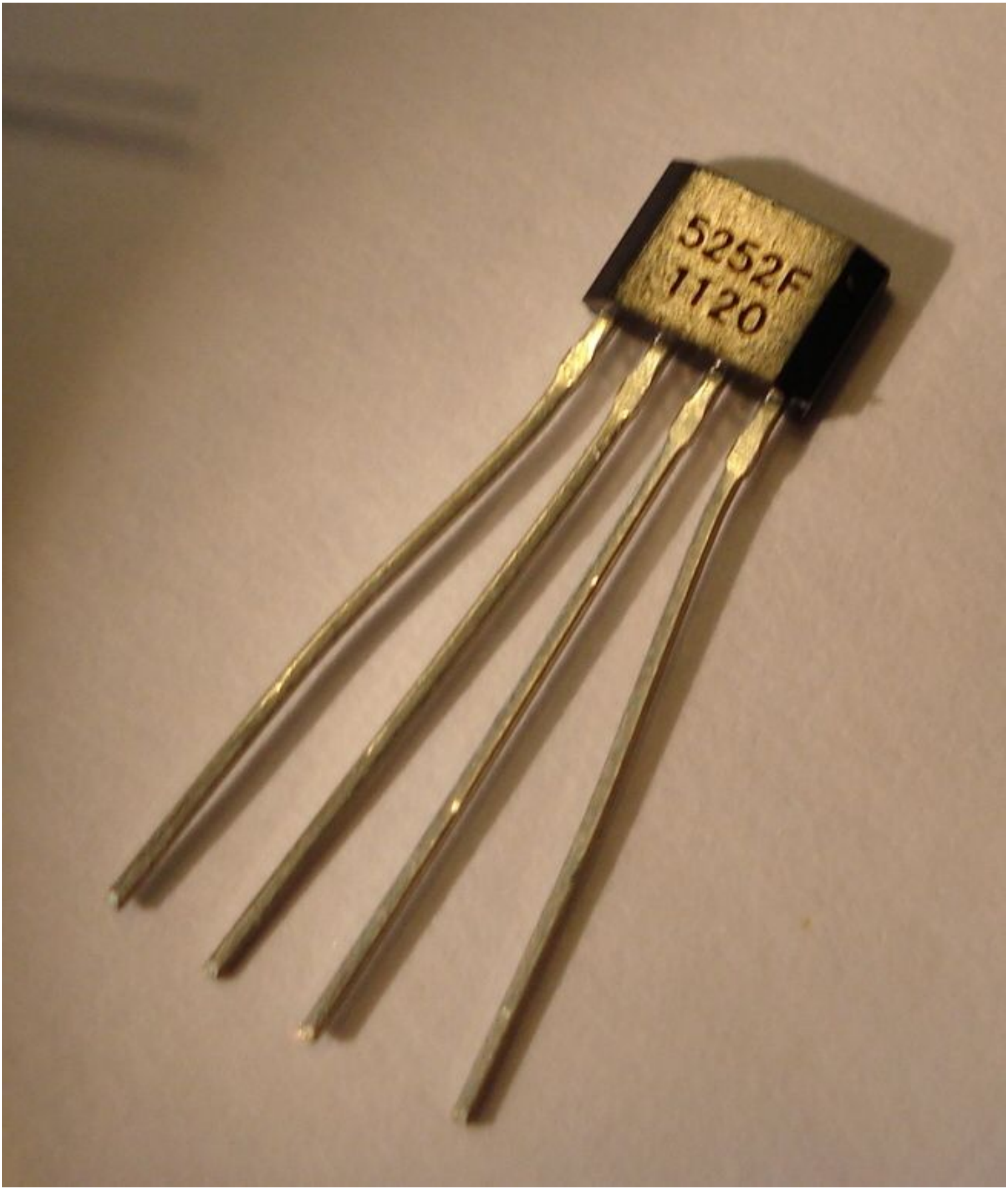
5252F
1120

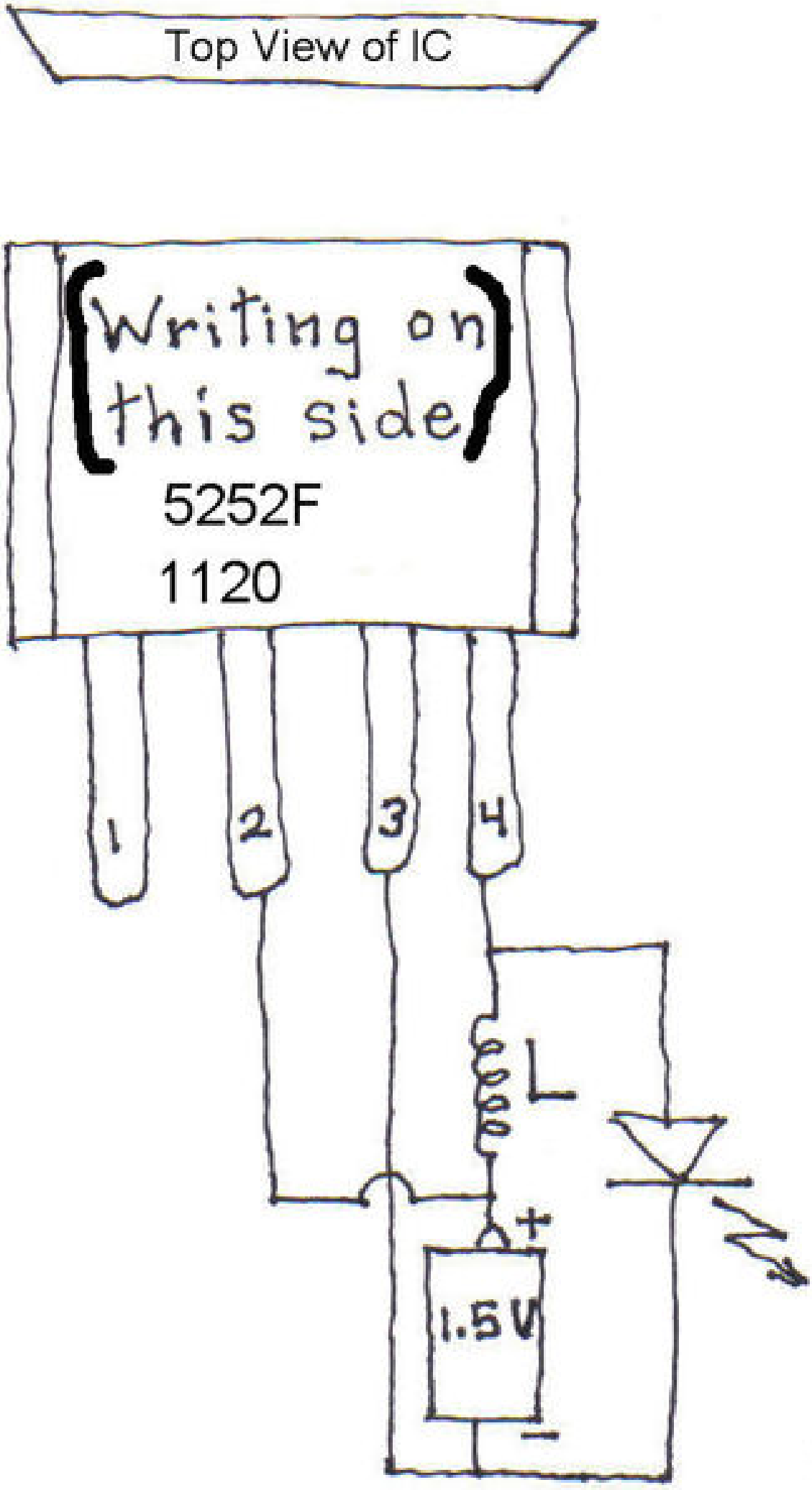
Top View of IC
Writing on this side
5252F
1120
1
2
3
4
L
+
1.5V
−

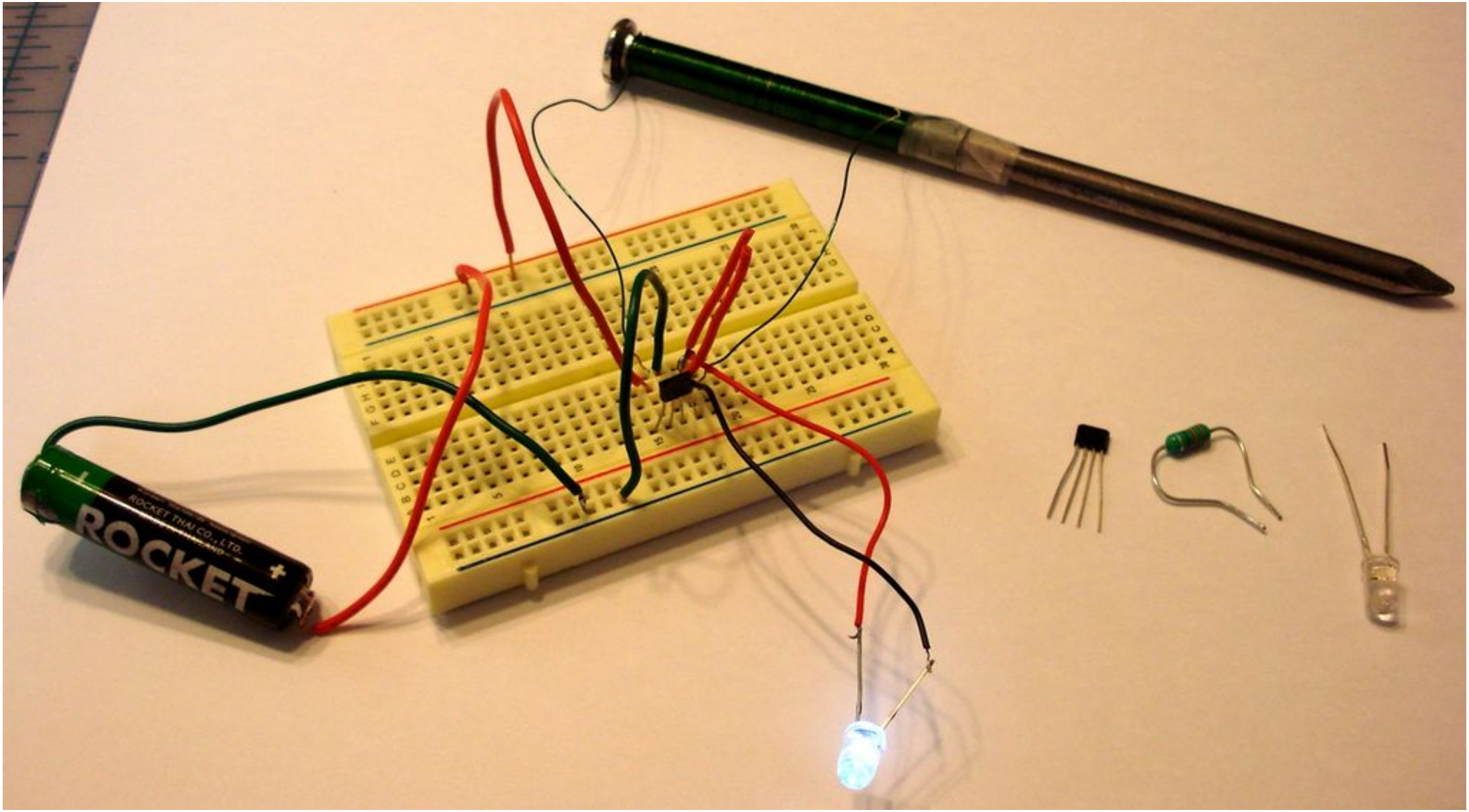
ROCKET
ROCKET THAI CO., LTD.

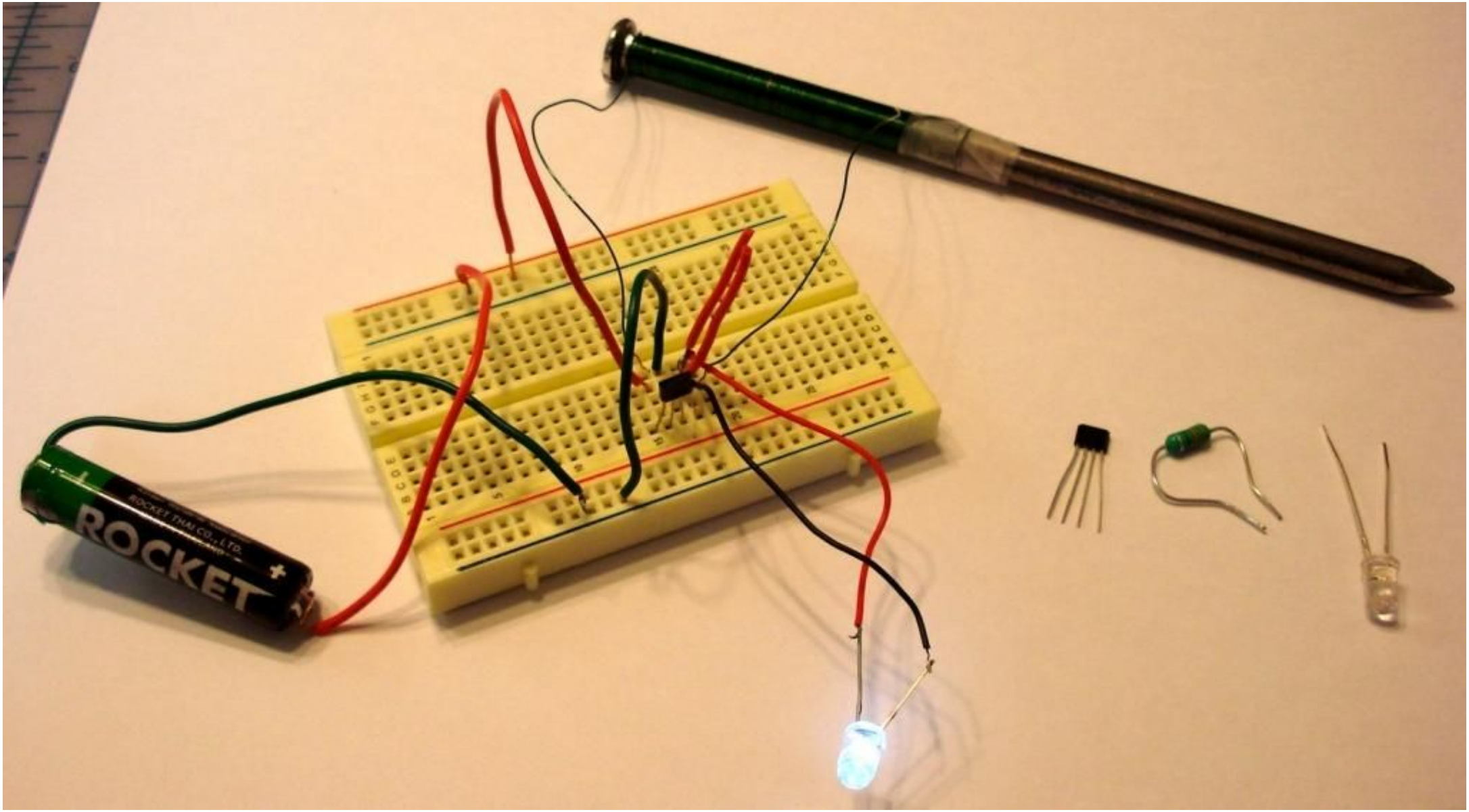
ROCKET
ROCKET THAI CO., LTD.

to be 50 mils wide. The final PCB design is shown in figure 13. The antenna, which can be seen at the top of the figure, is connected to the input of the processing circuitry from the direct-fed element of the antenna. The preliminary design does not contain a matching network, as this requires knowledge of the input impedance of the circuit, which can only be measured experimentally. The board dimensions are 89 mm x 57.5 mm.

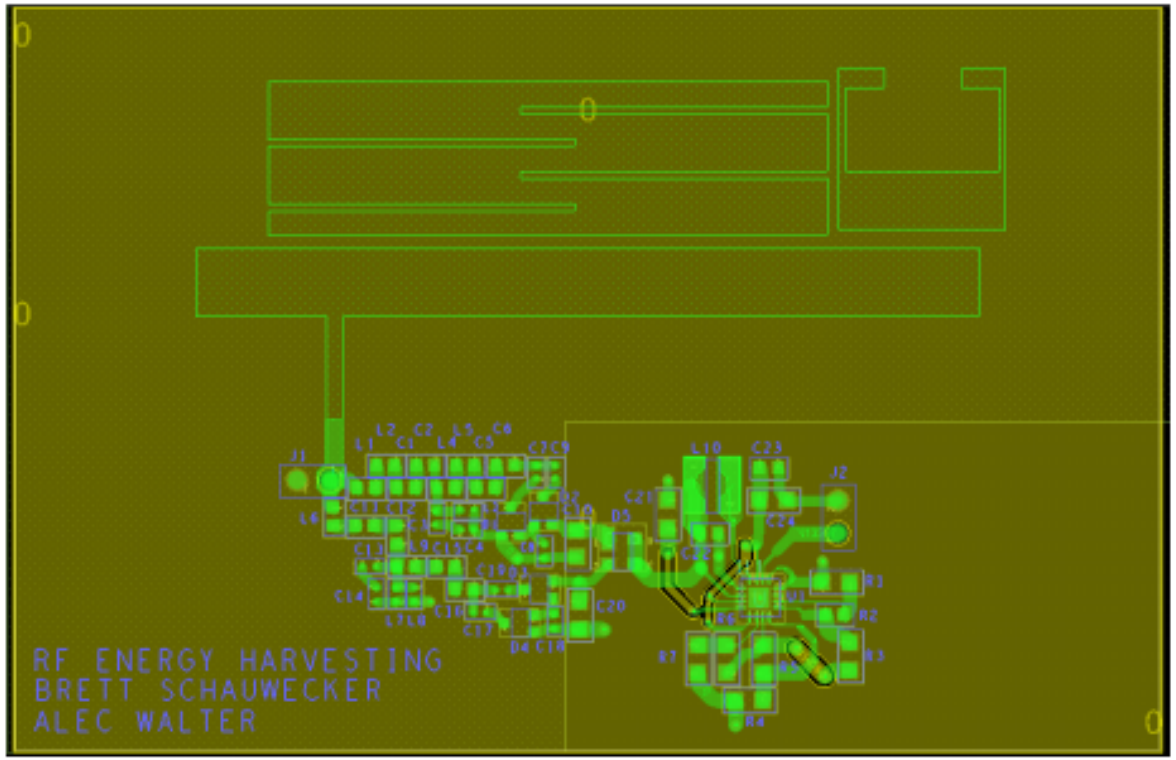

Figure 13. PCB Layout

With the size and quantity of small surface mount devices, all soldering was done with the use of water-soluble soldering paste and a heat gun. The only exception was the bq25504 Ultra Low-Power Boost Converter, which was soldered by tinning the pads on the board as well as the quad flat no-lead (qfn) package, and then heating up the solder with the soldering iron until a connection was made. Finally, a 470uF capacitor was connected to the output of the circuit for testing purposes. A capacitor was selected for testing instead of a Lithium-Ion battery for safety reasons, as improper charging of a Lithium-Ion battery can result in explosion. It is important to note that a capacitance of 470µF is considerably lower than the capacitance of a Lithium-Ion battery. However, charging of any size capacitor is sufficient to verify proof-of-concept, which is the primary purpose of this research. The completed board can be seen in figure 14.

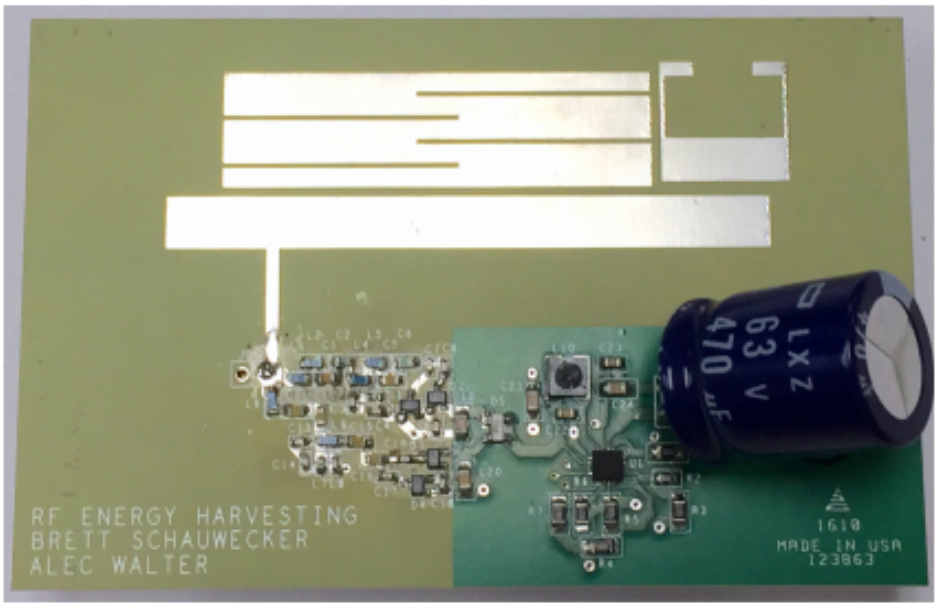

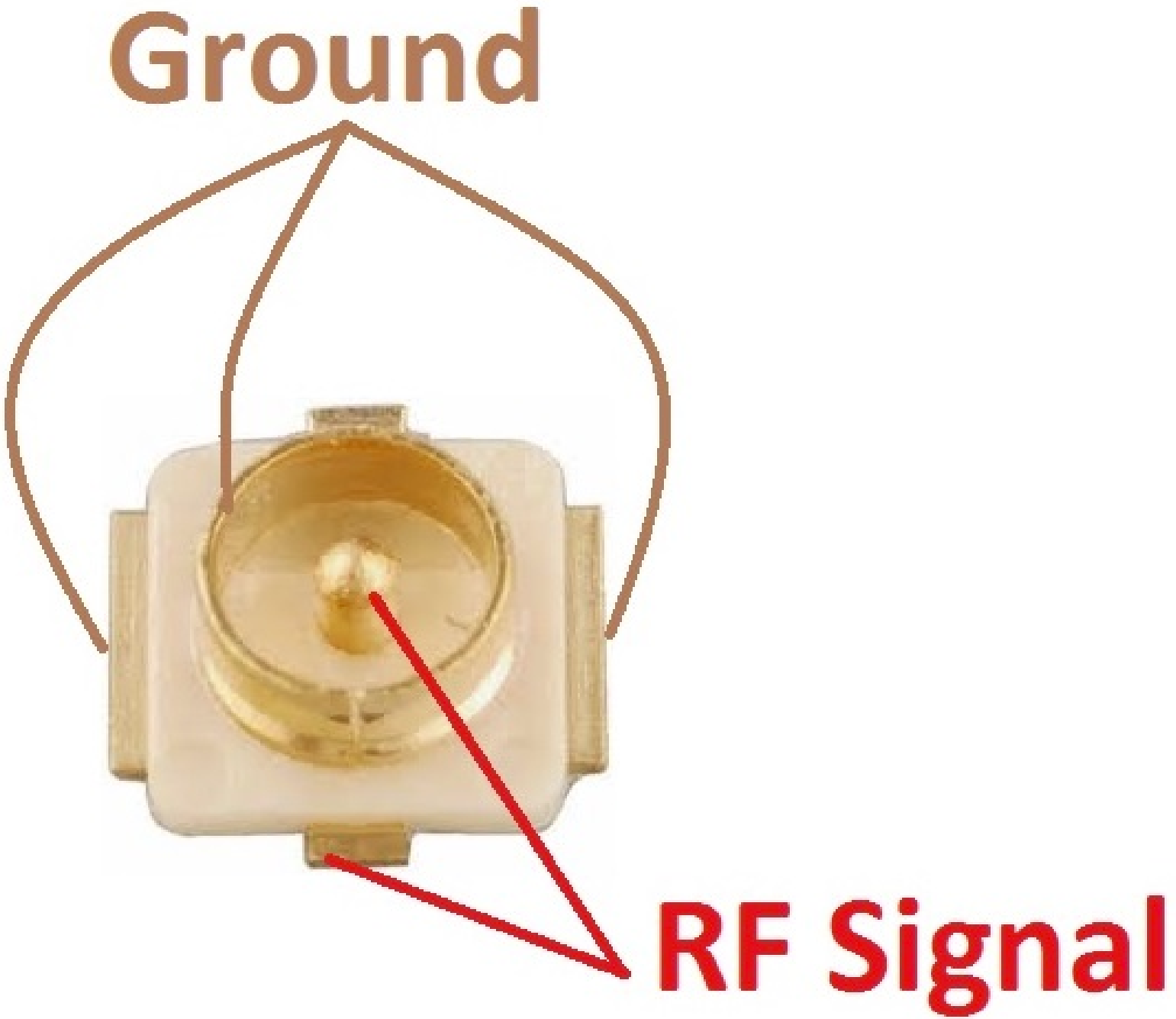
Ground
RF Signal

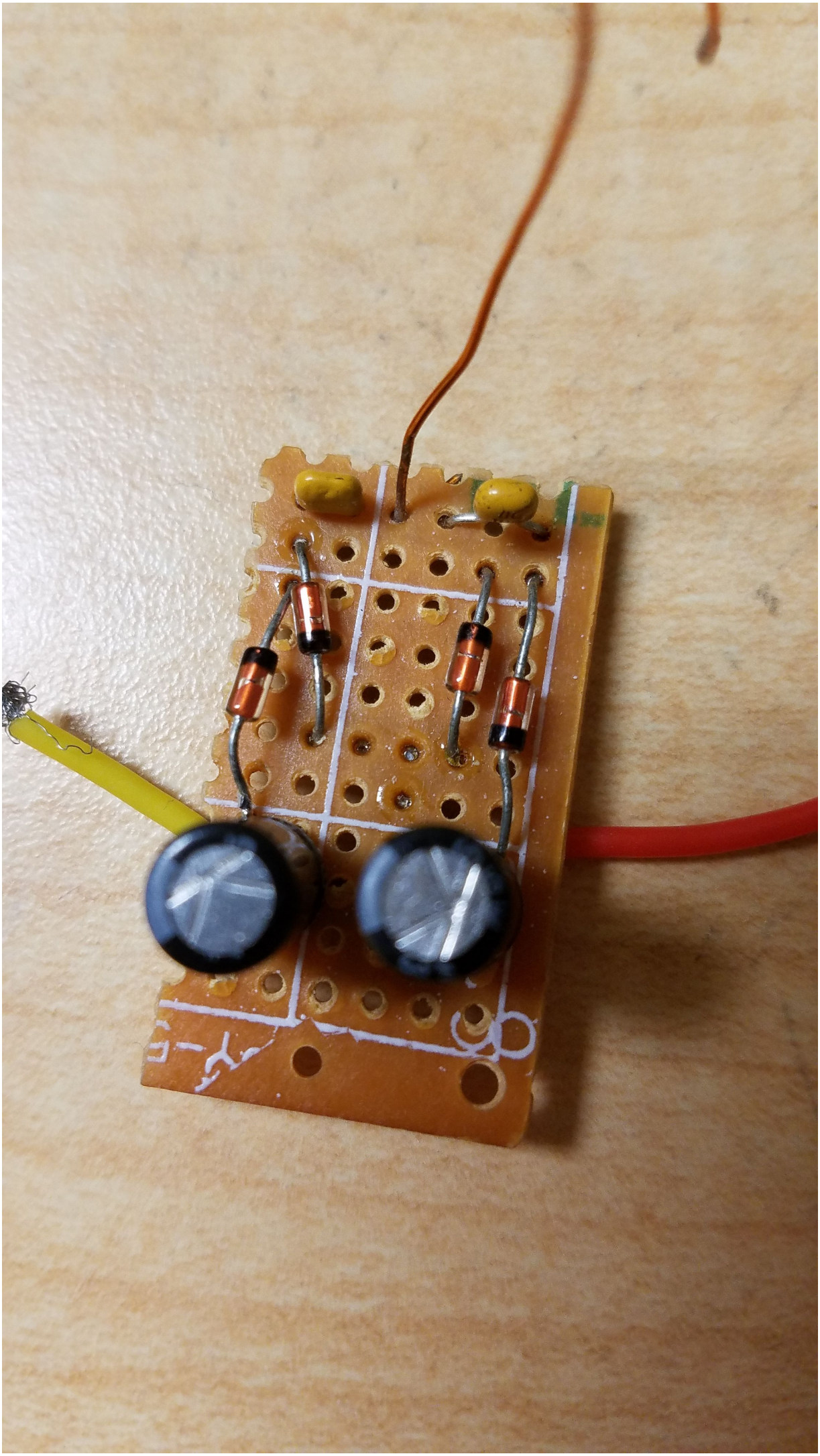

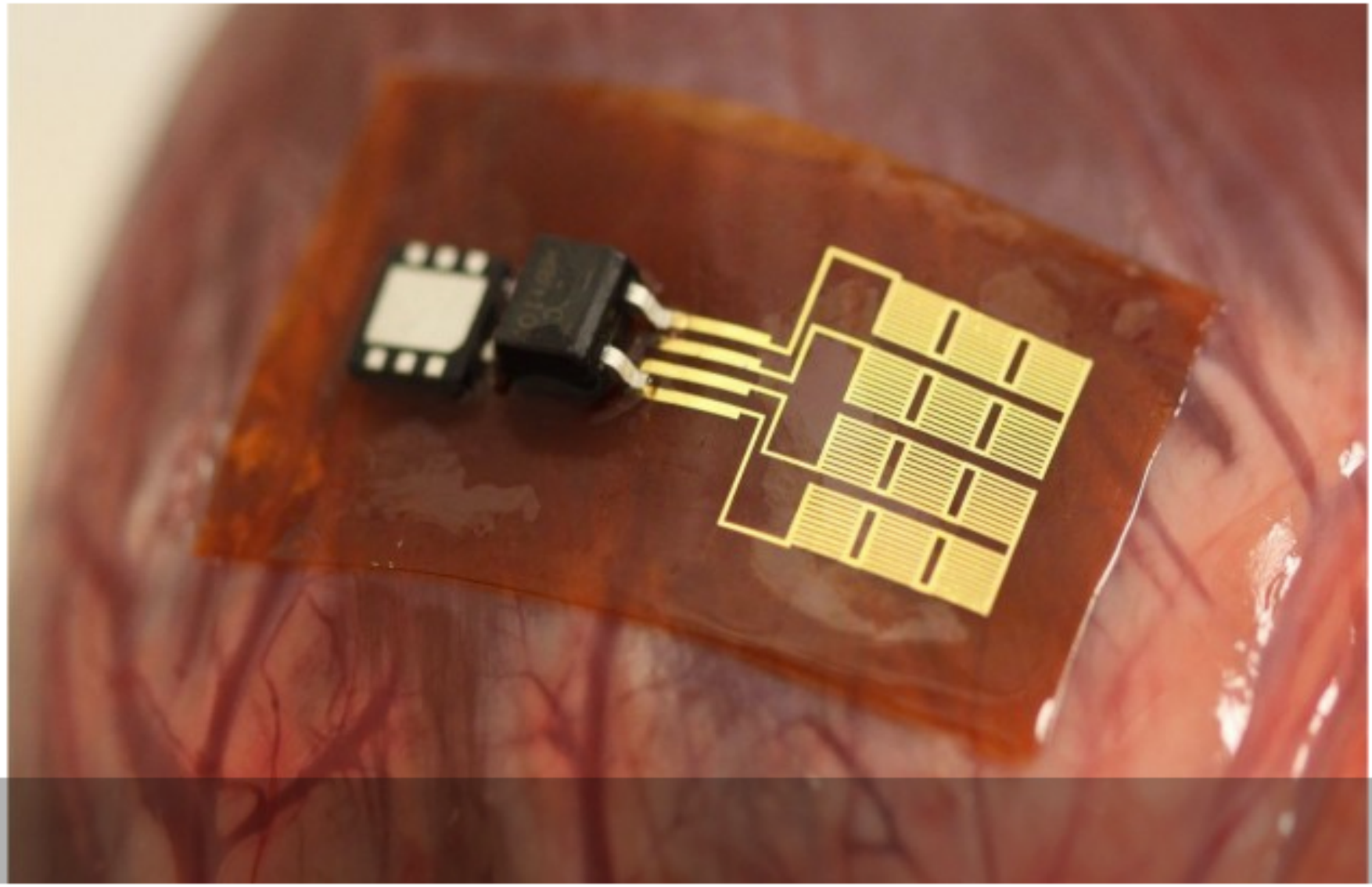

The implant mounted on the heart of a cow